

https://dspace.org/

Evaluation of metal nanocomposite polymer inclusion membranes (PIMs) for trace heavy metal extraction in natural waters

Maiphetlho, Kgomotso

2020

https://hdl.handle.net/10539/30195

Maiphetlho, Kgomotso Hendrick. (2019). Evaluation of metal nanocomposite polymer inclusion membranes (PIMs) for trace heavy metal extraction in natural waters, University of the Witwatersrand, https://hdl.handle.net/10539/30195

Downloaded from a DSpace repository. https://dspace.org/

Evaluation of metal nanocomposite polymer inclusion membranes (PIMs) for trace heavy metal extraction in natural waters



Kgomotso Maiphetlho

A dissertation submitted to the Faculty of Science, University of the Witwatersrand, Johannesburg, in fulfilment of the requirements of the Master of Science degree

University of the Witwatersrand

Johannesburg

2019

DECLARATION

I declare that this dissertation is my own work, unaided work. It is being submitted for the Degree of Master of Science at the University of Witwatersrand, Johannesburg. It has not been submitted before for any degree or Examination at any University.

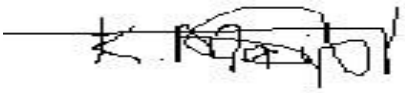

Kgomotso Maiphetlho

Date: 10/12/2019

ABSTRACT

The shortcomings of the conventional membranes in water applications such as low stability and the hydrophobic nature reduces the membrane productivity and lifespan. These result in expensive procedures that hinder membrane science technology. Hence, recent investigations have resulted in the synthesis of nanocomposite membranes as an alternative. In this work, silver nanocomposite polymer inclusion membranes (PIMs) were synthesized to evaluate the extraction of trace metal ions in natural waters. To characterise the PIMs, scanning electron microscope (SEM), energy-dispersive X-ray spectroscopy (EDX), contact angle measurements and water uptake measurements were used. The contact angle and the water uptake measurements highlighted that the introduction of the silver nanoparticles (Ag NPs) into the membrane, modified the membrane hydrophobic/hydrophilic character.

The evaluation of the synthesized PIMs demonstrated that the PIMs containing Ag NPs exhibit better extraction capacity as opposed to the bare PIMs and the PIM with (40 w.t% D2EHPA, 10 w.t% Ag NPs and 50 w.t% PVC) has the optimum composition. It was then used to optimise the parameters that are important for the extraction of trace metal ions and those were sample pH 5, 1 M HNO_3 of the receiving solution and 120 hrs for the extraction time. The selectivity of the nanocomposite PIM was investigated and it was found that its affinity towards a range of divalent cations (Co^{2+}, Ni^{2+}, Cu^{2+}, and Cd^{2+}) in synthetic water solutions, based on the percentage recovery factor of the extracted metal ions, follow the order; Cd^{2+} (94) > Cu^{2+} (87) > Ni^{2+} (78) > Co^{2+} (67), where the numerical data in the brackets correspond to the percentage recovery factor of metal ion extracted from the source solution, respectively. This order can be explained by the *Hard* and *Soft Acids* and *Bases Theory* and the hydration energy of the metal cations. However, the stability of the PIM was still compromised during repeated cycle operations despite an improvement of hydrophilicity with introduction of Ag NPs, this was indicated by an appreciable leaching of the carrier (D2EHPA) and Ag NPs in a 4:1 ratio (identical to the ratio of these components in the original membrane).

This silver nanocomposite PIM was tested in dam water. No matrix effect was observed on metal ion transport efficiency in such waters. The obtained transport efficiencies for the metal ions were Cd^{2+} (88), Cu^{2+} (80) , Ni^{2+} (62) , Co^{2+} (70) and Fe^{2+} (37) respectively. The newly synthesized PIM could be used for future extraction of the target metals in water systems. The designed PIM system has also the potential to be used as passive sampler for in situ extraction of the target metals in water systems. However, further studies are needed to improve the stability of both the carrier and nanoparticles in the membrane.

DEDICATION

This dissertation is dedicated to my late mother Boitumelo Maiphetlho.

ACKNOWLEGEMENTS

First and foremost, I would like to thank my supervisors Dr Heidi Richards and Prof. Luke Chimuka at the University of the Witwatersrand for grooming me towards finding solutions to environmental challenges through research in the use of membranes to extract trace metal ions in environmental samples. I appreciate all the contributions of time, ideas and funding to make my MSc productive and stimulating.

A special mention of Dr Izak Kotze, Dr Anita Etale, Dr Yannick Nuapia, Prof. Ewa Cukrowska and Prof. Hlanganani Tutu who were always present during my progress presentations. Your engagement and feedback were invaluable.

The Post Graduate students in the Environmental Analytical Chemistry research group have contributed immensely to my personal and professional growth. The group has been a source of friendship with invaluable moral support and intellectual guidance. *Ke leboga tirisano mmogo ya lona.* I would also like to mention Dr Nthabiseng Motsoane who encouraged me to pursue MSc and special thanks to Mrs Mokgaetji Monyai for training me to become a competent ICP-OES user. Ndivhuwo Shumbula (PhD candidate at the nanomaterials lab) is also acknowledged for help in synthesis of nanoparticles. To a 3rd year student (Craig Gurnell-2018) and an Honours student (Jessica Mhlongo-2019) thank you for affording me my first experience as a research supervisor.

Importantly, I would like to thank the Water Research Commission (WRC) and National Research Funding (NRF) of South Africa for their financial support towards this project.

Finally, I would like to acknowledge the only wise God, he who is full of wisdom, for the vision and divine enablement throughout this work.

TABLE OF CONTENTS

DECLARATION i

ABSTRACT ii

DEDICATION iii

ACKNOWLEGEMENTS iv

TABLE OF CONTENTS v

LIST OF FIGURES viii

LIST OF TABLES ix

LIST OF ABBREVIATIONS x

CHAPTER 1 1

1 INTRODUCTION 2

CHAPTER 2 6

2 LITERATURE REVIEW 7

2.1 Trace Heavy Metals 7

2.1.1 Definition 7

2.12 Metals: history, uses and abuses 8

2.1.3 Hazards of heavy metals to human health, plants and environment 9

2.1.4 Metals under study 11

2.1.4.1 Cadmium 12

2.1.4.2 Cobalt 12

2.4.1.3 Copper 13

2.4.1.4 Iron 13

2.4.1.5 Nickel 14

2.1.5 Metal extractions: the past, present and future 14

2.2 Membrane Technology 17

2.2.1 Polymer inclusion membranes (PIMs) 17
2.3 Membrane Characterisation 19
2.3.1 Morphology and structure 19
2.32 Permeability 20
2.3.3 Selectivity 22
2.3.4 Stability 23
2.3.5 Role of nanoparticles in nanocomposite PIMs 26
2.4 Transport Mechanism 28
2.4.1 Transport mechanism in PIMs 28
2.4.2 Critical parameters in transport of analytes 30
2.5 Sampling 30
2.5.1 Principle of passive sampling 30
CHAPTER 3 34
3 AIMS AND OBJECTIVES 35
3.1 Aim 35
3.2 Objectives 35
3.3 Justification 35
CHAPTER 4 36
4 RESEARCH METHODOLOGY 37
4.1 Chemicals and Reagents 37
4.2 Instrumentation 37
4.3 Synthesis of Silver Nanoparticles 38
4.4 Synthesis of nanocomposite PIMs 38
4.5 Water Uptake 39
4.6 Contact Angle Measurements 40
4.7 Transport Experiments 40
4.8 Sampling procedure 43

CHAPTER 5 44
5 RESULTS AND DISCUSSION 45
5.1 Characterisation of Silver Nanoparticles 45
5.2 Characterisation of the Silver nanocomposite PIMs 46
5.3 Transports Experiments 50
5.3.1 Optimisation of PIMs composition 50
5.3.2 Optimisation of critical parameters for the transport of analytes 52
5.3.2.1 Optimisation of receiver solution concentration 53
5.3.2.2 Optimisation of source solution pH 55
5.3.2.3 Effect of source solution concentration on extraction capacity 56
5.4 Selectivity 57
5.5 Stability 59
5.6 Influence of transport time 62
CHAPTER 6 64
6 Environmental Application 65
6.1 Sampling site 65
6.2 Physicochemical parameters of the water samples 66
6.3 Matrix effect 67
6.4 Analytical figures of merit 68
CHAPTER 7 70
7 CONCLUSIONS AND RECOMMENDATIONS 71
7.1 General conclusions 71
7.2 Recommendations and future work 72
REFERENCES 73
APPENDIX 92

LIST OF FIGURES

Figure 1 Toxicity effects of heavy metals in microorganisms 10
Figure 2 Polymer inclusion membrane 18
Figure 3 A typical lab-based PIM experimental setup..... 19
Figure 4 Schematic diagram of a nanocomposite PIM structure 27
Figure 5 Schematic of the facilitated transport of target analyte across a PIM 29
Figure 6 Analyte uptake profile of passive sampling devices 32
Figure 7 Schematic procedure for the preparation of a nanocomposite PIM 39
Figure 8 Scheme of the PIM-device system used for analytes preconcentration and transport experiment 42
Figure 9 UV-Vis spectra of Ag NPs 45
Figure 10 Particle size distribution of Ag NPs and TEM image 46
Figure 11 Surface morphology of the PVC/Ag NPs nanocomposite membranes 47
Figure 12 EDX spectra of the PVC/Ag NPs nanocomposite membranes 48
Figure 13 Water contact angles (a) and uptake of PVC/Ag NPs nanocomposite membranes 49
Figure 14 Photograph of the PVC/Ag NPs nanocomposite membranes 50
Figure 15 Influence of Ag NPs w.t% in PVC PIMs, for various metal extraction capacity.... 52
Figure 16 Effect of various acid receiver solutions on extraction ability 53
Figure 17 Effect of receiver solution concentration on extraction of metal ions..... 55
Figure 18 Effect of source solution pH on membrane extraction capacity..... 56
Figure 19 Effect source metal ion concentration on analyte extraction..... 57
Figure 20 Molecular structure of di-(2-ethylhexyl) phosphoric acid (D2EHPA)..... 58
Figure 21 Percentage mass loss of PIMs for metal ions extraction 60
Figure 22 RF values of bivalent cations vs number of cycles 61
Figure 23 Influence of the duration of transport on the transport efficiency of the metal ions studied..... 62
Figure 24 Sites used for the collection of water samples..... 65

LIST OF TABLES

Table 1 Standard fundamental toxicity data for heavy metals in drinking water 11
Table 2 Membrane technologies for separations and purifications of metal ions in aqueous solutions 15
Table 3 PIM lifetime and performance under continuous conditions 24
Table 4 Environmental applications of a PIM-based passive samplers. 33
Table 5 Compositions of the PIMs and their resulting flexibility 39
Table 6 The influence of silver nanoparticles on the initial flux of metal ions across a PIM . 51
Table 7 PIM extraction based recovery factors (RF) and initial flux (J) values for a range of metal cations 58
Table 8 Ionic sizes and the hydration energies of metal ions 59
Table 9 Characteristics of the water samples used for this study 66
Table 10 Effect of matrix effect on analytes transport efficiencies of the PIM 67
Table 11 Cationic species that were co-transported with the targets metal ions on the spiked tap water sample 68
Table 12 Summary of the analytical figures for calibration curves obtained with a nanocomposite PIM 69

LIST OF ABBREVIATIONS

AFM	Atomic force microscopy
Ag NPs	Silver nanoparticles
Aliquat 336	Trioctylmethylammonium chloride
AMD	Acid mine drainage
ANOVA	Analysis of variance
Bif-ILEs	Bifuntional ionic liquid extracts
PVDF	Polyvinylidene difluoride
Cd	Cadmium
Co	Cobalt
CTA	Cellulose triacetate
Cu	Copper
Cyphos® IL 101	Trihexyl (tetradecyl) phosphonium chloride
Cyphos® IL 104	Trihexyl (tetradecyl) phosphonium bis(2,4,4-trimethylpentyl) phosphinate
D2EHAF	N[N,Ndi (2-ethylhexyl) amino carbony lmethyl] phenylalanine
D2EHPA	Di-(2-ethylhexyl) phosphoric acid
DGT	Diffusion gradient in thin-films
DNNDS	2,4-dinitro-1-naphthol-7-sulfonic acid sodium salt
ELMs	Emulsion liquid membranes
EPA	Environmental Protection Agency
ESPLMs	Electrostatic pseudo liquid membranes
Fe	Iron
FFAT	Two phenylalanine in acid
FTIR	Fourier transform infared scpectroscopy
HFSLMs	Hollow fiber supported liquid membranes
Ils	Anion based ionic liquid
Ni	Nickel
NPOE	1-(2-Nitrophenoxy) octane
PIMs	Polymer inclusion membranes
POCISs	Polar organic chemical intergrative samplers
PVC	Polyvinyl chloride

PVDF-HFP	Poly (vinylidene fluoride-co-hexafluoro propylene)
RF	Recovery factor
SD	Standard deviation
SE	Solvent extraction
SEM	Scanning electron microscopy
SEM-EDS	Energy dispersive spectroscopy
SLMs	Supported liquid membranes
SMX	Sulfamethoxole
SPMDs	Semipermiable membrane devices
SPR	Surface plasma resonance
TEM	Transmission electron microscopy
TGA	Thermogravimetric analysis
THF	Tetrahydrofuran
TWA	Time weighted averages
USEPA	United States Environmental Protection Agency
WFD	Water Framework Directive
WHO	World Health Organisation

CHAPTER 1

This chapter gives a background on the trace metal pollution in natural waters, membrane extractions, and incorporations of nanoparticles in membranes to improve membrane stability.

1 INTRODUCTION

Water is an essential resource needed by all organisms for survival. However, many people do not have access to clean water, because only 2.6% of global water can be classified as fresh water, which is not enough for the global population (Simões and Simões 2013). It has been reported that water scarcity is a worldwide problem (Zeng et al. 2013). Some statistics on the global water situation are given below:

- About two-thirds of the global population live in severe water scarcity conditions for at least 1 month. Yearly half a billion people live with water scarcity (Mekonnen and Hoekstra 2016).
- Water scarcity is projected to worsen due to increase in temperatures as a result of climate change (Distefano and Kelly 2017).
- In 2015, 663 million people were officially recognized as being without access to an improved drinking water source (World Health Organization 2015).
- Globally, at least 2 billion people use a drinking water source that is contaminated with faeces (World Health Organisation 2018).

Besides the water scarcity problem and lack of access to proper sanitation, heavy metal pollution has become an international problem (Facchinelli et al. 2001). This is accelerated by overpopulation, rapid economic development and industrialisation. toxic heavy metals enter natural waters from anthropogenic sources such as mining activities, agricultural runoffs, open-pit latrines and industrial wastes. Exposure of humans to these metals can result in severe health issues, with the surrounding environment also affected. Some of these health issues have been investigated and it was reported that cadmium exposure can cause lung cancer, kidney dysfunction, bone fracture and pulmonary adenocarcinomas (Zukowska and Biziuk 2008). Long term exposure of zinc results in cholesterol imbalances and infertility (Zhang et al. 2012b). Lead exposure has an effect on blood enzymes and the central nervous system (Kaufmann et al. 2003). Other metals such as, nickel, copper and chromium also have an impact on human health at higher concentrations (USEPA 2000).

To tackle the water pollution problem as an attempt to minimise water scarcity, a technique that is cheap, simple and environmentally friendly is needed to constantly evaluate the level of trace pollutants in natural waters. Over the past decades, membrane extraction systems have been utilized as an alternative to the traditional solvent extraction methods. These methods have been widely applied in separating compounds such as organics and trace metal ions in

aqueous solutions. This is because membranes do not use extensive thermal operations that waste energy in heating, drying and distillation (Chen et al. 2018). Besides energy saving, there is also less usage of expensive organic solvents, thus making the extraction process cost effective and promising as a green analytical separation method.

The number of publications on the use of membranes to extract analytes in water samples, has risen exponentially in recent years (Almeida et al. 2012). Different types of membranes which have been used including, bulk liquid membranes (BLMs), emulsion liquid membranes (ELMs), supported liquid membranes (SLMs), hollow fibre supported liquid membranes (HFSLMs), and electrostatic pseudo liquid membrane (ESPLMs) (Nghiem et al. 2006; Chen et al. 2018).

However, since the first publication of membranes, different investigative approaches have been undertaken to improve the stability of the membranes. This was done in an attempt to improve hydrophilicity, specific selectivity, reduce biofouling and improve chemical and thermal stability of the membranes (Kang and Cao 2014). The above factors can render membranes susceptible to fouling when exposed to concentrated acids and in some cases alkaline solutions. Fouling is caused by the undesirable accumulation of solutes inside the membrane or on the membrane surface. It results in a decline in the life span of the membrane, reduced productivity and an increase in costs of the membranes (Khalid et al. 2017a).

Investigations resulted in a novel type of polymer-based liquid membrane known as polymer inclusion membranes (PIMs), which was introduced fifty years ago as an ion selective electrode and optode (Almeida et al. 2017). These PIMs consist of a base polymer, a carrier and a plasticizer. They are synthesized by casting a solution of a carrier, plasticizer and a base polymer to form a thin, flexible, but stable film. these membranes separate analytes of interest in a similar fashion as SLMs (Nghiem et al. 2006). Compared to SLMs however, PIMs have several advantages including higher transport efficiency, improved flux, easy setup, high selectivity and durability (Kim et al. 2001, 2000; Wang et al. 2000). PIMs that result in a no loss of carrier during a membrane extraction process can also be synthesized meaning that PIMs have less possibility of leaching in water applications as compared to the other membranes (Annane et al. 2015). There is also fast permeation and simple composition in PIMs (Chen et al. 2018). In general, PIMs have a relatively long lifespan and can be reused (Kaya et al. 2016; Wang et al. 2017).

PIMs can be used in passive samplers to monitor trace heavy metals in environmental water samples (Seethapathy et al. 2008). This minimises sampling errors, as pollution can be missed during grab (spot) sampling. It is also an easy technique that combines sampling, analyte isolation and preconcentration, thus saving time and tedious labour (Górecki and Namieśnik 2002). Costs of analysis are also reduced because passive samplers have no electrical requirements to function and uses less or no organic solvents. It can thus be regarded as an emerging green analytical chemistry techniques due to less or no usage of toxic solvents. The technique is based on free flow of analytes from sampled to collected medium due to a difference in chemical potential, which continues until equilibrium is reached or it is terminated by user (Górecki and Namieśnik 2002). Since passive samplers can be left in water samples over time, they allow calculation of time weighted averages (TWA) which gives an accurate overview of analyte concentrations in a weighted frame.

Although there was an improved reproducibility and reusability when PIMs were used in passive samplers, there was still a decrease in the membrane permeability after four or five successive transport cycles (Nghiem et al. 2006). The decline is caused by the leaching of the membrane liquid phase due to finite water solubility constituents (Kaya et al. 2016; Wang et al. 2017). This means that fouling, chemical and thermal stability were still affecting the reusability of PIMs. More investigations were then conducted to minimise these limitations (Yoshida et al. 2019; Sellami et al. 2019).

Nanomaterials can reduce fouling activity by improving hydrophilicity, surface roughness, porosity, chemical and mechanical strength of the membranes (Yin and Deng 2015). These include nano silver, nano titanium oxide, nano zinc oxide, nano alumna and graphene (Jhaveri and Murthy 2016; Johary et al. 2018; Mokkapati et al. 2017; Teow et al. 2015). Among the above nanoparticles, nano silver is reported as a superior material with the most improved membrane selectivity, permeability, good chemical, mechanical and thermal strength, together with good catalytic and antibacterial properties (Andrade et al. 2015; Yin and Deng 2015).

The present study targeted the extraction of trace heavy metals using metal nanocomposite PIMs in environmental water samples. Unlike bare / unmodified PIMs, PIMs using nanoparticle-modified membranes have improved membrane hydrophilicity and analytes transport efficiency, better reproducibility and reusability, thus minimising the costs of analysis. The method is also environmentally friendly since there is no clean-up or pre-

concentration step, thus saving time and the possibility of errors occurring during sample preparation.

CHAPTER 2

This chapter defines common terms used in this dissertation. Environmental trace metal pollution is discussed with a focus on various metal extraction techniques and an emphasis on passive sampling. The advantages of using polymer inclusion membranes in passive samplers are also discussed.

2 LITERATURE REVIEW

2.1 Trace Heavy Metals

2.1.1 Definition

There are several definitions given for heavy metals in the literature. Each definition is given to suit the relevant research question which might be confusing for target audiences since some of the given definitions are contradictory. The common definition follows the specific gravity approach, whereby metals with densities higher than 3.5 to 7.0 $g\ cm^{-3}$ are classified as heavy metals (El-Kady and Abdel-Wahhab 2018; Hodson 2004). Other authors identify heavy metals as those that have atomic number greater than 20 (El-Kady and Abdel-Wahhab 2018). This latter approach classifies scandium as a heavy metal even though following the specific gravity approach, it would not be classified as one, with a density of 3.0 $g\ cm^{-3}$ (at unspecified temperature and pressure).

There is also an atomic weight based definition whereby heavy metals are classified as those that have atomic weight greater than 23 (from magnesium onwards) and from atomic weight greater than 40 (from scandium onwards) (El-Kady and Abdel-Wahhab 2018). Other definitions are chemically related although uncommon, the first is based on properties of *s*, *p*, *d* and *f*-block elements. In this approach heavy metals are described as high atomic number *p*-block elements that bind strongly to sulphur, leading to a toxic effect. Still another approach is based on hard and soft metal ion classifications. Hard ions form ionic bonds which are easily displaced and mobile, while soft ions form covalent bonds with soft ligands such as sulphide or sulphur donors, and tends to accumulate in organisms with resultant toxicity. This method has a biological, toxicological and environmental relevance although it is the most uncommon approach to define heavy metals (Hodson 2004).

Besides these various definitions of heavy metals, none of them is universally accepted and there have been calls to stop scientists from using the term. However, the number of publications with the different definitive approaches has increased exponentially over the past 30 years (Pourret and Bollinger 2018). A better word to replace heavy metals has also been proposed: “potentially toxic metals” (Pourret and Bollinger 2018).

In this dissertation, therefore, I use the term to refer to potentially toxic metals, and "trace heavy metals" to refer to these potentially toxic metals when their average concentration is below 100 ppm.

2.12 Metals: history, uses and abuses

Metals occur naturally in the earth's crust. However, their release and distribution from rocks to various media of environment is influenced by climate and erosion factors (El-Kady and AbdelWahhab 2018). Anthropogenic sources like mining, agricultural run offs, industrial and car emissions also play a crucial role in transportation of these metals in aquatic media and dry environments.

They have properties such as rigidity, ductility, tensile strength, durability and highly resistant to natural wear and tear hence have a wide range of applications. In the past metals were mainly used for manufacturing farming tools, weapons and in locomotive wagons. With recent advancement in technology and innovation, almost all manufactured products use metals in one form or another, including as alloys in electronics, jewellery, building construction, machinery, automobiles, furniture, security systems, fertilizers, medicine and medical imaging.

Metals can be classified into two categories; essential and non-essential metals. Essential metals provide micronutrients needed for human health. They include zinc (Zn), calcium (Ca), copper (Cu) and manganese (Mn) (Nuapia et al. 2018). Non-essential metals are those that have no positive role in human biological activities and can be toxic at a low concentrations. They include cadmium (Cd), lead (Pb), chromium (Cr), mercury (Hg) and uranium (U) (El-Kady and Abdel-Wahhab 2018; Nuapia et al. 2018).

As opposed to organic pollutants, metals are highly soluble and accumulate in different matrix environments with some metals undergoing oxidation or chemical reactions forming compounds that show minimum lethal dose at low concentrations (Nthunya et al. 2017). This is a critical concern. Since South Africa is a developing country that is economically dependent on industries that release these metal pollutants in natural waters and the environment. Thus, making it difficult for law enforcement to act on industries that are guilty of such pollution. Once these metals are released into the aquatic environment, they are adsorbed onto sediments and transported through water systems.

Biomagnification and bioconcentration then become a source of health hazard through food chains as soon as the metal concentrations in the environment exceed the permissible limits. Humans are affected through the consumption of plants including foods and medicinal herbs grown in contaminated water, drinking polluted water, or inhaling metal contaminated dust (Nthunya et al. 2017; Okem et al. 2014).

2.1.3 Hazards of heavy metals to human health, plants and environment

Heavy metal contamination induces serious health and environmental hazards; they inhibit metabolic function and modulate genetic material of humans (Jacob et al. 2018). They have the ability to inhibit physiological processes like cell membrane distribution (Karthik et al. 2016; Khan et al. 2009). They bind to vital cellular components such as structural proteins, enzymes and nucleic acid which then interferes with their functions. This results in the inhibition of cell division, enzyme activity, and modification of protein molecular structure (Khan et al. 2009). Elevated heavy metal concentrations affect plant growth, symbiosis and crop yield which could become a threat to food security and consequently mass extinction of rare plant and animal species. (Sobol and Schiestl 2012). Figure 1 illustrates the effect of heavy metals on microorganisms.

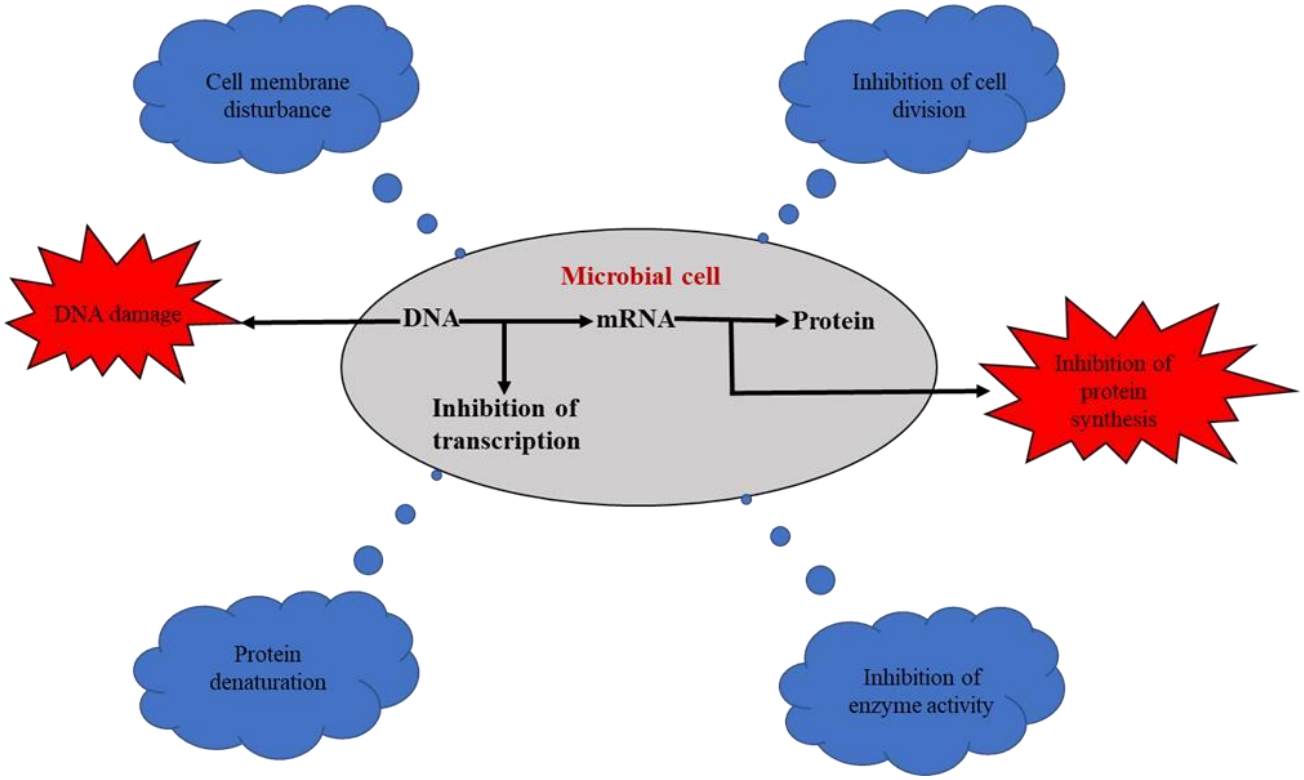

Figure 1 Toxicity effects of heavy metals in microorganisms (Jacob et al. 2018)

In humans, heavy metal exposure can result in cancers, kidney failure, skin disorder, lung disease, neurological disorders, schizophrenia and damage to functions of arteries and the liver (Kumar et al. 2017). Even the essential metals at elevated concentrations, pose a threat to living organisms (Jacob et al. 2018). Manganese (Mn) can lead to haemoglobin low levels, neurotoxicity and gastrointestinal accumulation at high levels (Fadel et al. 2017). Zinc (Zn) over-exposure may cause loss of appetite, muscular stiffness, irritability and nausea (Rangabhashiyam and Balasubramanian 2018), while high copper (Cu) concentrations may cause hair loss, hypoglycaemia, increased heart rate, severe headaches, anaemia, kidney damage, lethargy and anorexia (Pellera et al. 2012; Rangabhashiyam and Balasubramanian 2018).

Considering the threats posed by heavy metals, strategies have been developed to control levels of these metals in environments through the establishment of scientific toxicity studies and guidelines from World Health Organisation (WHO), Environmental Protection Agency (EPA) and Department of Water and Sanitation of South Africa (DWWSA). Table 1 shows the toxicity data for heavy metals in drinking water.

Table 1 Standard fundamental toxicity data for heavy metals in drinking water, as recommended by the WHO, EPA (Kumar et al. 2017) and DWWSA (SANS 2006)

Heavy metals	Scientific toxicity standards		
	WHO (mg L^{-1})	EPA (mg L^{-1})	DWWSA (µg L^{-1})
Ni	0.07	0.04	150
Cu	2	1.3	1000
Zn	3	5	5.0*
Cd	0.003	0.005	5
Hg	0.001	0.002	1
Pb	0.010	0.015	20
As	0.010	0.010	10

X* -unit is mg L^{-1}

The South African economy is largely dependent on industries and farming. Heavy metal contamination of water resources is therefore likely to continue posing a threat to living and non-living organisms. It is thus essential to scientifically evaluate and monitor heavy metal concentrations in water systems, which starts with the development of viable and cheaper metal extraction techniques.

2.1.4 Metals under study

The water quality in Gauteng, Mpumalanga and North West province is impacted by acid mine drainage (AMD) from abandoned and operational gold mines in the Witwatersrand (Wits) basin (Durand 2012). Elevated concentrations of heavy metals such as cadmium, cobalt, iron, copper and nickel in the Wits basin have been observed in rivers close to mine slime dumps (Tutu et al. 2008). These concentrations can be as high as 1010 mg L^{-1} iron content, 11.43 mg L^{-1} copper, 17.11 mg L^{-1} cobalt and 42.33 mg L^{-1} nickel (Tutu et al. 2008). Depending on concentration and duration of exposure, these metals can be fatal to humans and the ecosystem.

2.1.4.1 Cadmium

Cadmium (Cd) is a non-essential metal. Overexposure to this element is associated with kidney disease, and negative effects on skeletal and respiratory systems (Larsson and Wolk 2016). The United States Environmental Protection Agency (USEPA) has classified this metal as a possible human carcinogen (Geng and Wang 2019). A few studies have reported that Cd accumulation is higher in women than in men. During breastfeeding, Cd can be secreted into the milk, accumulating in the offspring's body, and impacting their memory and learning ability (Dharmadasa et al. 2017). Hence, the European Food Standards Authority has recommended the weekly Cd intake of 2.5 $\mu g\,kg^{-1}$ body weight (Turner 2019). In unpolluted soil, Cd concentration is 1 $mg\,kg^{-1}$, but in mine tailings the concentration ranges between 6.4 and 11.7 $mg\,kg^{-1}$ (Fashola et al. 2016). Cd has an exceptionally long biological half-life (>20 years), is highly mobile in soil-plant systems and exert a great effect on the proper functioning of the ecosystems. This is a serious concern due to its ability to accumulate through the food chain, drinking water and soil.

2.1.4.2 Cobalt

Cobalt (Co) is important in humanbiological systems due to its role in vitamin B_{12} (Strachan 2010). Vitamin B_{12} is a water-soluble vitamin that has a significant role in the normal function of the brain and nervous system and the biosynthesis of important blood components (Gille and Schmid 2015). However, Co can be toxic if exposure is excessive (Leyssens et al. 2017). It predominantly occurs in the cobaltous (Co^{2+}) and cobaltic (Co^{3+}) states, with the Co^{2+} state being the most environmentally available although both states are widely distributed in nature (Paustenbach et al. 2013). Due to persistent stability of Co in soil and water, it should be carefully monitored since high exposure is classified as a possible human carcinogen. there is also a suggested correlation between cobalt exposure and lung disease in humans, including asthma and alveolitis (Behl et al. 2015).

2.4.1.3 Copper

In the environment, Cu is widely distributed in sulphides, arsenites, chlorides and carbonates and exists in two states; the oxidized state Cu^{2+} and reduced state Cu^{+}. (Fashola et al. 2016). The mean concentration of 5 to 70 mg kg^{-1} exists in unpolluted soil, while higher concentrations (92.17 mg kg^{-1}) are found in contaminated environments like mining sites (Fashola et al. 2016; Bempah et al. 2013).

In the human body, Cu is the third most abundant *d*-metal in the human body and an essential element (Linder 2013). It participates in the formation of connective tissue, as collagen and keratine in the human body. However, at high concentrations, Cu can be toxic because it is able to replace zinc and iron from metalloproteins (Zoroddu et al. 2019). Hence, 100 mg per 70 kg body weight is the recommended daily intake (Maret 2016). Elevated copper levels in tap water can cause blue water, clogging of filters and staining of sinks and tubs (Lytle et al. 2019).

2.4.1.4 Iron

Iron (Fe) is the most abundant *d*-metal in the human body and an essential element for all living organisms (Zoroddu et al. 2019). It is particularly vital for normal heart functioning (LakhalLittleton 2019). However, excess concentrations can lead to ischemic heart disease, arthrosclerosis, suppression of the antitumor action of macrophages thus facilitating the growth of cancerous cells (Gujja et al. 2010; Moghimi Benhangi et al. 2019). In addition, a few neurodegenerative abnormalities are associated with inappropriate metabolism of iron in the brain, such as aceruloplasminemia and neuroferritinopathy (Papanikolaou and Pantopoulos 2005). Hence, the recommended daily intake is 5 g per 70 kg body weight (Maret 2016).

In natural waters, iron occurs as Fe^{2+} and Fe^{3+} (Chen et al. 2015). These include different fractions of particulate, colloidal and dissolved metal, existing as charged and neutral inorganic ions (for Fe^{2+}, it is primarily Fe^{2+}, $FeCl^{+}$, $FeSO_4$, $FeCO_3$ and $FeOH^{+}$; while for Fe^{3+}, different hydroxide species, such as $Fe(OH)^{2+}$, $Fe(OH)_2^{+}$ and $Fe(OH)_3$ are predominant with only partial contribution of Fe^{3+}) (Granado-Castro et al. 2018). Diverse organic complexes of Fe^{2+} and Fe^{3+} of different lability, as well as operationally defined fractions also exist in natural waters (Rivaro et al. 2012). Fe content can be as high as 1010 mg L^{-1} in water sources close to acid

mine drainage (AMD) (Tutu et al. 2008), posing a threat to human and aquatic life. It is therefore, essential to monitor iron concentrations in natural waters.

2.4.1.5 Nickel

Nickel (Ni) is the 22nd most abundant element in the earth crust and an important trace metal since it plays a role in the creation of red blood cells (Hussain et al. 2013). It is an essential microelement for normal plant growth and part of several biological functions. However, it is still not clear weather Ni is an essential or non- essential metal for humans (Zoroddu et al. 2019). It commonly exists in the 0 and +2 oxidation states and less often in the −1, +1, +3 and +4 oxidation states. The +4 oxidation state is more toxic and carcinogenic compared to the +2 state (Fashola et al. 2016). Ni concentrations can reach up to 26 g kg^{-1} and 0.2 mg L^{-1} in polluted soils and surface water respectively, which is 20–30 times higher than unpolluted areas (Cempel and Nikel 2006). This suggests that soil and water contamination with Ni has become a serious problem worldwide, requiring innovative solutions to be addressed (Shahzad et al. 2018).

2.1.5 Metal extractions: the past, present and future

Environmental pollution has been identified as the biggest threat to humans and global diversity with metals classified as priority environmental pollutants (Sikder et al. 2019). This is a crisis in aquatic systems since water scarcity is taking its toll. Everywhere in the world, water is a basic necessity, however 40% of the world population is facing water scarcity (Calzadilla et al. 2011). This means that the use of recycled water would be key for tackling not only the pollution, but also the shortage problem.

Over the past centuries, various methods have been developed to extract heavy metals from aqueous solutions. They include precipitation, ion exchange remedies, coagulation/flocculation, membrane filtration, electrochemical treatment, adsorption, photocatalysis, biological treatment, electrodialysis and oxidation (Khalid et al. 2017b; Hashim et al. 2011; Fu and Wang 2011). All these methods have advantages and disadvantages. Ion exchange has high transformation of components but removes only limited ions and operational costs are high (Farooq et al. 2010). Coagulation is cheap, has dewatering qualities, but involves the use of chemicals and results in the generation of large volumes of sludge. Filtration has a

very high metal removal efficiency, but is expensive due to membrane fouling (Ahmed and Ahmaruzzaman 2016).

Electrical treatment has low chemical usage for important heavy metal removal, although initial investment is high due to the need for an electrical supply (Ahmed and Ahmaruzzaman 2016). Adsorption is easy to operate, low cost and there is less sludge generation. However, there is a need for desorption (Ruihua et al. 2011). Photocatalysis can remove organic pollutants and heavy metals simultaneously, but takes longer to remove metal ions (Ihsanullah et al. 2016). Biological treatment is good for heavy metal removal but still needs further development (Ahmaruzzaman 2009). Electrodialysis provides good separation of metals without the need for electrical energy but has challenges such as clogging of the membrane, loss of energy, oxidation, and rusting (Nguyen et al. 2013; Patil et al. 2016).

As a result, these methods are usually used combined as no single method can yield metals of high quality. However, Song *et al.* have reported membrane techniques as superior due to high selectivity and low footprint (Song et al. 2018). This is because membrane transport is a non-equilibrium mass transfer process which is not limited by thermodynamic equilibrium conditions. Membrane strategies involve the permeation of solutes across the membrane surfaces from feed to receiving phase driven by the concentration gradient of target and other forces such as pH (Chen et al. 2018). Membranes such as the BLMs, ELMs, SLMs, HFSLMs, ESPLMs and PIMs have been explored for heavy metal extractions (Nghiem et al. 2006; Chen et al. 2018). Table 2 lists the advantages and disadvantages of these membranes.

Table 2 Membrane technologies for separations and purifications of metal ions in aqueous solutions

Technologies	Advantages and disadvantages	Reference
BLMs	Combines extraction with back-extraction, separates and pre-concentrates analytes but transport flux is hindered by low interfacial area-to-volume ratio.	(Granado-Castro et al. 2018; Nghiem et al. 2006; X. J. Yang et al. 2002)

ELMs	Utilised for both solvent and solid-phase extraction and has higher transport rates than BLMs but hindered by membrane leakage and emulsion swellings.	(Chen et al. 2018; Song et al. 2018)
SLMs	Highly selective and easier to operate than BLMs and ELMs but long-term stability a problem.	(Jean et al. 2018; Onac et al. 2019**)**
HFSLMs	Highly efficient transport and separation with high interfacial area per volume but has poor selectivity for rare earth elements and there is loss of extract from micropores of hollow fiber.	(Sribudda et al. 2015; Wongkaew et al. 2015)
ESPLMs	High production and preconcentration of target analytes but extra care is needed for the electrodes.	(Chen et al. 2018)
PIMs	PIMs have highest transport efficiency, improved flux, easy setup, high selectivity and durability, less usage of expensive carriers, preconcentrates analytes, can be used in passive samplers for over a month, but long-term stability compromised due to membrane fouling	(Almeida et al. 2017; Chen et al. 2018; Kim et al. 2001, 2000; Wang et al. 2000).

As observed from Table 2 above, it is evident that PIMs offer promising solutions for large scale extraction of heavy metals in aqueous solutions. This suggests that robust investigations must be conducted to solve the fouling that occurs in these polymer membranes.

2.2 Membrane Technology

2.2.1 Polymer inclusion membranes (PIMs)

PIMs is a relatively new branch of membrane separation technologies. PIMs have great potential in the safe and effective separation of metallic, non-metallic ions and small organic molecules from aqueous solutions (Nghiem et al. 2006). They mimic properties of traditional solvent extraction (SE) methods but in PIMs, extraction and back extraction occur simultaneously (Almeida et al. 2012). Furthermore, SE uses large inventories of often volatile and toxic diluents and large quantities of active extracts. Thus, it is most suitable for the recovery of metals from leachates obtained from high grade ores but less cost effective for the recovery of metals from solutions containing metals in low concentrations such as effluents and waste waters, making the use of PIMs a better alternative (Wang et al. 2017).

PIMs have the same properties as filtration membranes and consist of a base polymer, carrier (extract) and in some cases a plasticizer. The base polymer is responsible for the structure and mechanical support of the membrane (Bonggotgetsakul et al. 2015). Polyvinyl chloride (PVC) and cellulose triacetate (CTA) are the two most commonly used polymers in engineering applications because they can be dissolved in an organic solvent to prepare a thin film using a very simple procedure. CTA is slightly hydrated while PVC is generally not. PVC is mostly preferred in waste water treatment as it does not undergo hydrolysis in acidic environments. However, PVC undergoes dehydrochlorination in alkaline solutions while CTA is more stable under these conditions. The carrier is a complexing agent or ion exchanger responsible for binding target analytes and transporting them across the membrane. Carriers can be acidic and chelating, basic, neutral/solvating or macrocyclic depending on the type of target analytes and application (Almeida et al. 2012). Plasticizers are organic compounds containing a hydrophobic alkyl backbone with one or several highly solvating polar groups (Sellami et al. 2019). They are used to increase membrane softness, flexibility, permeability, and the compatibility of membrane components (Pereira et al. 2009). However, when carriers such as quaternary ammonium salts and phosphoric acid esters are used, a plasticizer is not required because these carriers also have plasticizer properties (Argiropoulos et al. 1998; Wang et al. 2000).



Figure 2 Polymer inclusion membrane (Kubota et al. 2019)

The PIM is formed by casting a solution of the base polymer, extract and if essential a plasticizer allowing the solvent to evaporate to form a thin, flexible and stable membrane illustrated in Figure 2. The PIM has the capability to selectively extract heavy metals and organic pollutants in aqueous solutions. These experiments are usually carried out in a system consisting of two compartments with mechanically stirred solutions and a membrane sandwiched between them (Figure 3). One of the compartments contains the source solution with a known initial concentration of the target solute, while the other contains the receiver solution with a suitable stripping reagent. The concentration of the target solute in each compartment is monitored over time. A change in concentration in each compartment allows the determination of the rate of extraction across the membrane. The main advantage of such a system is that, its selectivity towards heavy metals can be enhanced by using a suitable carrier in the form of a complexing compound or ion exchange for target analyte.

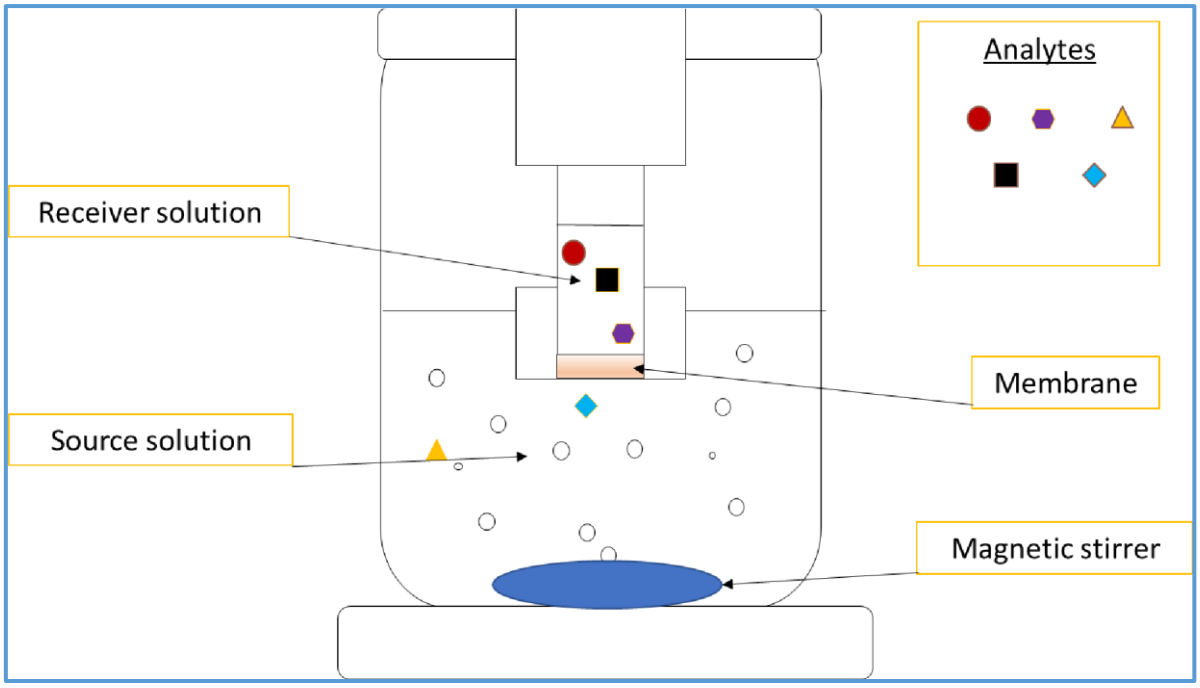

Figure 3 A typical lab-based PIM experimental setup

2.3 Membrane Characterisation

2.3.1 Morphology and structure

The microstructure of PIMs is one of the most important aspects in membrane extractions since it determines the distribution of carriers in the polymer matrix, which further affects the membrane transport efficiency. Different sophisticated and advanced techniques have been used to determine whether the morphology and structure of PIMs is homogenous, porous, and where pores are filled by the carrier. Most studies have reported PIMs as being homogenous, but this is based on naked eye observations or under an optical microscope. Some studies have tried to understand interactions of membrane components in order to understand their transport and extraction properties (Almeida et al. 2012).

Techniques that have been mostly used to study the morphology and structure of membranes alone or in conjunction with each other include scanning electron microscopy (SEM) or energy dispersive spectroscopy (SEM-EDS), atomic force microscopy (AFM), thermogravimetric

analysis (TGA), Fourier transform infrared spectroscopy (FTIR) and contact angle measurements. SEM is used to study the surface morphology and structure of PIM in order to provide information on the distribution of the carrier and plasticizer in the PIM (Almeida et al. 2012). SEM samples are usually dried and coated with a conductive material such as chromium, gold or carbon before analysis. Due to a relatively low resolution that makes it difficult to observe PIM features at nanometre scale or lower, AFM is often employed with SEM to improve resolution (Nghiem et al. 2006). TGA links the mass change at a specific temperature to the degradation of a particular compound (Kebiche-Senhadji et al. 2011), It is used to determine thermal stability of the membranes. FTIR is mostly used to understand the type of interactions between the PIM components (Saf et al. 2011) while the contact angle measurements are employed to study the hydrophilicity of membranes.

2.32 Permeability

The rate of transport through PIMs is one of the factors that has driven interest in polymer-based membranes. Most studies to date have reported on this important parameter since it is very important in characterising PIM transport performance (St John et al. 2013). In some cases, the permeate flux of SLMs is higher than that of PIMs (Nghiem et al. 2006). This is because the diffusion coefficient of SLMs is usually one or two times that of PIMs. Diffusion coefficient of PIMs can also be comparable (Fontàs et al. 2005; Scindia et al. 2005; Tayeb et al. 2005) or even higher than that of SLMs (Fontàs et al. 2005; Kim et al. 2001), giving PIMs an advantage.

For both SLMs and PIMs, transport is influenced by membrane morphology, membrane composition, solution chemistry of both source and receiving solution, as well as temperature. However, PIMs and SLMs have very different and surface morphologies. SLMs consist of a porous supporting layer impregnated with carrier and diluent and metal ions are transported through a network of fluid-filled micro channels (Almeida et al. 2012; Nghiem et al. 2006). This means that transport is subject to the tortuosity of this network and is limited by the available surface area. In contrast, PIMs do not have a micro channel network in which metal ion transport can take place. As a result, the whole membrane is available for transport (Nghiem et al. 2006).

The ability to alter the membrane thickness to enhance analyte permeability also makes PIMs attractive. Nghiem *et al.* have reported that thinner membranes improve analyte permeability through PIMs (Nghiem et al. 2006), though other authors believe that thicker membranes have a better permeability (Kolev et al. 2013). This gives PIMs an advantage to offer competitive analytes flux intakes since the thickness can altered to improve the flux. However, careful consideration of experimental conditions is required when reporting and comparing permeability of analytes in membranes due to variety of membrane components that can be used. Several researchers have explored how features such as membrane morphology, surface roughness, membrane composition and solution chemistry affect the permeability of analytes in membranes.

Results from these PIM studies indicate permeability can be strongly influenced by membrane morphology. In some cases, high concentration of carrier result in a crystalline thin film with distinctively separate layers. This morphology was found to be unfavourable for transport in PIMs which is associated with the observed poor target solute fluxes (Arous et al. 2004; Gherrou et al. 2005, 2004). Membrane surface roughness is also an important morphology parameter. When the rougher side of the membrane is exposed to the source solution, the analyte permeability improves (Wang et al. 2000). This is consistent with other studies were there was a positive correlation between permeability and the surface roughness of membranes (Kozlowski and Walkowiak 2005; Scindia et al. 2005).

An increase in PIM surface roughness can also be achieved by an addition of a plasticizer (Nghiem et al. 2006), implying that membrane surface roughness is related to membrane composition. Results from most PIM studies also indicate an influence of membrane composition on the permeability of analytes. Wang *et al.* have reported membrane composition as the most crucial factor for determining transport properties of the membrane (Wang et al. 2017). However, reported data remain scattered with variation in permeate flux as a result of any changes in membrane composition which depends on the characteristics of each membrane component involved. Generally, to achieve a reasonable permeability of target analyte, membrane composition (base polymer, carrier and plasticizer concentration) must be optimised as observed from most PIM studies (Cho et al. 2011; GarciaRodríguez et al. 2015; Wang et al. 2016).

Solution chemistry of both the source and the receiving solution also influences the permeate flux of analytes. This is because the driving force of a PIM system is the concentration gradient across the membrane. Kozlowski and Walkowiak (2005) studied the effect of source solution

pH on Cr^{4+} transport on a CTA based PIM. They observed that the permeate flux increased with a decrease in pH of the source. Levitskaia *et al.* reported that the driving form can also be influenced by mobility of coupled-transport ion within the organic phase of membrane (Levitskaia et al. 2000). Generally, the efficiency of the coupled transport ions increases in the opposite order of their hydrated radii as follows (Nghiem et al. 2006):

$$F^- < CI^- < Br^- < NO_3^- < SCN^- < I^- < IO_4^- < CIO_4^- \; picrate^-$$

This is demonstrated in a number of studies (under a similar concentration gradient) whereby better permeability of target metal ion is reported when lower hydrated ions were employed as the driving ion (Lacan et al. 1995; Lamb and Nazarenko 1997; Thunhorst et al. 1999).

In addition, the permeability of target analytes is also influenced by competition with other ions present in the aqueous phase. St John *et al.* reported that the presence of Fe^{3+} on the extraction rate of U^{6+} decreased (St John et al. 2012).

2.3.3 Selectivity

Selectivity is an important issue for implementations of PIMs for the following reasons:

(1) In environmental applications, metal ion concentration can be very low thus needing high selectivity for effective treatment.
(2) In hydrometallurgy, purity is a key factor in determining the commodity price of a given metal, especially those of high value (Sole et al. 2005).
(3) Impurities also affect downstream processing such as electrowinning where only a certain level of impurity can be tolerated (Ivanov 2004).

In solvent extractions (SE), selectivity of metals ions mainly depends on lipophilicity of metal complexes (Nghiem et al. 2006). This results in low selectivity and the requirement for several extraction steps. The advantage of performing several steps is, unfortunately, not available in membrane systems. Fortunately, Nghiem *et al.* had reported limited data

currently available to prove that membrane systems (PIMs and SLMs) are more selective than the conventional SE systems (Nghiem et al. 2006).

The high selectivity of membrane systems can be attributed to difference in extraction mechanisms when compared to SE. In membranes, the availability of the carrier is restricted while in SE it is possible to have an excess. Additionally, extraction and back extraction occur simultaneously in membranes which is not the case for SE systems. This suggests that it is wrong to classify mass transfer in membranes as analogues of SE. When it comes to using the limited data to compare the selectivity of PIMs and SLMs. PIMs have demonstrated a better selectivity under similar conditions (Nghiem et al. 2006). However, in a PIM-based metal ion extraction system, there is a dilemma on what to compromise between selectivity and stability, and due to the limited data on selectivity of analytes in PIM extraction systems, more studies must be conducted to understand this phenomenon and the parameters that either decrease or increase analyte selectivity.

2.3.4 Stability

The SLMs have had a limited commercial use due to far too low stability (de Gyves and Rodríguez de San Miguel 1999; Sastre et al. 1998). This became a major motivation for the development of PIMs. Generally, PIMs are more stable as compared to other membranes as demonstrated by reusability experiments where a membrane used for different source and the receiving solutions / experiments. Even though PIMs have a higher stability than SLMs, several studies have demonstrated that the initial flux of PIMs is usually lower than that of the SLMs (Ashok Kumar et al. 2010; Scindia et al. 2005; Tor et al. 2009). The low stability of SLMs is attributed to its structure since it has a capillary force responsible for binding membrane liquid phase to support pores. This force is weak which then result in membrane breakdown due to shear forces, emulsion formation and leaching of carrier to the aqueous phase (Danesi et al. 1987).

PIMs are formed by a carrier, a base polymer and a plasticizer that are well integrated to form a homogenous thin film. However, a few FTIR studies have demonstrated that there is no sign of covalent bonds between the PIM components (Saf et al. 2011; Arous et al. 2010b). This suggests that the PIM components are held together by secondary forces such as the Van der Waals forces, hydrogen bonds and hydrophobic bonds, which are stronger than capillary

forces (Almeida et al. 2012). Several stability comparisons have been done between SLMs and PIMs (Kim et al. 2000; Scindia et al. 2005; Tayeb et al. 2005), with evidence that the PIM is more stable than the SLM.

Although PIMs have a high resistance of plasticizer and carrier leakage under certain conditions, some studies have reported the loss of carrier in PIMs (Gherasim et al. 2011; Guo et al. 2012). Leaching has been reported to occur for hydrophilic carriers with octanol-water partitioning coefficient of less than 5 (Aguilar et al. 2001; Levitskaia et al. 2002). The leaching behaviour of carriers is also influenced by hydrophobicity and water solubility. Nghiem *et al.* have reported that the hydrophobicity of the carrier can be influenced by the chemistry of the aqueous phase (Nghiem et al. 2006). This is demonstrated by another study with evidence that the solution pH has influence on the solubility of the carrier and subsequently on the stability of the membranes using the carrier (Argiropoulos et al. 1998).

Despite many studies devoted to investigating the stability of membranes. There is no reported benchmark for the satisfactory membrane life time. Table 3 gives a summary of some PIM stability studies.

Table 3 PIM lifetime and performance under continuous conditions

Membrane composition (polymer/carrier/plasticizer)	Membrane lifetime and performance	Reference
CTA/D2EHAF	Excellent stability in 5 cycles with insignificant deterioration in performance (24 hrs each)	(Yoshida et al. 2019)
PVDF-HFP/Cyphos® IL 101/NPOE	PIM can be used for at least five extraction/back-extraction cycles without loss of its extraction capacity (24 hrs each)	(Yaftian et al. 2018)
PVDF-HFP/Cyphos® IL 104	Small decrease in extraction efficiency at 5th cycle attributed to 3% membrane loss in 1st cycle but little mass change from 2nd cycle (24 hrs each)	(Bonggotgetsakul et al. 2016)

PVC/D2EHPA	Small variation in performance over 5 cycles of extraction and back-extraction; however, the variation in performance was well within the range of the experimental error corresponding to the 95% confidence interval (8 hrs each)	(St John et al. 2012)
CTA/FFAT/NPOE	No loss of transport efficiency during the first 4 cycles (10 hrs each)	(Saf et al. 2011)
PVC/D2EHPA	Gradual decrease in flux for first 9 cycles then the membrane becomes inefficient for further use (12 hrs each)	(Gherasim et al. 2011)
CTA/Crown ethers/NPOE	Flux remained constant after 2 weeks	(Arous et al. 2010a)
BVDF/Bif-ILEs/Ils	Permeability was decreased to 76% after 5 cycles	(Guo et al. 2012)
CTA/DNNDS/NPOE	PIM was reused for 2 months without a change in its performance	(Ocampo et al. 2009)

(Full names of membranes components in list of abbreviations)

Data from Table 3 shows the complexity of controlling the stability of PIMs. This suggest that further investigations are required in order to properly understand the critical parameters that influence the stability of PIMs.

2.3.5 Role of nanoparticles in nanocomposite PIMs

Nanocomposite membranes (polymer membranes blended with nanoparticles; illustrated in Figure 4) have become an area of interest due to their simple fabrication (Al Aani et al. 2017). Nanoparticles have a large surface-to-volume ratio, unique functionalities and potential for improving the antifouling of membrane by tuning membrane physicochemical properties such as surface roughness, porosity, hydrophilicity, and mechanical properties (Yin and Deng 2015). Incorporating hydrophilic nanoparticles into hydrophobic membranes makes membranes hydrophilic, providing resistance against hydrophobic fouling agents (Johary et al. 2018; Kumar and Lawler 2014; Safarpour et al. 2015).

Metallic, metal oxides and carbon based nanoparticles have been incorporated in membranes to introduce antifouling ability and hydrophilicity (Khalid et al. 2017a). Silver nanoparticles are the most widely explored antimicrobial agent in nanocomposite membranes due to excellent biocidal properties in different applications (Yin and Deng 2015). The synthesized silver nanocomposite membranes have resulted in improved selectivity, good chemical and mechanical stability, good conductivity and the introduction of catalytic and antifouling properties (Figueiredo et al. 2015; Koseoglu-Imer et al. 2013). Even though the silver nanocomposite membranes are common, the mode of action of silver nanoparticles on microorganisms is not well understood (Kim et al. 2007).

Other nanoparticles such as copper, cobalt selenium, iron, silica, titanium, nickel and zirconia based have been explored (Akar et al. 2013; Bassyouni et al. 2019; Dasari et al. 2012; Nasir et al. 2019).

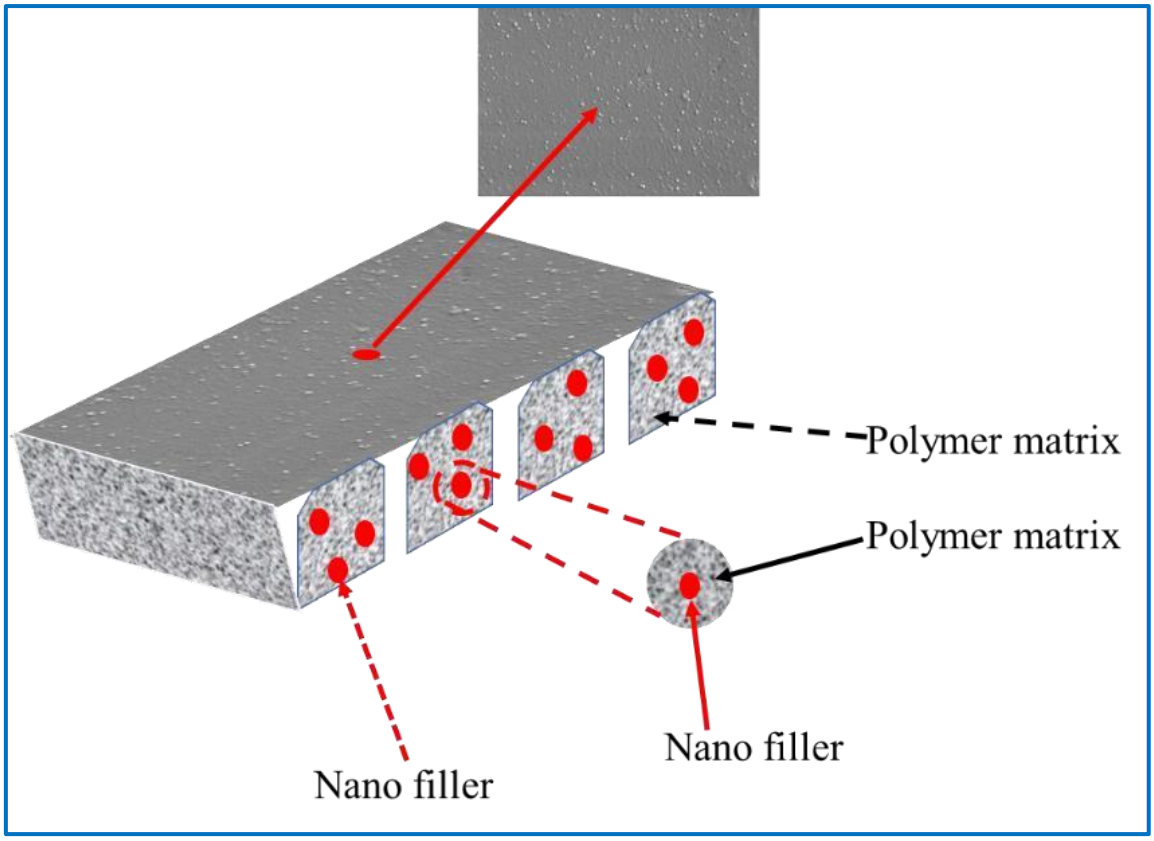

Figure 4 Schematic diagram of a nanocomposite PIM structure

2.4 Transport Mechanism

2.4.1 Transport mechanism in PIMs

The overall transport in PIMs consists of two processes namely.

(1) Transfer of target analytes across the source phase and at the receiving phase.
(2) Diffusion of analytes through the membrane.

In the first step, the target analyte at the source solution/PIM interface reacts with the selective carrier in PIM to form a complex. The analyte is then replaced by another molecule of the carrier. For extraction of cations by acidic and chelating carrier, there is an exchange of metal ion for a proton of carrier. Consequently, counter-transport of protons is the driving force achieved by maintaining a pH difference between source and receiving solution. The target analyte that formed a complex with the carrier then diffuses through the PIM towards the receiving phase. Lastly, at the PIM/receiving solution interface. Target analyte is released into the receiving solution, which is the reverse of what is happening at the source solution. Figure 5 illustrates the overall process, and it has been previously named facilitated transport (Nghiem et al. 2006).

This mechanism is advantageous since the transport of target analyte across the PIM continues even when the total analyte concentration in the receiving solution is higher than the one in the source phase (Almeida et al. 2014).

The above mechanism for bivalent metal ions in complexation with an acidic chelating carrier such as di-(2-ethylhexyl) phosphoric acid (D2EHPA) is reported as follows.

$$M_{(2aq+)} + n(RH)_{2(org)} \rightleftharpoons MR_2(RH)_{2n-2(org)} + 2H_{(+aq)}$$

where *M* is the metal ions, *RH* is D2EHPA molecule, *n* is the stoichiometric coefficient, and *aq* and *org* are the aqueous and the organic phase of the membrane respectively (Gega and Otrembska 2014).

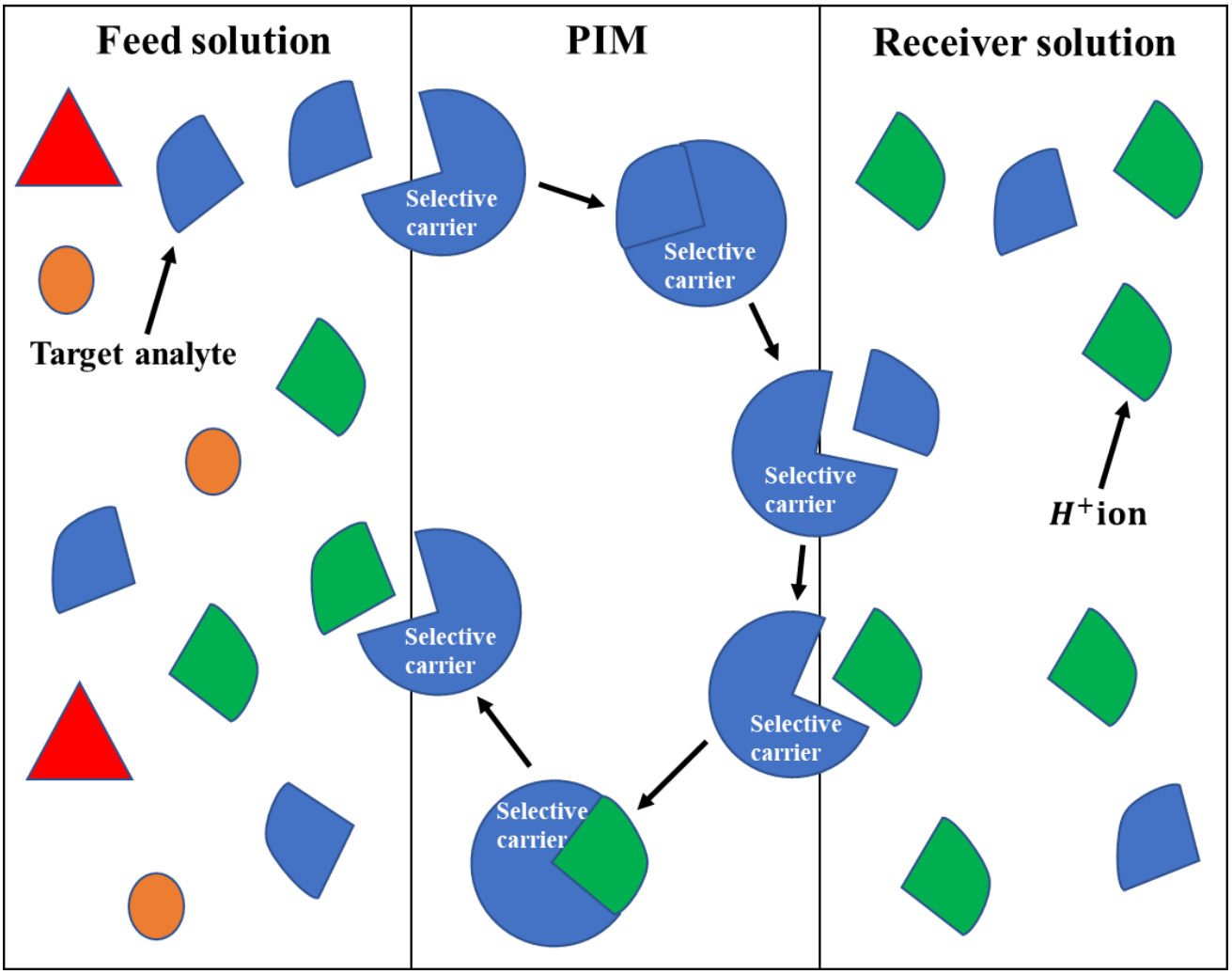

Figure 5 Schematic of the facilitated transport of target analyte across a PIM

During transport, the partition coefficient (*Kp*) of the target analyte/carrier complex between the organic phase of the membrane and the aqueous solution, $K_p{}^s$ (superscript s representing the source solution), must be as high as possible to favour the extraction process. In contrast, the partition coefficient of the receiving solution ($K_p{}^r$) must be sufficiently low to favour back extraction of the target solute from the membrane phase. Within the membrane phase, there is a concentration gradient of the target analyte/carrier complex or ion pair acting as a driving force for its transport across the membrane. This suggests that uphill transport only takes place with respect to the total analyte concentration in the source solution, while in the membrane phase it is downhill transport of chemical species diffusing across the membrane. In practice, such a difference in *Kp* between the source and receiving solutions can be maintained with a suitable chemical composition of these solutions thus increasing transport efficiency.

2.4.2 Critical parameters in transport of analytes

Transport of analytes in PIMs is a complex process that is affected by many parameters. These include membrane composition, pH of solutions, concentration of both source and receiving solutions, membrane thickness, stirring rate, solution chemistry and extraction time. These parameters should be optimised to achieve satisfactory extraction rates, improved membrane lifetime and good analyte selectivity in a variety of matrixes.

When the PIM is applied in environmental waters as passive sampler, external factors such as water flow pattern and temperature should also be considered when reporting the detected analytes.

2.5 Sampling

2.5.1 Principle of passive sampling

Sampling is an important step in any analytical quantification procedure since errors at this stage cannot be corrected. Spot sampling (collection of discreet water samples) was the main sampling technique that has been used to evaluate metal ions in aqueous environments. However, this sampling technique resulted in 70-90% of analysis time being spent on sampling and preparation; tedious work that caused more errors in the analysed sample (Górecki and Namieśnik 2002). This meant that there was a need for an alternative sampling technique.

Passive samplers allow for pollutants of interest to be collected on site, over an extended period (Almeida et al. 2016). These devices were introduced for the first time in 1972 for the semi-quantitative determination of CO (g) (Gordon and Lowe 1927) and in 1973 a full quantitative passive sampler was developed (Palmes and Gunnison 1973). Since then, thousands of papers devoted to the development of passive samplers have been published.

These samplers can sample organic and inorganic pollutants in air, soil and water and have been recommended by the European Commission Water Framework Directive (WFD) to

improve confidence in water monitoring data since they have advantages over spot or grab sampling (Miège et al. 2015).

The advantages include the improved limit of quantification by accumulation and concentration of analytes due to long term deployments that allows for the calculations of time weighted average (TWA) concentrations that are almost impossible to calculate in spot sampling (Miège et al. 2015). There is easy deployment, no power requirements for operation and the samplers are cost effective since they can be re-used (Criquet et al. 2017). It is also a solvent-less method thus a green technique (Górecki and Namieśnik 2002).

Over the last 30 years, different passive sampling devices have been developed (Vrana et al. 2005). They include the polar organic chemical integrative samplers (POCISs), semi-permeable membrane devices (SPMDs), Chemcatcher and diffusion gradient in thin-films (DGT) (Harman et al. 2012; Esteve-Turrillas et al. 2008; Ahkola et al. 2013; Davison and Zhang 2012). Each device is developed for a specific type of analyte and almost all of these passive samplers consist of a barrier and a sorbent, with their material and geometry chosen for a specific kind of analytes and the matrix. The barrier can be a static layer or a polymer membrane for diffusion and permeation type of samplers respectively. In the barrier convective transport is avoided and transport of analytes occurs due to molecular diffusion or permeation following Fick's laws (Seethapathy et al. 2008). When a passive sampler is exposed to a source solution, uptake of analytes occurs (Figure 6). Depending on the barrier type, sampler geometry, as well as sampling time, a passive sampler can function in the linear region, equilibrium region, or the curvilinear region.
However, for a passive sampler to function effectively two conditions must be met;

(1) The amount of analyte collected by the sampler per unit time at constant concentration in the surrounding medium must remain constant throughout the sampling session (Górecki and Namieśnik 2002);
(2) The receiving solution must act as a so-called ''zero sink'', which means that it should not let the trapped molecules be released back to the source even if the concentration of the analyte around the sampler decreases to zero (Seethapathy et al. 2008).

This suggests that careful consideration of a barrier type and the receiver solution is important for the use of passive samplers in the monitoring of analytes in water samples.

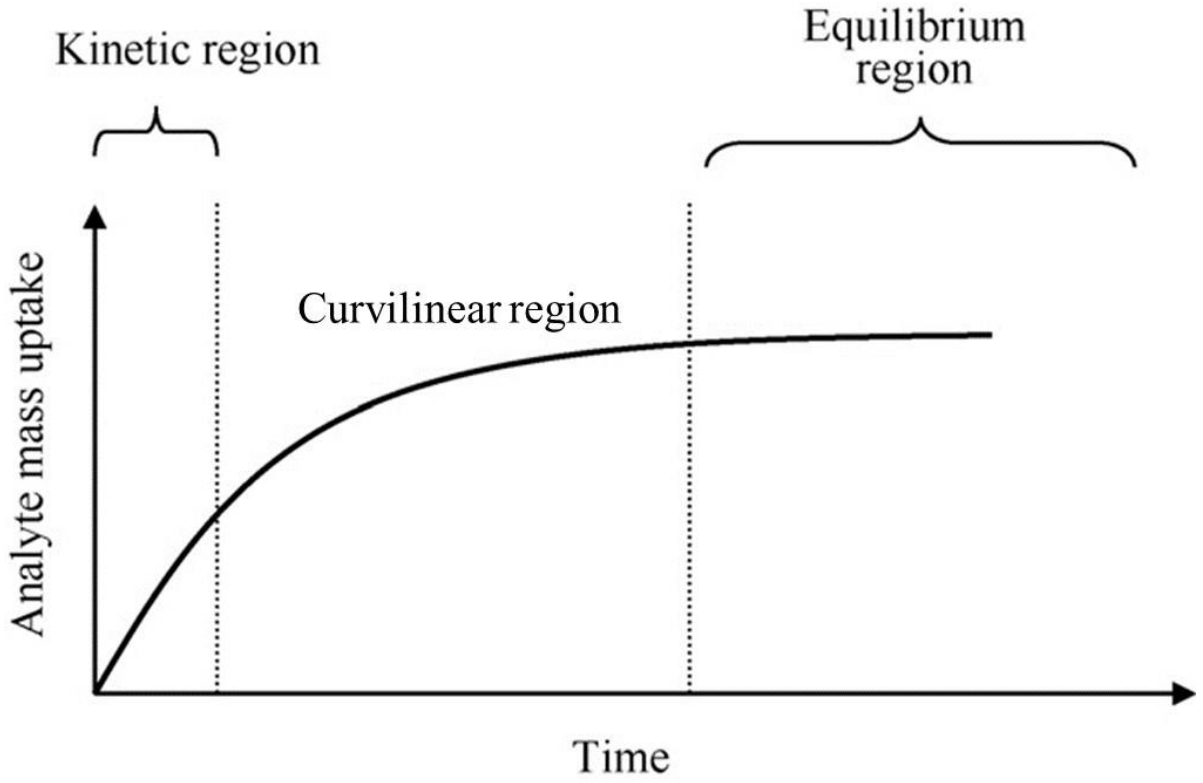

Figure 6 Analyte uptake profile of passive sampling devices [Modified from (Seethapathy et al. 2008)]

Despite several advantages that passive samplers possess over spot sampling, environmental conditions affect the accuracy of data obtained in passive sampling. This is because passive sampling theory is based on Fick's laws with assumptions of steady state conditions. In reality this does not hold since analyte uptake varies depending of factors which influence permeation or diffusion of analytes such as temperature, velocity in aqueous environments and concentration. In addition, the presence of particulates or biological matter in the source matrix can cause fouling of the barrier in the case of membranes. Thus, for environmental applications, passive sampling needs to be validated with spot sampling methods conducted in parallel (Seethapathy et al. 2008), and passive samplers need to be calibrated in a laboratory before deployment (Almeida et al. 2017).

Recently, PIM-based passive samplers have been applied in environmental waters to determine the TWA of zinc, sulfamethoxazole (SMX) and ammonia as summarized in Table 4. These samplers were first calibrated under laboratory conditions before environmental application. A good correlation between spot and passive sampling was obtained. The SMX passive sampler did not only monitor the analyte, the effect of flow pattern in the aquatic system was also investigated and appropriate measures taken to minimize this effect.

Table 4 Environmental applications of a PIM-based passive samplers. Membrane compositions are presented as mass percentages (w.t%)

Target analyte	PIM composition	Application	Sampling period	References
Zn^{2+}	60% PVC 40% D2EHPA	Urban-pond water	7 days	(Almeida et al. 2014)
SMX	30% CTA 26% Aliquat 336 44% NPOE	Natural water	100 hrs	(Garcia-Rodríguez et al. 2016)
Ammonia	55% PVC 35% DNNS 10% Tetradecanol	Creek	7 days	(Almeida et al. 2016)

CHAPTER 3

The main aim and objectives of this research are outlined in this chapter. The motivation and novelty of this work are also discussed.

3 AIMS AND OBJECTIVES

3.1 Aim

The aim of this research was to investigate the extraction of trace heavy metals in natural waters using silver nanocomposite polymer inclusion membranes (PIMs).

3.2 Objectives

i. To synthesize and characterize silver nanocomposite PIMs;

ii. To select an optimal composition of the nanocomposite PIM for simultaneous extraction of (Co, Ni, Cu, and Cd) in natural waters;

iii. To optimise extraction conditions such as pH (2-7), type of receiver solution (H_2SO_4, HCl and HNO_3), concentration of receiver solution (0.25-1.25 M) and the effect of the source solution concentration (0.50 – 2.50 mg L^{-1});

iv. To evaluate the extraction efficiency, permeability, selectivity and the stability of the nanocomposite PIM;

v. To study the effect of extraction time on transport efficiency and apply the nanocomposite PIM in environmental samples.

3.3 Justification

Membrane stability has been a stumbling block for the commercialisation of PIMs. This is due to biofouling that occurs on membrane surfaces and leaching of the carrier into the aqueous solutions. Even though a few investigations on synthesis and characterisation of nanocomposite membranes have previously been conducted and resulted in an improved stability (Johary et al. 2018; Khalid et al. 2017a), studies on transport of trace heavy metals ions using metal nanocomposite PIMs have not been reported in the literature (Chen et al. 2018). This research investigated the use of nanocomposite PIMs on transport of trace metal ions in environmental water samples. These nanoparticle-containing PIMs could be promising for the future large-scale industrial applications of PIMs.

CHAPTER 4

This chapter focuses on all materials and instrumentation used in this study. This extends to all synthesis and procedures undertaken to achieve the main aim and objectives.

4 RESEARCH METHODOLOGY

4.1 Chemicals and Reagents

All chemicals used in this study were purchased as analytically pure reagents, and no further purifications were done unless as otherwise stated. Polyvinyl chloride (PVC), di-(2-ethylhexyl) phosphoric acid (D2EHPA), tetrahydrofuran (THF), nitric acid (HNO_3), sulphuric acid (H_2SO_4), hydrochloric acid (HCl), sodium hydroxide (NaOH), cobalt nitrate hexahydrate ($Co(NO_3)_2{\cdot}6H_2O$), nickel nitrate hexahydrate ($Ni(NO_3)_2\cdot6H_2O$), iron nitrate $Fe(NO_3)_2$, copper nitrate trihydrate ($Cu(NO_3)_2{\cdot}3H_2O$), cadmium nitrate tetrahydrate ($Cd(NO_3)_2{\cdot}4H_2O$), Silver nitrate ($AgNO_3$, 99%) and trisodium citrate ($C_6H_5Na_3O_7.\,2H_2O$, 99.9%) were purchased from Sigma-Aldrich (Johannesburg, South Africa). Glycerol [$C_3H_5(OH)_3$] was purchased from Associated chemical enterprises (PTY) LTD, South Africa. Metal stock solutions were prepared by dispersing a suitable mass of the metal salt in deionized water (18.2 MΩ cm). The pH of the solutions was adjusted using 1.0 mol L^{-1} HNO_3 and/or 1.0 mol L^{-1} NaOH solutions.

4.2 Instrumentation

The absorption spectra were acquired using the UV-Vis spectrophotometer supplied by Analytikjena (Specord 210/plus, Germany). Transmission electron microscopy (TEM) images were obtained from Tecnai-12 JEM 12kV (ThermoFisher Scientific, USA). All metal ions measurements were performed on a Spectro Genesis inductively coupled plasma mass spectrometry ICP-MS (Agilent 7700 Series, USA) for low concentrations and ICP-OES (Spectro Genesis Spectro Analytical Instruments GmbH) for more concentrated metals (Kleve, Germany). Solution pH measurements were performed on a Five easy FE20 pH meter (Mettler Toledo,Johannesburg, South Africa). The anion concentrations were determined using a Metrohm ECO IC (Herisau, Switzerland). Deionized water was obtained from a Millipore water system (Massachusetts, USA). For all mass measurements, an analytical balance with up to 4 decimal places and 220 g capacity supplied by OHAUS (Johannesburg, South Africa) was used. The morphology, structural configuration and roughness of the synthesized membranes were studied using a scanning electron microscope (SEM) (Joel IT300, Tokyo, Japan). The

membrane thickness was measured by electronic outside micro meter 0-25 mm, 0.001 mm shut geometrical metrology (Trossingen, Germany). Water contact angle was measured using a Kruss Drop Shape Analyzer, DSA30 (KRUSS GmbH, Germany). Membrane casting machine Elcometer 3570 micrometric film applicator (Manchester, UK) was used to cast the membrane to the desired thickness.

4.3 Synthesis of Silver Nanoparticles

Silver nanoparticles (Ag NPs) were synthesized using a modified Lee and Meisel method (Lee and Meisel 2002). In a typical procedure, 10 mg of $AgNO_3$ was dissolved in 40% glycerol-water solution. The solution was then heated to a boiling temperature; about 97°C. To a boiling solution 0.3 ml of 3% trisodium citrate solution was added. The mixture was then stirred vigorously while heating. A change in colour of the mixture from colourless to pale yellow after 5 minutes was an indication of the formation of Ag NPs. It is also important to note that the volumetric flask from which Ag NPs where synthesized in, was wrapped with aluminium foil to avoid the interaction of light with NPs.

4.4 Synthesis of nanocomposite PIMs

For each experiment a batch of fresh membranes was prepared. Unless otherwise stated, the total mass of all membrane components is 1000 mg. To prepare a batch, an appropriate mass of PVC was dissolved in 15 mL THF in a 100 mL beaker using a magnetic stirrer. The appropriate amounts of D2EHPA and nanoparticles solutions were then added to a PVC-THF solution and stirred for 3 hours to form a homogenous casting solution. The casting solution was then spread evenly on a levelled glass surface using a membrane casting machine for uniform PIM formation. The glass was then covered, whereby THF was left to evaporate over a 24 hours period at room temperature to form a flexible and mechanically strong nanocomposite PIM. The average thickness of the PIMs was determined as 50 ± 5 μm. Figure 7 gives a schematic representation for the PIMs preparation. All the synthesized nanoparticles are presented in Table 5 and Section 5.3.1.

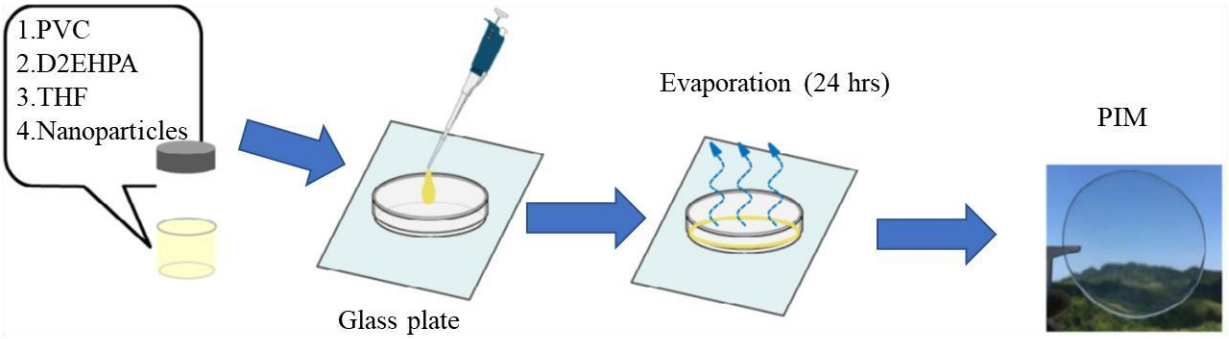

Figure 7 Schematic procedure for the preparation of a nanocomposite PIM [Modified from (Kubota et al. 2019)]

Table 5 Compositions of the PIMs containing 40 w.t% carrier and their resulting flexibility

PVC (w.t %)	D2EHPA (w.t%)	Ag NPs (w.t%)	Flexibility
60	40	0	Flexible
55	40	5	Flexible
50	40	10	Flexible
45	40	15	Flexible

4.5 Water Uptake

Evaluation of water adsorption by the PIMs was done by immersing circular pieces of membranes with a diameter of 25 mm in water for 24 hrs. PIMs were then carefully removed, wiped with paper towel to remove excess water, then weighed accurately. After that, PIMs were vacuum dried overnight at 60℃ and weighed again. Water uptake was calculated as follows (M.S et al. 2017):

$$U\ (\%) = \frac{W_{wet} - W_{dry}}{W_{dry}} \times 100 \qquad (1)$$

where W_{wet} is the weight of the wet membrane and W_{dry} is the weight of the dry membrane (g). Three values were recorded, and the average was reported in Figure 13b.

4.6 Contact Angle Measurements

Contact angle measurements were performed by dropping 1 μL of deionised water on the membrane surface at a rate of 1 μL s^{-1}. For each membrane composition, at least 10 measurements were taken on dry membranes. Obtained angles were averaged and to obtain reliable values, they were measured at different locations with highest and lowest values eliminated.

4.7 Transport Experiments

Batch transport experiments were carried out in a system consisting of a two-compartment unit (Figure 8a). A PIM segment was sandwiched between the two surfaces of the two compartments, so that it separated the feed and receiving solutions located in the corresponding compartments of the transport cell. The PIM set up was designed and constructed in our laboratory (Figure 8b). The source solution consisted of 3500 mL of water containing the target metals as solutes, while the receiver solution consisted of 8 mL the of acid solution. The diameter of the circular membrane surface area exposed to the solution on each side of the membrane was 20.0 mm (effective surface area $A = 3.14 \times 10^{-4}\ m^2$). A magnetic stirrer, operating at 100 rpm, was used to drive the stirring magnet (70 mm in length, 30 mm in diameter) in the source solution. The temperature of the solutions in the two compartments was maintained at room temperature. Samples (8 mL) of the source and receiving solutions were taken at regular time intervals, and their metal composition was analysed by ICP-OES/MS. A synthetic metal solution consisting of (Co^{2+}, Ni^{2+}, Cu^{2+} and Cd^{2+}) was used as the feed solution. The permeation cell unit was manufactured using Polytetrafluoroethylene (PTFE). This transport experiments were used to evaluate the permeation, selectivity, stability, and the extraction capacity of silver nanocomposite PIMs. These were evaluated in terms of its initial flux (*J*), defined by Equation 2, recovery factor (RF) [Equation 3] and transport efficiency (Equation 4).

$$J = \left(\frac{V}{A}\right)\left(\frac{\Delta[M^{2+}]}{\Delta t}\right) \qquad (2)$$

Where $V = 3.50 \times 10^{-3}$ m^3 is the feed solution volume, $A = 3.14 \times 10^{-4}$ m^2 is the membrane area exposed to feed solution, $\Delta[M^{2+}]$ is the change in the metal ion concentration in receiver solution (mol m^{-3}), and t = 86400 s.

$$RF = \frac{C_i - C_f}{C_i} 100 \quad (3)$$

where C_i is the initial molar concentration of the cation in the feed solution prior to PIM extraction and C_f is the final molar concentration of the cation in the feed solution at the end of the PIM extraction experiment.

$$(\%)TE = \left(\frac{V_r}{V_s}\right)\left(\frac{[M^{2+}]_r}{[M^{2+}]_s}\right) \times 100 \quad (4)$$

where $[M^{2+}]r$ denotes the metal ion concentration in the receiving phase at time *t*, $[M^{2+}]s$ is the initial metal ions concentration in the water sample and *Vr* and *Vs* are the volume of receiving and source solution, respectively.

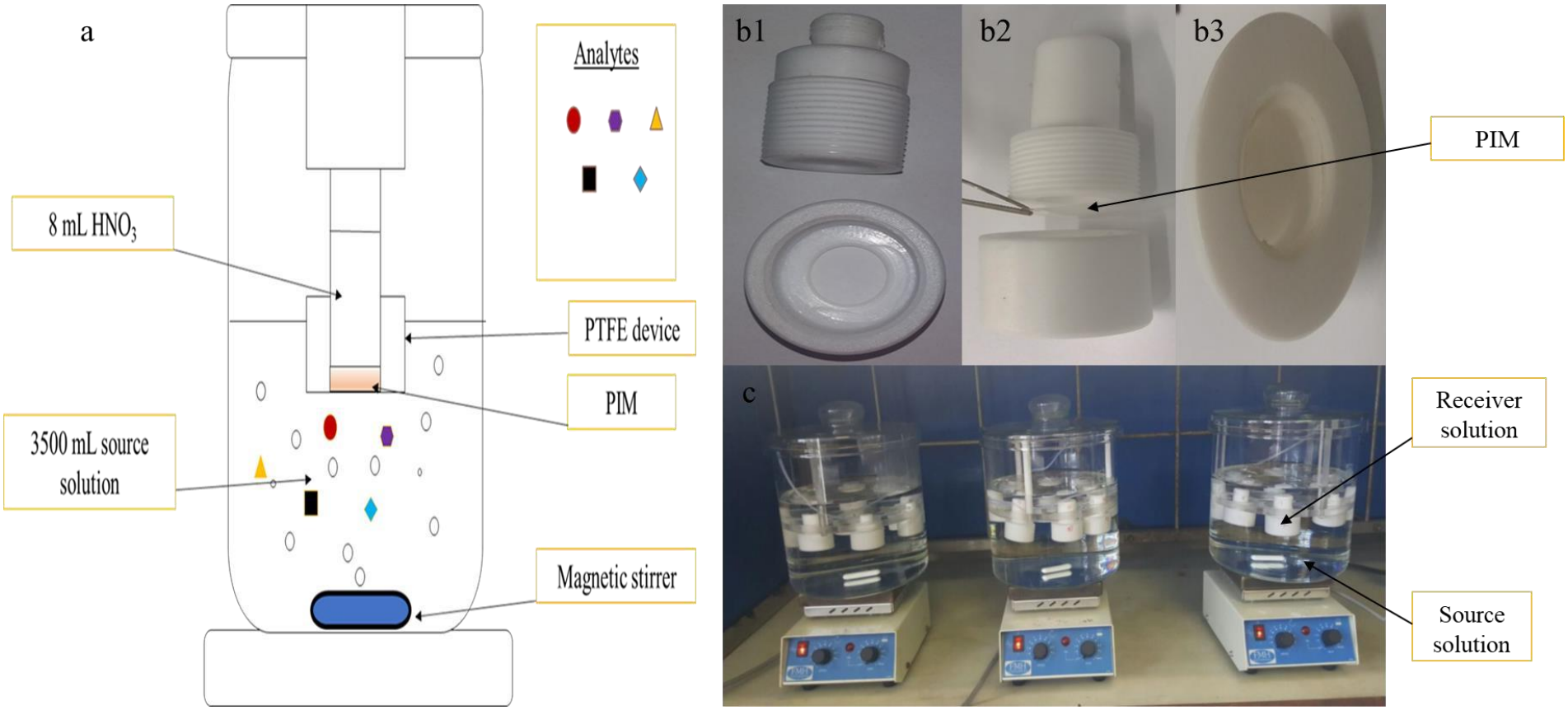

Figure 8 (a) Scheme of the PIM-device system used for analytes preconcentration and transport experiment, (b1) receiver solution chamber and a screw with opening window, (b2) unassembled PIM passive sampler, (b3) assembled PIM sampler with area to be exposed to source solution, (c) PIM passive sampler deployed in the laboratory

4.8 Sampling procedure

Clear polyethylene bottles were used for sample collection. The bottles were cleaned with detergent, rinsed with tap water followed by deionized water before soaking in 10% nitric acid. The nitric acid bath was used to remove any metals that could be adsorbed onto the containers. On the day of sampling (March 2019), the containers were thoroughly rinsed with deionized water and at each sampling site, they were further rinsed with tap and dam water, respectively, before collecting the sample.

CHAPTER 5

In this chapter, the membrane and nanoparticles characterisation results are presented. The PIM is then optimised for effective metal extractions.

5 RESULTS AND DISCUSSION

5.1 Characterisation of Silver Nanoparticles

The UV-Vis absorption spectra (Figure 9) shows the surface plasma resonance (SPR) absorption bands of citrate capped Ag NPs. The spectra showed the SPR band at 414 nm, which indicate the presence of spherical or spherical-like Ag NPs. Similar observations have been reported by a number of studies (Alula et al. 2018; Frost et al. 2017; Ma et al. 2016).

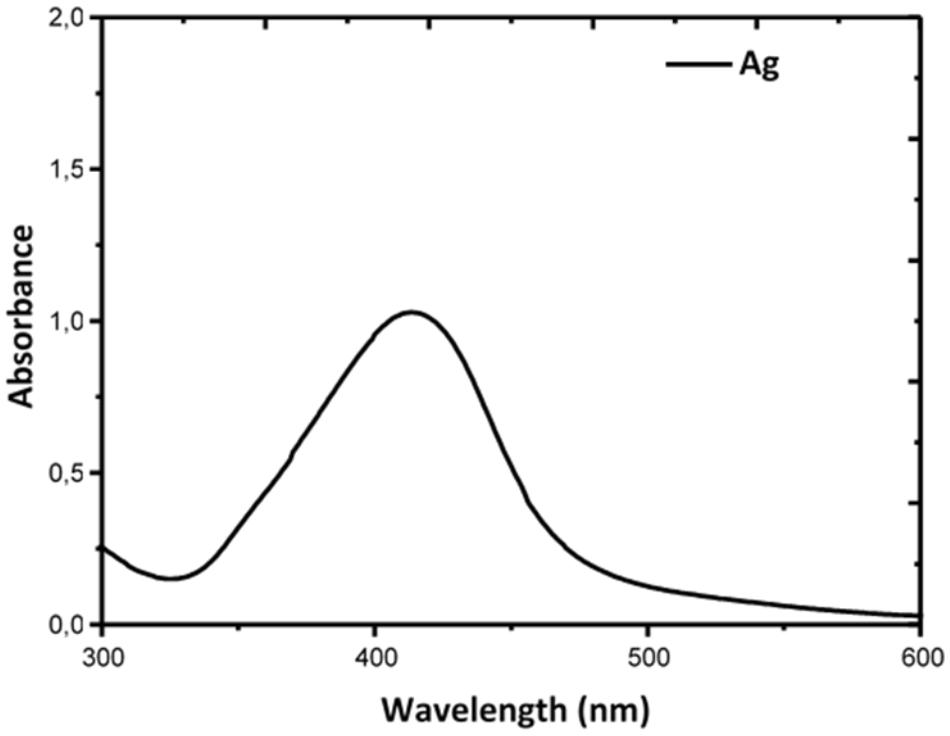

Figure 9 UV-Vis spectra of Ag NPs

Transmission electron microscopy (TEM) was used to determine the average particle size distribution of the nanoparticles. Figure 10 (a, b) presents the TEM micrographs that show monodispersed Ag NPs with spherical-like morphology, the sizes of the Ag NPs are ranged between 18 and 30 nm; the average diameter was about 25 nm. Since the citrate capped Ag NPs in colloidal solution characteristically possess anions adsorbed to the surface, the negative charges on the surface influenced the repulsive force between the particles and further promoted

dispersion in solution as observed on the TEM image. This results are similar to previous studies although Ramanathan *et al.* used a different synthetic approach (Alula et al. 2018; Ramanathan et al. 2018).

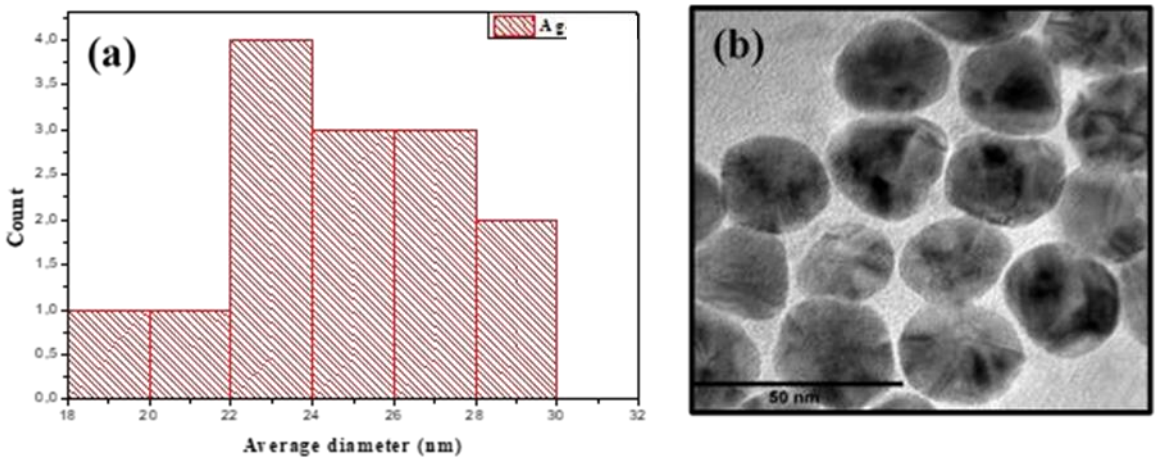

Figure 10 Particle size distribution of Ag NPs (a) and TEM image (b)

5.2 Characterisation of the Silver nanocomposite PIMs

The surface morphology of the PIMs was analysed with SEM at different magnifications (high and low respectively), as shown in Figure 11. It is observable that the bare PIM and the nanocomposite PIMs with up to 10 w.t% Ag NPs were smooth and homogenous without obvious agglomeration of nanoparticles on PIM surface. This indicates a uniform distribution of Ag NPs on the nanocomposite PIMs. They were no signs of obvious cracks or imperfections on membrane surface which confirm that the incorporation of Ag NPs on PIM did not negatively affect the membrane stability. In contrast, the nanocomposite PIM prepared with 15 w.t % Ag NPs loadings [Figure 11 (d, h)] exhibited noticeable cracks (highlighted by the yellow box) on the membrane surface in comparison to the other nanocomposite PIMs. These cracks are detrimental to membrane stability and can affect the membrane trace metal ion transport capacity.

In order to determine if the Ag NPs were incorporated into the PVC membranes, energy dispersive X-ray analysis (EDX) was done. There was no evidence of Ag element in the bare

PIM (Figure 12a). However, the nanocomposite PIMs showed the presence of Ag NPs as confirmed by the peak at around 3 keV [Figure 12 (b-d)], similar observations have been reported previously (Marulasiddeshwara et al. 2017; Panzarini et al. 2017; Patil et al. 2018; Rasheed et al. 2018) and the present study results are in good agreement with these.

This confirms the incorporation of Ag element into the PIMs. Hence, it can be concluded that the silver nanocomposite PIMs were successfully synthesized.

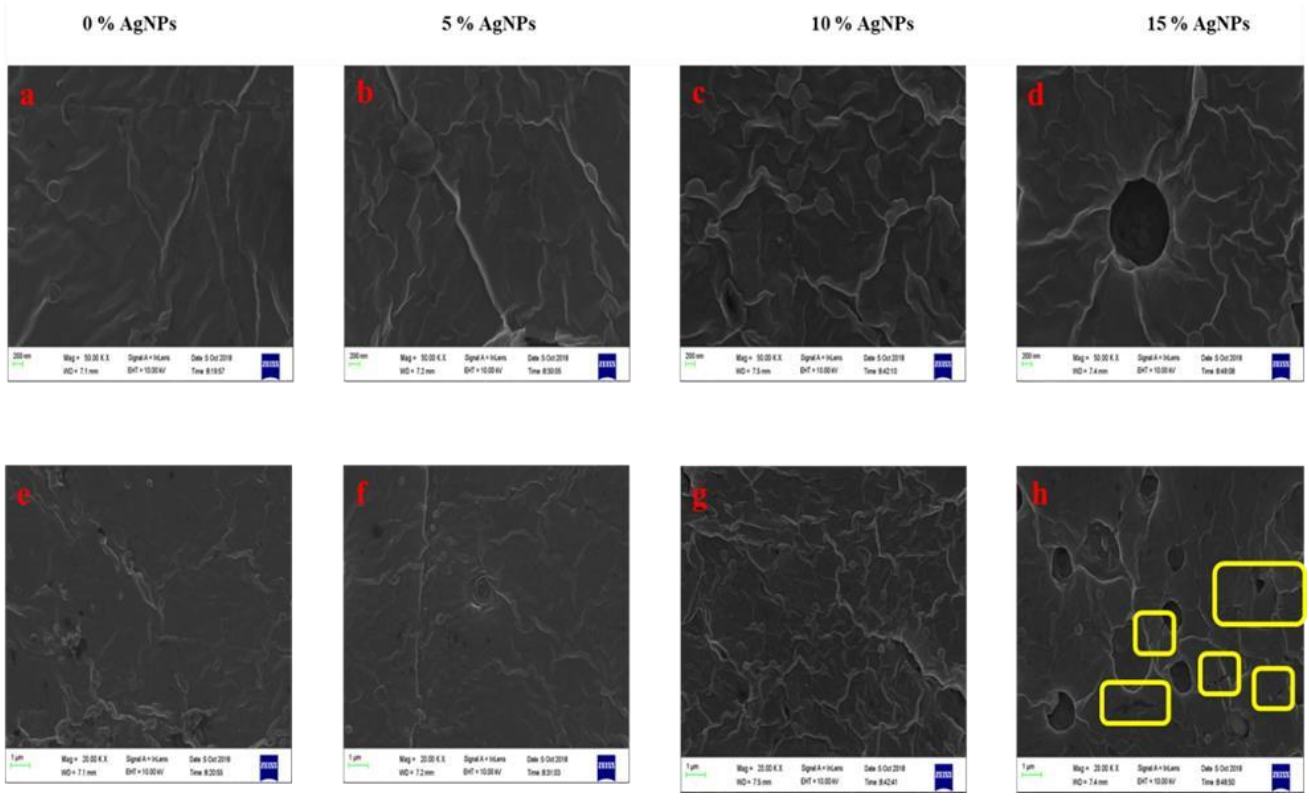

Figure 11 Surface morphology of the PVC/Ag NPs nanocomposite membranes at (a–d) a lower magnification (200 µm) and (e–h) a higher magnification (1 µm) with a corresponding Ag NPs loadings of 0, 5, 10 and 15 w.t% in the casting solutions

To determine the hydrophilicity of the PIM at different compositions, water uptake experiments and the contact angle experiments were conducted.

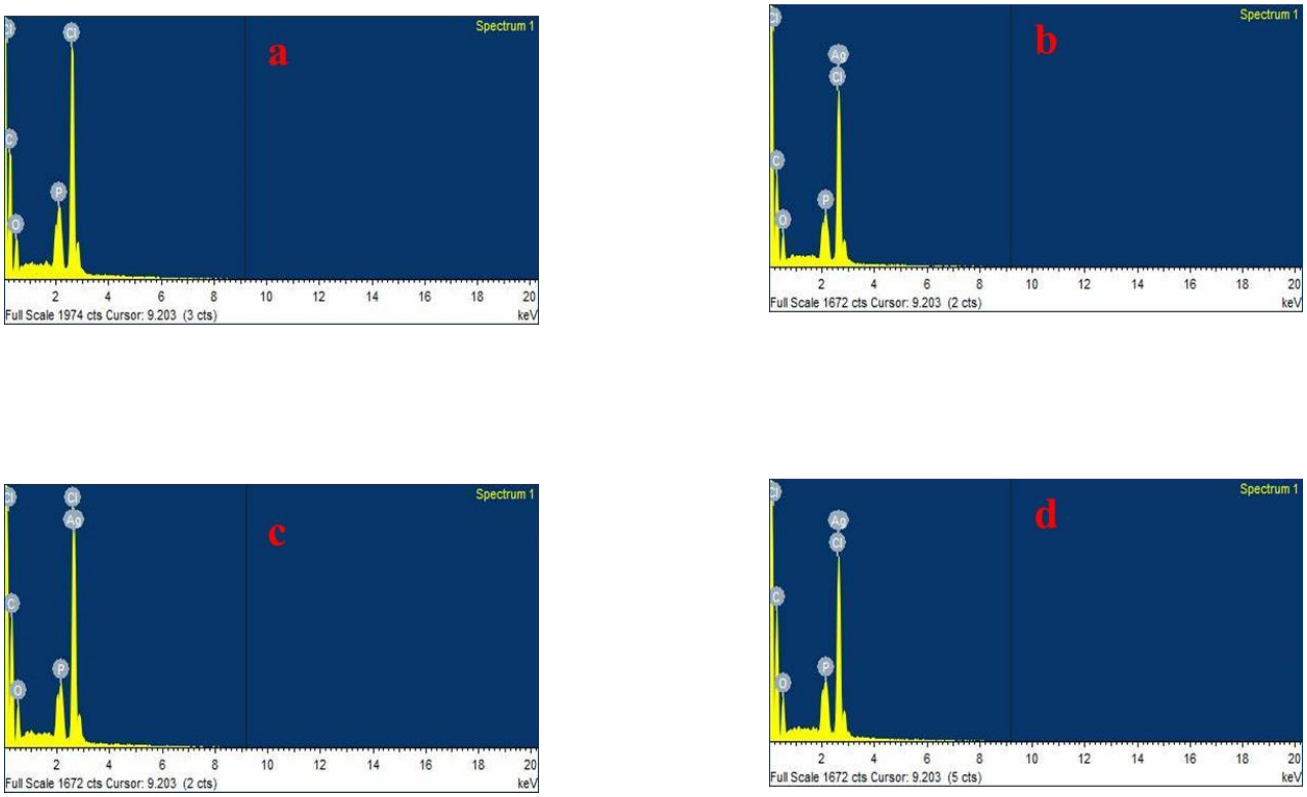

Figure 12 EDX spectra of the PVC/Ag NPs nanocomposite membranes with 0 w.t% (a), 5 w.t% (b), 10 w.t% (c) and 15 w.t% (d) loadings of the Ag NPs

From the water contact angle measurements, it was observed that Ag NPs have an influence in the hydrophilicity of the PIMs. As shown in Figure 13a, the water contact angle decreased with an increase in w.t% Ag NPs that is incorporated into the membrane surface; lower contact angle means strongest hydrophilicity. Pure membranes had a water contact angle of 89° and this was reduced to 67° on membranes with 15 w.t% Ag NPs. Increasing Ag NPs on a PVC based PIM therefore resulted in a decrease in water contact angle values and improved hydrophilicity. These results are in agreement with those obtained by another study (Khalid et al. 2017a). However, the water contact angle remained the same for 5 w.t% and the 10 w.t % Ag-PVC nanocomposite PIMs, this is confirmed by the contact angle of 70° for both PIMs. Vatanpour *et al*. have reported the above trend as occurring due to non-uniform dispersion of nanoparticles on the PIM surface, caused by the strong Van der Waals forces between PIM components (Vatanpour et al. 2011). However, the SEM images in Figure 11 did not demonstrate any assemblage of nanoparticles in these nanocomposite PIMs.

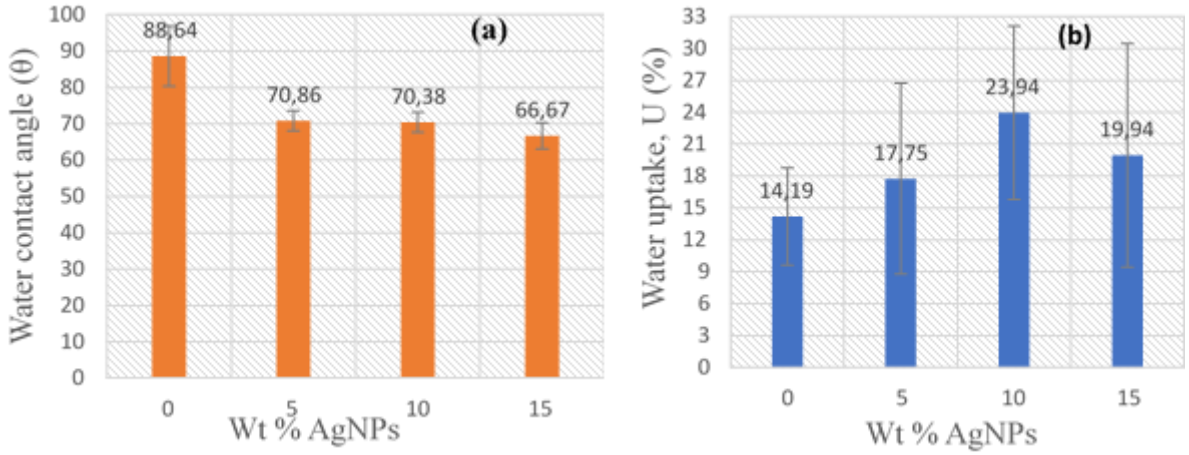

Figure 13 Water contact angles (a) and uptake of PVC/Ag NPs nanocomposite membranes with different loadings of Ag NPs (b). The error bars are ± SD (standard deviation)

The water contact angle measurements results were then analysed by a one-factor analysis of variance (ANOVA) with Bonferroni's post-hoc test to determine whether there is significant contribution of the Ag NPs loadings on membrane hydrophilicity. The significance level was set at $p < 0.05$ for all the calculations. The results showed that there was a statistically significant difference between the analysed PIMs with $p < 0.05$ (Table A1 in appendix). This meant that adding Ag NPs to the bare PVC based PIM had a considerable influence in the hydrophilicity. To determine which Ag NPs w.t% had a significant influence on hydrophilicity a Bonferroni correction was done on the *p* value followed by a *t*-test between two sets of PIMs. The *t*-test results showed that the hydrophobicity of each of the nanocomposite PIMs was significantly different from that of the bare PIM (0 w.t% Ag NPs) since $p < 0.008$ (Table A2).

However, the *t*-test results between the nanocomposite PIMs (5-15 w.t%) showed that there is no significant difference in water contact angle of the PIMs since $p > 0.008$ (Table A2). This suggests that an initial loading of Ag NPs into the PIM surface influenced its water contact angle (i.e. hydrophilicity), but adding more of the Ag NPs in the same PIM did not .

Similar to the contact angle measurements, water uptake (Figure 13b) measurements also showed that w.t% Ag NPs had an influence on the hydrophilicity of the PVC nanocomposite PIMs, membrane with the higher water uptake has the strongest hydrophilicity. Initially the bare membrane had an uptake of 14.19%. However, when Ag NPs were increased in a range of 5 to 10 w.t%. There was an increase in the water uptake capacity indicating an improvement in the hydrophilicity, with the highest value being 23.94% for the 10 w.t% Ag NPs

nanocomposite PIM. When the Ag NPs w.t% was further increased, a slight drop in the uptake was observed. This phenomenon can be attributed to the poor dispersion of Ag NPs on membrane surface which results in a cracked surface (highlighted yellow in Figure 11). Contrary to these, ANOVA results showed that w.t% Ag NPs loadings on the PIM surface had no significant influence in the PIM water uptake since $p > 0.05$ (Table A3).

5.3 Transports Experiments

5.3.1 Optimisation of PIMs composition

The PIM composition is crucial in determining the mechanical, extraction and transport properties of the membrane. As such, PIMs with various compositions using PVC as the base polymer, D2EHPA as the carrier and different metal nanoparticles loaded on the PIM were studied to obtain the optimal compositions. The plasticizer was not used in this case since the carrier used has plasticizer properties. As the amount of nanoparticles was increased the amount of polymer was decreased to maintain the carrier (D2EHPA) at 40 w.t%. The PIMs compositions and the flexibility are listed in Table 5. the PIM with no Ag NPs was optically transparent while PIMs with the Ag NPs were slightly opaque (Figure 14). However, all the membranes incorporated with silver nanoparticles (Ag NPs) were mechanically strong, flexible and all appeared homogenous to the naked eye. As such, all the synthesized PIMs were characterized and evaluated for various metal extraction capacity.

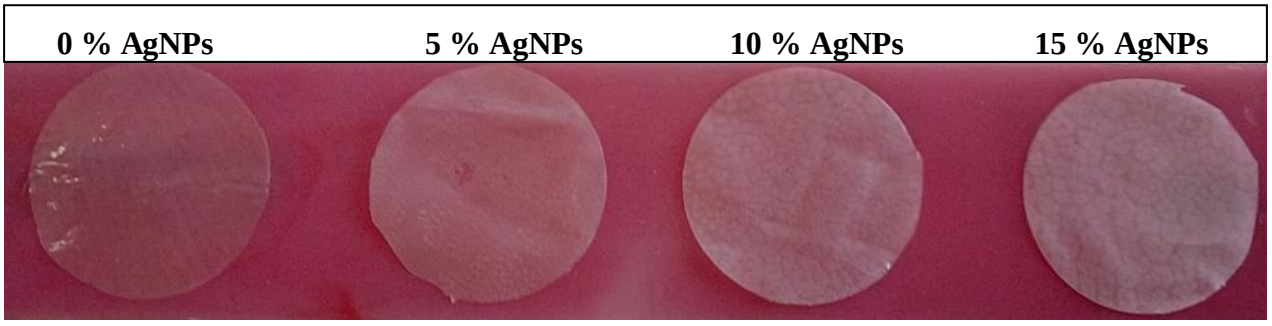

Figure 14 Photograph of the PVC/Ag NPs nanocomposite membranes with 0, 5, 10 and 15 w.t% loadings of the Ag NPs in the casting solution

Permeability studies were performed in order to select the optimum composition for the three different metal nanocomposite PIMs. This is the most important parameter in aspects for the commercialisation of PIMs (St John et al. 2013). Thus, the value of the flux intake ($J, mol\, m^{-2}s^{-1}$) at the PIM/solution interface was used to assess the extraction rate of the PIMs using Equation 2.

Table 6 The influence of silver nanoparticles on the initial flux ($10^8\, J, mol\, m^{-2}s^{-1}$) of metal ions across a PIM. (Feed solution:1 mg L^{-1} of metal ions at pH 5, extraction period of 24 hrs, and receiver solution: 0.10 M HNO_3)

Ag NPs w.t% Analyte	0	5	10	15
Cobalt	1.32	2.99	8.57	6.98
nickel	1.01	2.28	7.38	5.85
Copper	0.15	2.31	5.78	6.54
Cadmium	0.53	1.67	3.93	3.25

Results from Table 6 indicate that there is a strong connection between PIM composition and its performance. PIM with 10 w.t% Ag NPs loadings had the highest flux for all metal ions. Bare PIM had the lowest fluxes with an improvement >126% for all metal ions when 5 w.t % Ag NPs loadings are incorporated into the PIM. The observed fluxes of the silver nanocomposite PIMs are higher as compared to that of bare PIMs investigated by (Ershad et al. 2018) and (Pont et al. 2008) although different PIM components were used. As observed in the water uptake capacity of silver PVC nanocomposite PIM, the flux dropped slightly when w.t% Ag NPs loading is increased from 10-15 w.t % for most metal ions. This suggests that 10 w.t% Ag NPs is the optimum composition due to homogenous distribution of Ag NPs in the PIM surface, highest water uptake and the high permeability.

The extraction capacity of these PIMs was also used to validate the permeability results. As observed in Figure 15. Addition of Ag NPs on PIM had an influence in various metal extraction capacity. An initial increase in concentration of Ag NPs on PIM, similar to increasing the antifouling activity (antibacterial properties) of membrane, lead to an improvement in

extraction capacity as compared to the bare PVC PIM. However, when w.t% Ag NPs is greater than 10, a decline in extraction capacity for most metal ions is observed. Khalid *et al* have reported that a higher w.t% of Ag NPs in membrane result in a nonhomogeneous deposition of silver across the polymer matrix which causes a decline in membrane properties (Khalid et al. 2017a). This study showed cracks on nanocomposite PIM with 15 w.t% of Ag NPs [Figure 11 (d, h)], which potentially affected the PIM stability hence the observed drop in the extraction capacity.

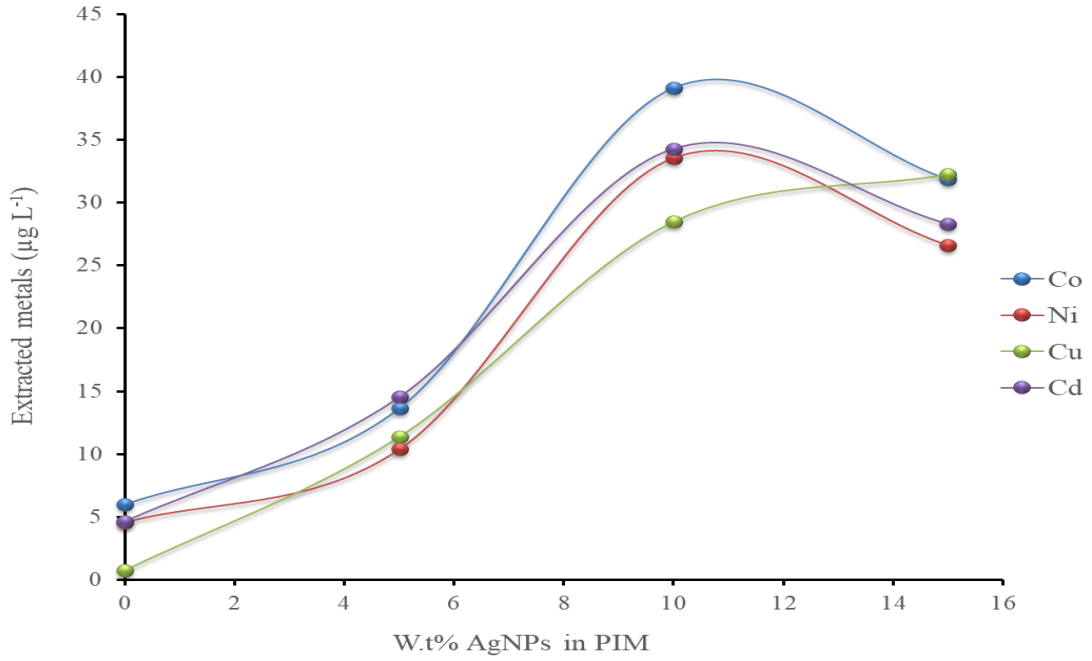

Figure 15 Influence of Ag NPs w.t% in PVC PIMs, for various metal extraction capacity (Feed solution:1 µg L^{-1} of metal ions at pH 5, extraction period 24 hrs and receiver solution: 0.10 M HNO_3)

5.3.2 Optimisation of critical parameters for the transport of analytes

When a PIM is used for transport of metal ions, firstly the metal ion has to be extracted from the source phase. This is followed by a facilitated transport through a membrane, and the final step happens when the metal is released to the receiving solution. The above steps take place simultaneously thus, a proper pH balance, receiver solution concentration and the optimised membrane composition are needed to avoid the accumulation of metal in the membrane that leads to a decrease in efficiency. Given this; parameters that affect analyte transport in PIMs should be effectively optimised. In this study, the optimised silver nanocomposite PIM was used to optimise these critical transport parameters.

5.3.2.1 Optimisation of receiver solution concentration

The effective stripping of the membrane is necessary for the system to be used in practical situations. Three different acid receiver solutions (1 mol L^{-1} each; H_2SO_4, HCl and HNO_3) were used to evaluate the stripping of Co^{2+}, Ni^{2+}, Cu^{2+}, and Cd^{2+} from the optimised Ag/PVC nanocomposite PIM. In order to optimise this parameter, the concentration of the source solution containing target analytes was kept at 1 mg L^{-1}, and a stirring rate of 100 rpm and membrane with thickness of 50 ± 5 µm was used. The pH of the source solution was kept at 2 because at pH > 3 the D2EHPA based PIM becomes unstable since the pKa of D2EHPA is ≈ 3.5, making its ionization at pH > 3 to enhance leaching of the carrier in the both the source and the receiving phase (Bonggotgetsakul et al. 2015; Croft et al. 2018). At pH 2, PVC is also less likely to undergo dehydrochlorination, making the membrane more stable. The PIM devices were deployed for 24 hrs.

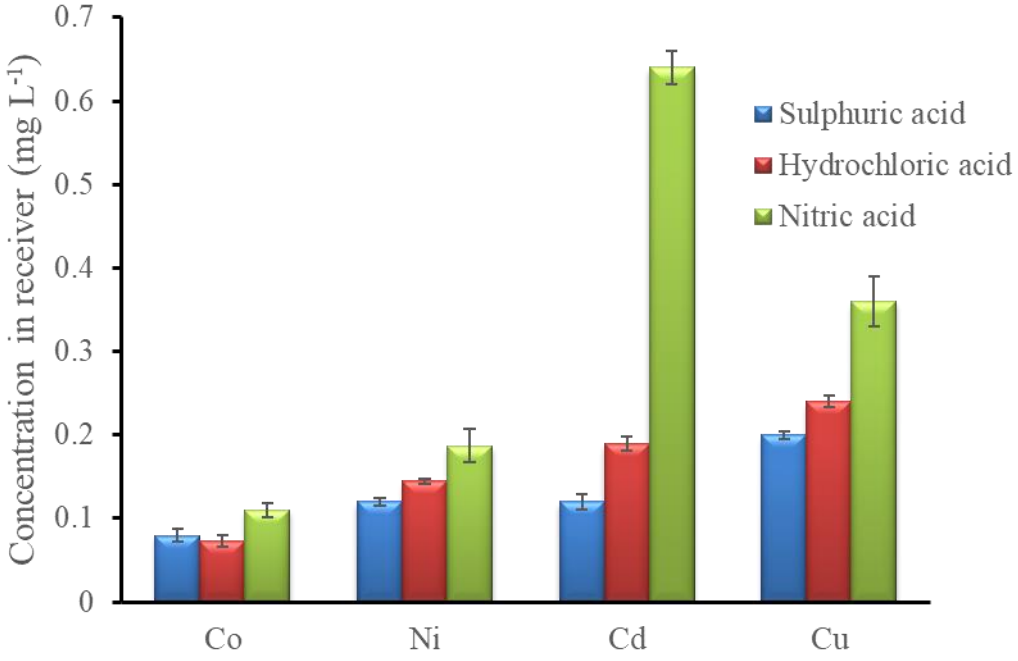

Figure 16 Effect of various acid receiver solutions on extraction ability (n = 3). (Feed solution: 1 mg L^{-1} of metal ions at pH 2, extraction time of 24 hrs, 1 mol L^{-1} for each receiver solution, membrane composition of 40 w.t% D2EHPA, 10 w.t% Ag NPs and 50 w.t% PVC). The error bars are ± SD (standard deviation).

It is notable that the stripping of analytes using HNO_3 as the receiver solution gave the highest uptake of metal ions from the source to the receiver solution (Figure 16). This was followed by HCl and H_2SO_4. This suggests that effective facilitative transport of Co^{2+}, Ni^{2+}, Cu^{2+}, and Cd^{2+} through Ag/PVC PIMs can be achieved with H^+ concentration gradient across the membrane from nitric acid. To optimize the acidity in the receiving phase membrane transport experiments were carried out with 0.25-1.25 M of nitric acid in the receiving phase. This is because transport of metal ions from the source to receiving phase is coupled to the transport of H^+ in the opposite direction so thus increasing the H^+ concentration gradient across the membrane increases the driving force of the transport process. Since the source solution pH was kept constant at 2, the concentration gradient of H^+ across the membrane can only be increased by varying the concentration of nitric acid in the receiving phase. In Figure 17, it notable that an increase in nitric acid concentration resulted in an improved metal uptake up to 1 M nitric acid. This could be attributed to high concentration of protons in the receiver phase which leads to an increase in the driving force, that accelerates the separation of the metal ion-D2EHPA complex at the membrane-receiver interface. However, it appears that the uptake decreases when the concentration is increased from 1.0 M to 1.25 M although this difference is not statistically significant This suggests that there is no benefit in increasing the concentration of acid higher than 1 M. Since a desirable acid receiving solution concentration should be as low as possible for costs and safety (St John et al. 2012). 1 M nitric acid was therefore used for subsequent experiments.

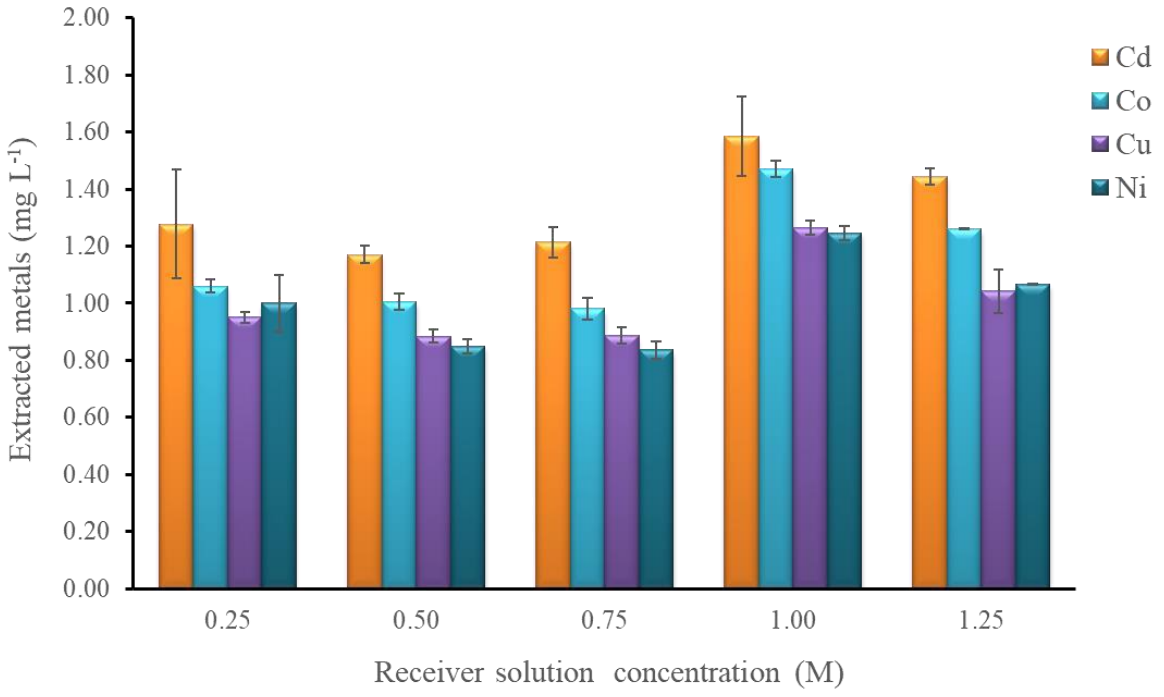

Figure 17 Effect of receiver solution concentration on extraction of metal ions (n = 3). Feed solution:1 mg L^{-1} of metal ions at pH 2, extraction time:24 hrs, membrane composition of 40 w.t% D2EHPA, 10 w.t% Ag NPs and 50 w.t% PVC. The error bars are ± SD

5.3.2.2 Optimisation of source solution pH

The pH gradient between source and receiving phase generates the potential gradient across the membrane, which is the driving force for the permeation of metal complex towards the receiver phase. In order to assess the role of the source phase pH on the extraction of Co^{2+}, Cu^{2+}, Ni^{2+} and Cd^{2+}, the pH of the source solution was investigated from pH 2-7 for 24 hrs. pH was the only varied factor in this study while other parameters remained constant. Since D2EHPA is an acidic extract, it is expected that the extraction capacity is enhanced by increasing the pH of the source solution since H^+ are the driving force in the extraction and the greater the H^+ difference concentration between the source and receiver solutions, the better the expected transport efficiency. Figure 18 illustrates that extraction capacity increases with increasing source solution pH. It could be argued that this would result in the leaching of the carrier (D2EHPA) when the pH is above 3. However, in PIM studies, in order to achieve a desirable transport efficiency there is always a dilemma on what to compromise between stability and selectivity (Nghiem et al. 2006). When the pH was above 5 the metal ions began to precipitate and were no longer available hence the observed drop in the concentration of extracted metal ions. Thus, the optimum pH for effective metal ion extraction is pH 5.

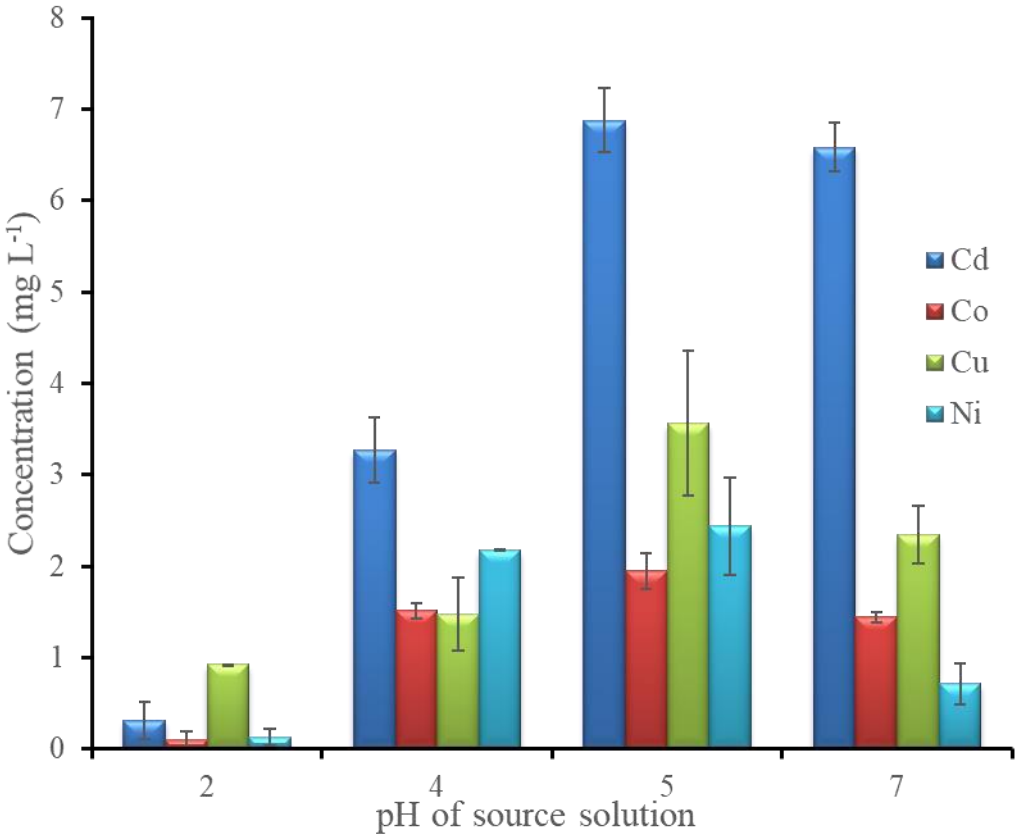

Figure 18 Effect of source solution pH on membrane extraction capacity (n = 3). Feed solution:1 mg L^{-1} of metal ions, extraction time of 24 hrs, 1 mol L^{-1} of HNO_3 as receiver solution, membrane composition of 40 w.t% D2EHPA, 10 w.t% Ag NPs and 50 w.t% PVC. The error bars are ± SD

5.3.2.3 Effect of source solution concentration on extraction capacity

The effect of metal ion concentration in source solution (deionised water) was investigated in a range of 0.50 – 2.50 mg L^{-1}. Figure 19 shows the curves obtained for the analysis of the metal ion concentrations in the receiving phase versus the initial metals present in the water sample. As observed, the concentration of the analytes in the receiving phase increased with an increase in the source phase. This suggest that the silver nanocomposite PIM device can determine the amount of metal ions in natural waters after its pre-concentration over a wide range of concentrations.

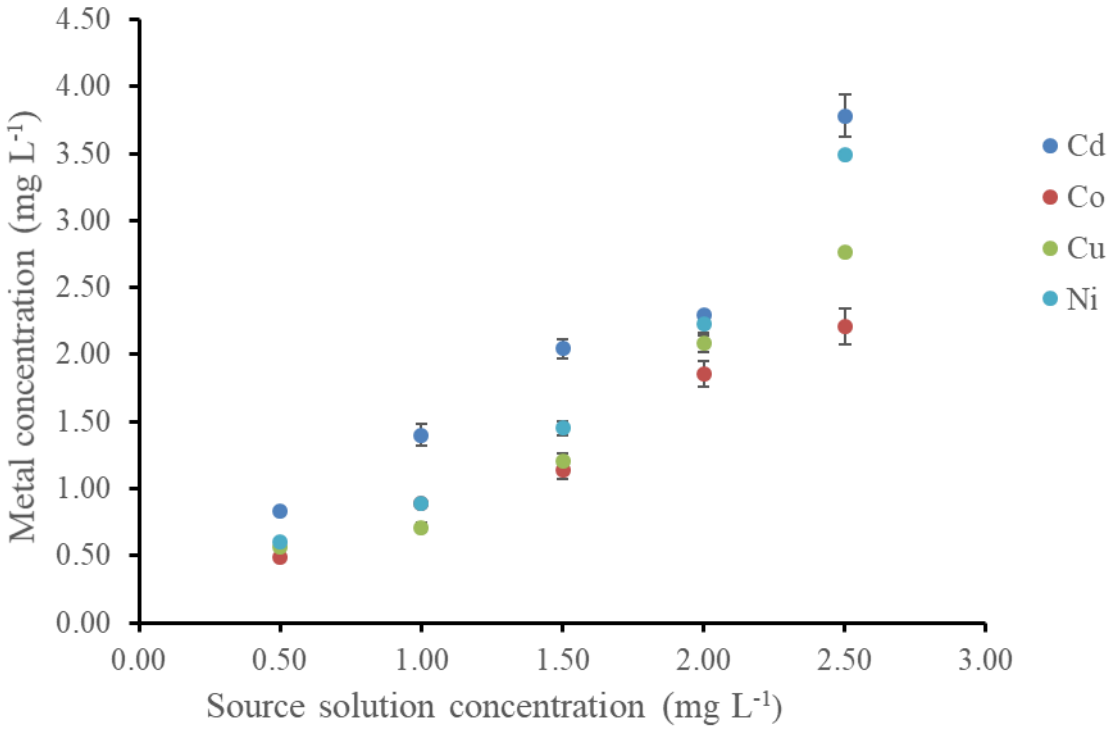

Figure 19 Effect source metal ion concentration on analyte extraction (n = 3). (Feed metal ions solution at pH 2,extraction time of 24 hrs, 1 mol L^{-1} HNO_3 as receiver solution, membrane composition of 40 w.t% D2EHPA, 10 w.t% Ag NPs and 50 w.t% PVC). The error bars are ± SD

5.4 Selectivity

The affinity of the D2EHPA-based silver nanocomposite PIM (40 w.t% D2EHPA, 10 w.t% Ag NPs and 50 w.t% PVC) towards a range of metal cations was assessed in extraction experiments (Figure 8) using aqueous feed solution, containing 1 mg L^{-1} of each individual cation. The membrane selectivity for each of the cations studied was quantified by the corresponding recovery factor (RF) and the initial flux (equation 2). The RF and initial flux (J) values of the cations studied are reported in Table 7. The recovery factor (RF) [Equation 3] was calculated as the percentage of the extracted metal ion and was used to determine the order of selectivity of the D2EHPA-based silver nanocomposite PIM for the extracted metal ions.

Table 7 PIM extraction based recovery factors (RF) and initial flux (J) values for a range of metal cations (40 w.t% D2EHPA, 10 w.t% Ag NPs and 50 w.t% PVC); feed solution 1 mg L^{-1} of the cations at pH 5 and extraction period of 24 hrs

Extracted species	RF (%)	$\boldsymbol{J \times 10^6}$ ($\boldsymbol{mol\, m^{-2} s^{-1}}$)
Cd^{2+}	94.3	7.90
Cu^{2+}	83.7	7.24
Ni^{2+}	78.4	5.35
Co^{2+}	67.2	4.27

Recovery efficiency is affected by the ability of the metal cation to form an ion-pair with the conjugated base of the carrier (Ershad et al. 2018). This can be assessed based on the *Hard* and *Soft Acids* and *Bases Theory* whereby soft bases have a high affinity to soft acids (Zoroddu et al. 2019). The RF values in Table 7 provide the following order of affinity of the D2EHPA-based PIM for the extracted cations in water solutions: $Cd^{2+} > Cu^{2+} > Ni^{2+} > Co^{2+}$. These results are broadly in line with the *Hard* and *Soft Acids* and *Bases Theory* mentioned above since the PIM has the highest affinity for the soft Cd^{2+} metal ion (D2EHPA in Figure 20 has a soft conjugate base) and the lowest affinity for the other divalent metal ions which are in the borderline of being hard/soft acids (Zoroddu et al. 2019).

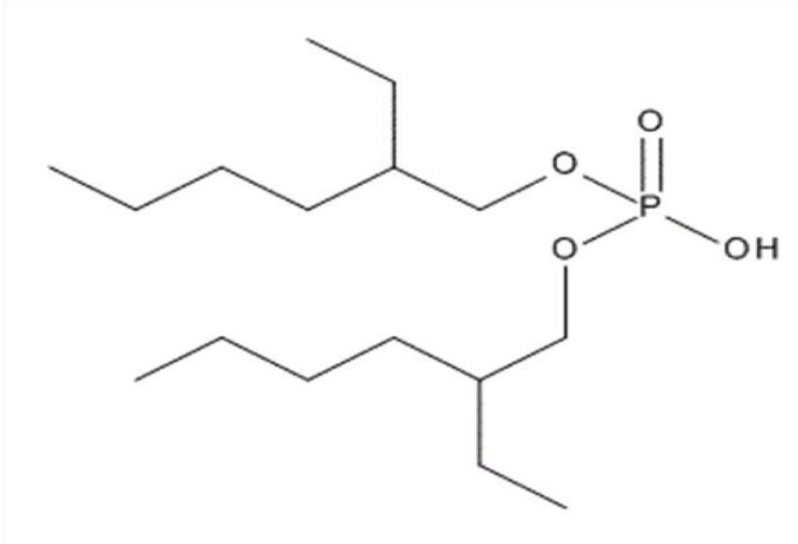

Figure 20 Molecular structure of di-(2-ethylhexyl) phosphoric acid (D2EHPA)

The results showed that the silver nanocomposite D2EHPA-PIM had a significantly higher affinity for Cd^{2+} compared to the other divalent cations despite the fact that the corresponding ion sizes (Table 8) are not significantly different thus corresponding to similar electron densities.

Table 8 Ionic sizes and the hydration energies of metal ions (Atkins and Overton 2010; G. Wulfsberg 1987)

Metal ion	Ionic radius (pm)	Hydration energy (kJ mol^{-1})
Cd^{2+}	95	1806
Cu^{2+}	73	2100
Ni^{2+}	69	2106
Co^{2+}	65	2054

The most likely reason for this observation lies in the fact that Cd^{2+} can more readily shed its hydration sphere to be able to enter the hydrophobic PIM environment. This is reflected by the hydration energies of the cations mentioned above which for Cd^{2+} is 1806 kJ mol^{-1}, whereas the values for Cu^{2+}, Ni^{2+} and Co^{2+} are 2100, 2106 and 2054 kJ mol^{-1} respectively. These results are consistent with those reported by other authors (Ershad et al. 2018) and as expected, the initial flux values follow approximately the order of the corresponding RF values.

5.5 Stability

The instability of PIMs is generally related to loss of the membrane liquid phase to the aqueous solutions in contact with the membrane and can be quantified by determining the mass loss hence determining membrane reusability. Thus, the stability of PIMs containing 40 w.t% D2EHPA, 10 w.t% Ag NPs and 50 w.t% PVC was assessed by weighing them before and after repeated cycles of metal ions extraction using the same membranes while replacing the feed and the receiving solution after each cycle. The average percentage mass losses after 24 hrs of exposure based on experiments conducted in triplicate are presented in Figure 21. Results show a gradual mass loss between the first and the fifth cycles with a total mass loss of 21% after the fifth cycle. For the sake of clarity, the weight of the initial fresh membrane (before first cycle metal extraction) was assumed to be 100%. Most authors have reported the mass loss occurs as a result of the loss of the carrier to the aqueous phase as the membrane is being reused

(Bonggotgetsakul et al. 2016; Cai et al. 2019; Yoshida et al. 2019). In this case since there are nanoparticles and the carrier in the membrane morphology, there is a possibility of losing both the silver nanoparticles and the carrier into the aqueous phase. Since the data did not allow the accurate identification of the extent of leaching of each individual component (i.e. D2EHPA and Ag NPs), the concentrations of phosphorus and Ag NPs in the aqueous phases after each cycle were measured by ICP-OES. This enabled the determination of the amount of D2EHPA and Ag NPs that leached. The total mass loss was 21% of the initial fresh membrane mass and 82.4% of this was due to the loss of D2EHPA and 17.6% due to Ag NPs. These mass losses are in the ratio of approximately 4:1, which is in agreement with the mass ratios of the corresponding components in the original membrane (i.e. 40 w.t% D2EHPA and 10 w.t% Ag NPs). The membrane mass loss seems to approach a constant from the fifth to the tenth cycles which suggests that there is a stable membrane composition that depends on factors such as solution pH and ionic composition of the contacting aqueous phase(s) as had been reported by other authors (Zhang et al. 2012a).

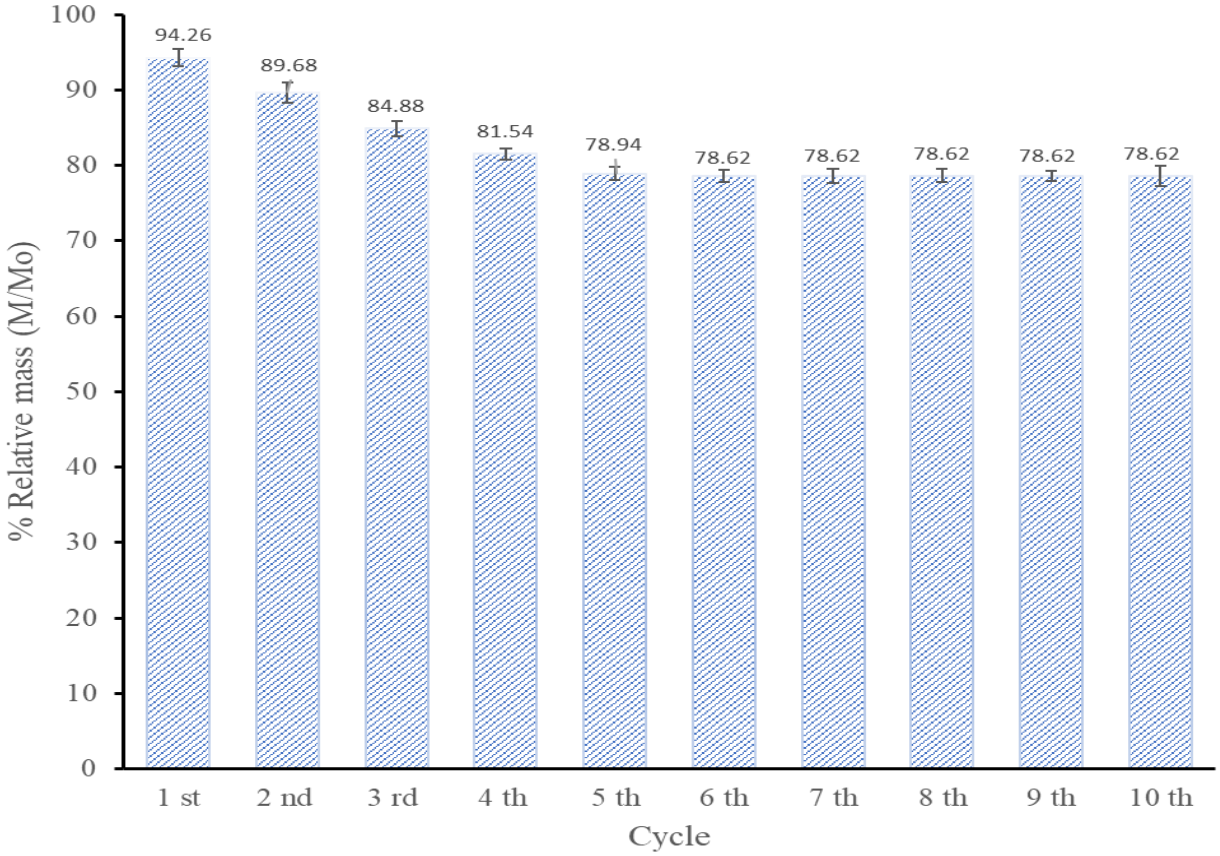

Figure 21 Percentage mass loss of PIMs (n = 3) containing 40 w.t% D2EHPA, 10 w.t% Ag NPs and 50 w.t% PVC for metal ions extraction (feed solution 1 mg L^{-1} of the cations at pH 5 and initial PIM mass 31.97 ± 1.45 mg). The error bars are ± SD

It was noticed that as the membrane was reused for the fourth time, it became yellow and rigid which might be the result of metal ions remaining in the membrane surface. Rigid membranes have been reported to decrease transport efficiency (Wang et al. 2017). The membrane thickness also decreased as the membrane was reused: the initial thickness of ~ 50 µm decreased to ~ 43 µm after the fifth cycle then to ~ 41 µm after the tenth cycle. This phenomenon has been reported to negatively affect the membrane transport performance (Sellami et al. 2019).

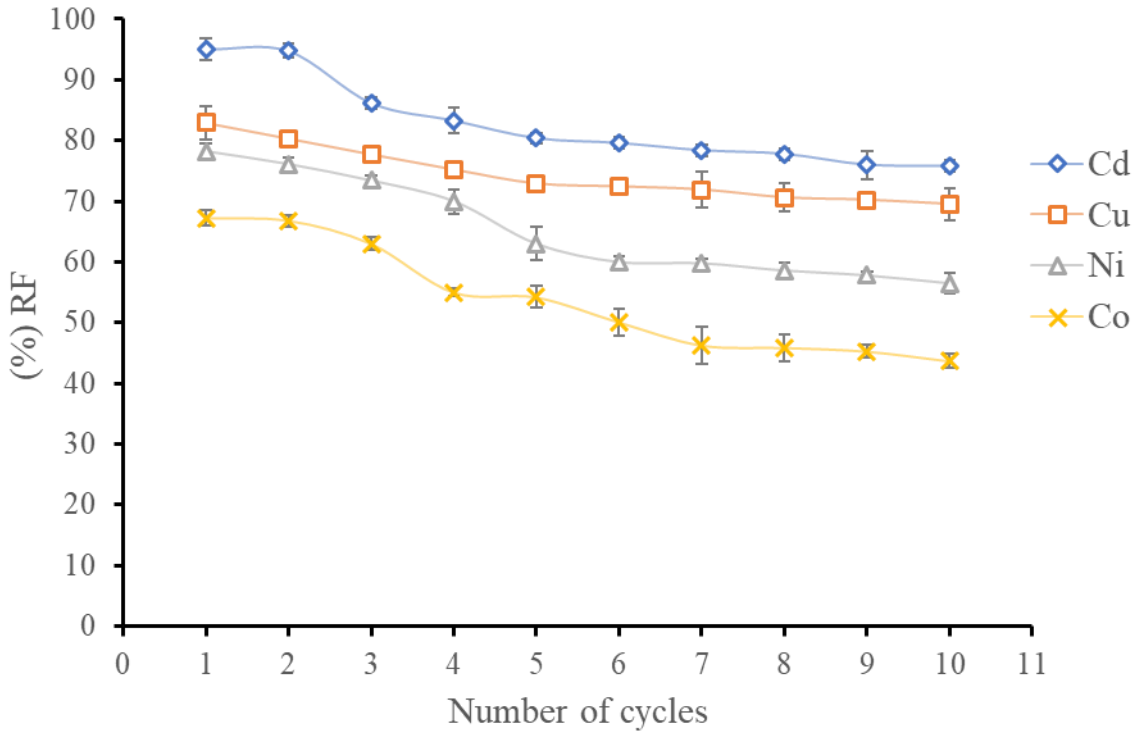

Figure 22 RF values of bivalent cations vs number of cycles (24 hrs each) of extractions (*n*=3). (Experimental conditions: feed solution 1 mg L^{-1} of the cations at pH 5, membrane composition of 40 w.t% D2EHPA, 10 w.t% Ag NPs and 50 w.t% PVC and PIM mass of 31.97 ± 1.45 mg). The error bars are ± SD

As a result of a decrease in relative mass of the silver nanocomposite PIM as the membrane is reused. Recovery factor (RF) [equation 3], of the metal ions was assessed to investigate the membrane transport performance. Figure 22 highlights that, in consistence with the mass loss of the PIM, the (%) RF values of all the metal ions were declining as the D2EHPA and the silver nanoparticles were leaching into the aqueous phase (first-fifth cycle). It was also important to note that all (%) RF values of metals reached a plateau were the relative mass remained constant (fifth-tenth cycle). This suggests that the stability of a membrane is directly

related to the membrane transport performance. This particular trend has been previously observed although other authors preferred to evaluate one monovalent metal ion analyte (Cai et al. 2019). In order to avoid loss of membrane performance due to reusability, investigations could be conducted on the use of cleaning agents that would prevent accumulations of foreign substances on or inside the membrane surface that promote fouling. This would mean that there would be a possibility of the membrane being used several times, without a significant loss in analyte transport efficiency.

5.6 Influence of transport time

In order to investigate the influence of exposure time of the membrane to performance and efficiency. Transport efficiency (TE) was used (Equation 4).

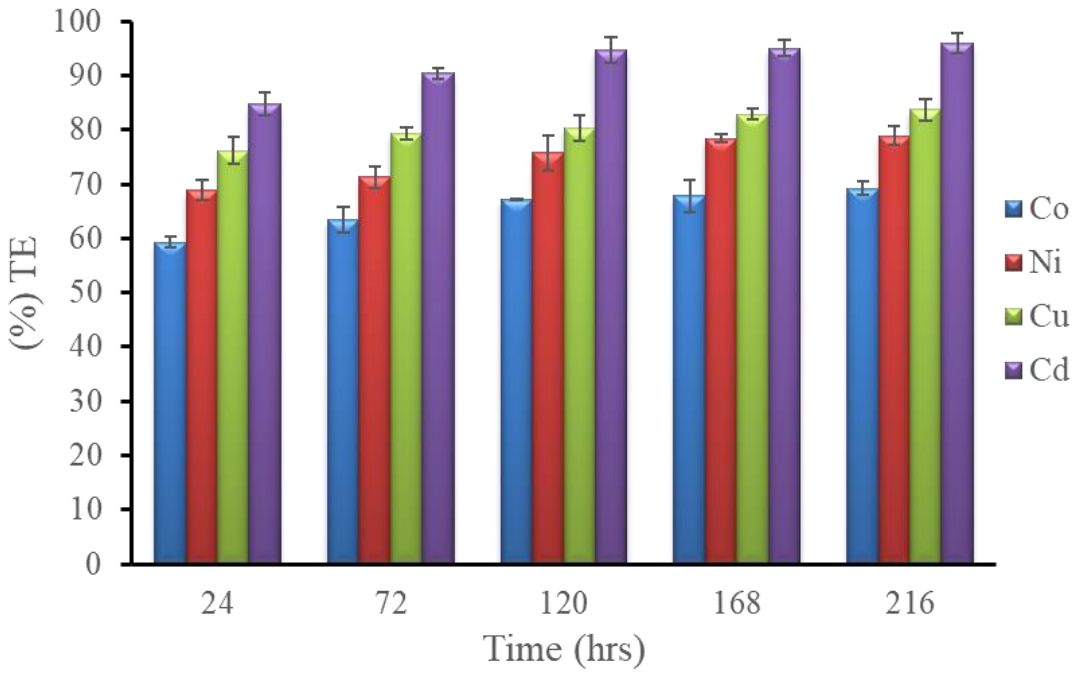

Figure 23 Influence of the duration of transport on the transport efficiency of the metal ions studied (*n*=3). The feed solutions contained 1 mg L^{-1} of the individual metal ions studied at pH 5. The stripping solution contained 1 M HNO_3. The PIM was composed of 40 w.t% D2EHPA, 10 w.t% Ag NPs and 50 w.t% PVC. The error bars are ± SD

Figure 23 shows the dependence of metal ion transport efficiency over different transport times (24, 72, 120, 168 and 216 hrs). As expected, the lower transport efficiencies were obtained after 24 hrs improved after 72 and 120 hrs. This means that in this period (24 - 120 hrs), the PIM based two compartment transport system was operating in the kinetic region where accumulated analytes increased with time. Hence the resultant increase in the individual metal ions transport efficiencies. However, from 120-216 hrs there was no change in the transport efficiency of all metal ions. The transport system was now operating in the equilibrium region where the amount of the analyte collected did not change with time, provided that the source solution concentration did not change. Hence 120 hrs was chosen as the optimum time since there was no significant change in transport efficiencies observed after this period. For the sake of clarity, other factors that can potentially affect the efficiency such as working temperature and the area of the membrane exposed to source solution were held constant.

CHAPTER 6

This chapter focuses on the applications of the optimised silver nanocomposite PIM in environmental samples.

6 Environmental Application

6.1 Sampling site

To evaluate the effect of water composition on metal ions transport, natural water samples were tested. Samples were collected in different locations in Gauteng (March 2019): dam water (DW) near mine tailing dumps was collected in Bekkersdal at Donaldson dam (26°17'17.50"S 27°41'56.64"E). Additionally, tap water from the University of the Witwatersrand Braamfontein East Campus (26°11'27.75"S 28°01'52.09"E), was collected to study the possibility of the cationic interferences in the transport of the target analytes.

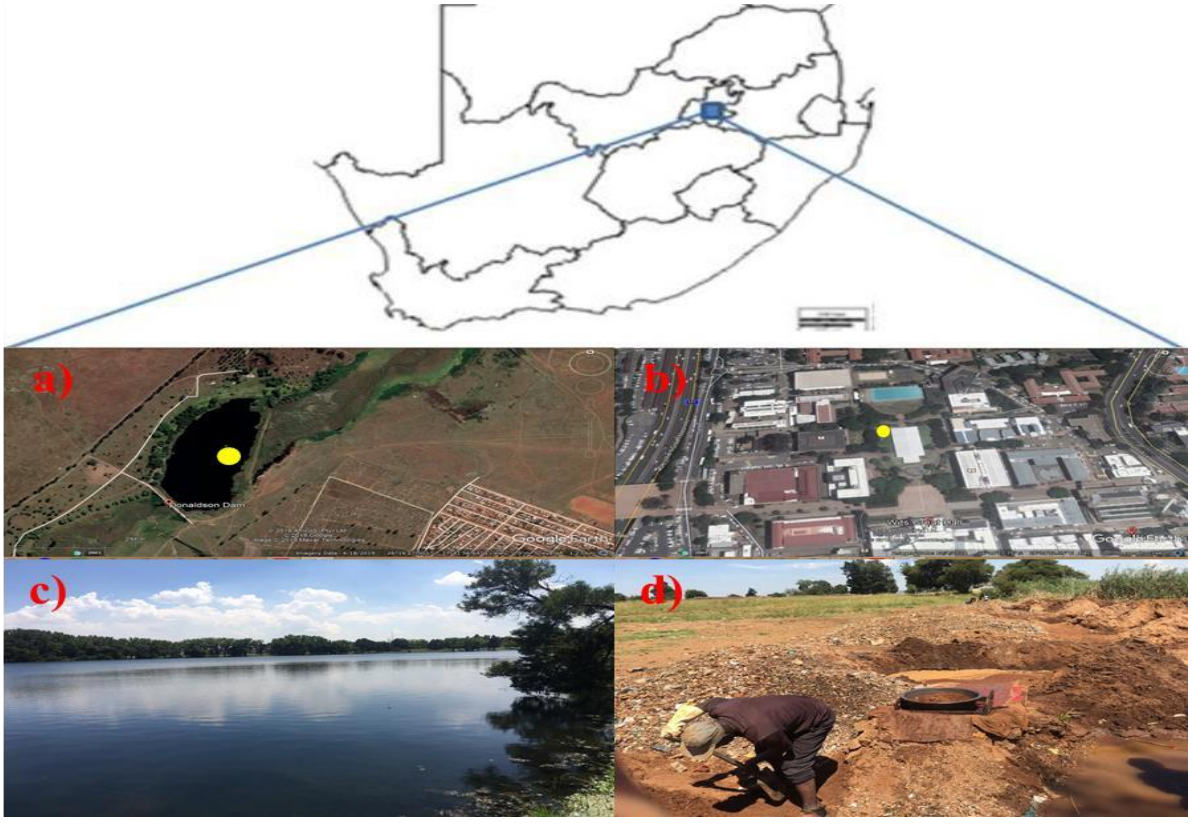

Figure 24 Sites used for the collection of water samples; a) Donaldson dam impacted by mine tailings, b) Braamfontein East campus, c) picture representation of the dam, d) Zama Zama (illegal gold miner) trying to recover gold next to the dam. (yellow colour represents sampling sites spots).

6.2 Physicochemical parameters of the water samples

Two points were selected in the dam area for sampling. The collected water samples had different physicochemical parameters which are presented in Table 9.

Table 9 Characteristics of the water samples used for this study with DWSSA stipulated limits (SANS 2006)

Sample characteristics	Dam water 1	Dam water 2	Tap water	DWWSA
Conductivity (µS)	1980	2 820	212	<150^
pH	5.20	4.62	7.90	5.0-9.50
Al^{3+}	3.65	2.06	1.29	<300*
Ca^{2+}	>75	>128	14.21	<150
Mg^{2+}	8.71	10.33	4.02	<70.00
Cd^{2+}	1.92	0.61	<0.10	<5.00*
Cu^{2+}	0.17	0.79	<0.10	<1000*
Ni^{2+}	0.75	2.38	1.17	<150*
Co^{2+}	0.76	0.56	<0.08	<500*
Zn^{2+}	<0.11	<0.11	0.28	<5.00
Sn^{2+}	1.487	<0.08	<0.08	-
Mo^{2+}	2.25	7.24	2.57	-
V^{2+}	0.726	2.35	<0.18	<200*
Li^{+}	0.06	0.08	0.05	-
K^{+}	7.86	11.33	1.46	<50.00
Na^{+}	>112	>142	10.00	<200
F^{-}	0.31	0.36	0.16	<1.00
Cl^{-}	44.67	48.6	9.54	<200
SO_4^{2-}	-	6.41	48.81	<400
TDS	1.61*	1.87	141	<1000
ORP (mV)	201	209	-76.3	-

Concentrations are given in milligram per litre,

*Concentration in parts per trillion, ^mS/m

Cations determined with ICP-OES and anions with IC.

6.3 Matrix effect

The presence of other components in natural water samples can affect the efficiency of the membrane. Additionally, for the transport of metal ions as target species, other major ionic species could interfere by competing with the target analytes for active sites on the carrier. This effect was observed in a study of the transport of arsenate using a PIM based device whereby the high conductivity of the hot spring water hindered the analyte transport due to high chloride content in the sample (Fontàs et al. 2014). On the other hand, other ions can act as complexation agents thus affecting metal speciation (Elias et al. 2019).

To evaluate these matrix effects, we tested transport efficiency for the dam water containing the target analytes as well as Millipore and tap water from Braamfontein spiked with the target analytes and iron (Fe^{2+}) as a potential interference. This is because natural waters closer to mine tailings usually have a high iron content (Tutu et al. 2008).

Since the pH of the dam water was in the range of the optimised pH for efficient analytes transport (Table 9). Only the tap and the Millipore water pH's were adjusted prior to the evaluation of the membrane transport efficiency of the proposed samples. The obtained transport efficiencies are presented in Table 10.

Table 10 Effect of matrix effect on analytes transport efficiencies of the PIM (40 w.t% D2EHPA, 10 w.t% Ag NPs and 50 w.t% PVC). The stripping solution contained 1 M HNO_3 and extraction time of 120 hrs

	Analyte (%) Transport efficiency				
Water sample	[Cd]	[Cu]	[Co]	[Ni]	[Fe]
Millipore*	96	83	74	66	40
Tap water*	92	82	67	59	55
Dam water 1	88	80	70	62	37
Dam water 2	82	77	66	58	41

*Samples spiked with 1 mg L^{-1} of the individual target analytes

Even though the conductivity of the waters studied, the composition and the initial targets analytes concentrations were different (Table 9), no significant differences were observed in the transport efficiencies of the analytes in all water samples despite the presence of iron as a potential interferer. In the case of the spiked tap water and the dam water, other metals were co-transported with the target analytes and the concentrations for the spiked tap water are presented in Table 11. However, the transport efficiencies of these other metal ions were very

low expect for zinc which has the same properties as the target analyte (cadmium). The results indicate that the silver nanocomposite PIM is efficiently able to pre-concentrate and transport metal ion analytes even in the presence of other ionic species, thus revealing a great robustness of the proposed detection method.

Table 11 Cationic species that were co-transported with the targets metal ions on the spiked tap water sample

Metal ion	Initial concentration (mg L^{-})	Concentration in receiver solution (mg L^{-})	(%)Transport efficiency
Ca	27.8	138	1.13
Mg	6.02	7.65	0.29
Na	11.07	9.55	0.19
Zn	0.28	27.9	22.8
Si	1.81	3.16	0.40
Mo	2.60	2.78	0.24
K	1.46	2.15	0.34
V	0.80	1.59	0.45
Al	1.29	2.00	0.35

6.4 Analytical figures of merit

The silver nanocomposite PIM was applied to investigate the effect of metal ion concentration (Co, Cu, Ni and Cd) to standards containing 0.50 to 2.00 mg L^{-1} in Millipore and tap water whereby ICP-OES was used to measure the concentration in the receiver solution. Table 12 shows summary of the calibration curves (Figure A1) for the analysis of analyte concentration in the receiving phase plotted vs the initial analyte present in the water samples. Both the Millipore and tap water calibration curves had a regression coefficient higher than 0.99 for all metal ions analytes, which indicates a good linearity throughout the working range. The similarity of the slopes between the two waters (tap water and Millipore) for all metal ions studied revealed also the lack of matrix effect. These results are highly noteworthy since they demonstrate that a single calibration is enough to determine the initial amount of a metal ion present in a water sample after its pre-concentration by a PIM-device.

Table 12 Summary of the analytical figures for calibration curves obtained with a nanocomposite PIM (*n* = 3) (40 w.t% D2EHPA, 10 w.t% Ag NPs and 50 w.t% PVC). Feed phase: 3500 mL with 0.5 – 2.0 mg L^{-1} analytes and extraction period: 24 hrs. The stripping solution contained 8 mL 1 M HNO_3

Analytical figure	Tap water	Millipore water	Metal analyte
R^2 value	0.99	0.99	
Slope	6.12	5.76	
LOD	0.47	0.28	Cd
LOQ	1.42	0.86	
R^2 value	0.99	0.99	
Slope	5.30	4.78	
LOD	0.05	0.31	Co
LOQ	0.15	0.96	
R^2 value	0.99	0.99	
Slope	6.06	5.48	
LOD	0.59	0.33	Cu
LOQ	1.78	1.01	
R^2 value	0.99	0.99	
Slope	5.53	5.22	
LOD	0.68	0.35	Ni
LOQ	2.07	1.06	

The limit of detection (LOD) and the limit of quantification (LOQ) were calculated for each metal analyte. The values of the LOD were found to be higher than those stipulated by the WHO, the EPA and the Department of Water and Sanitation of South Africa (DWSSA) for drinking water. Hence the nanocomposite PIMs still need further developments to improve the LOD to these limits. However, these PIMs can be used to monitor metal ions in natural waters such as dams, rivers, ground water, the sea and springs. The inter-day repeatability was evaluated at two cadmium concentration levels; 0.50 mg L^{-1} (n = 3) and 2.00 mg L^{-1} (n = 3) with the standard deviations of these measurements being 0.08 mg L^{-1} and 0.27 mg L^{-1} respectively.

CHAPTER 7

This chapter discusses the conclusions drawn from the experimental findings of this study. The recommendations for future work are also presented.

7 CONCLUSIONS AND RECOMMENDATIONS

7.1 General conclusions

The silver nanocomposite PIM was successfully synthesized and characterized. The incorporation of Ag NPs into the PIM improved the membrane hydrophilicity thus inducing an antifouling property to the nanocomposite PIMs. Evaluation of the PIMs demonstrated that PVC-D2EHPA based PIMs containing Ag NPs exhibited better extraction capacity compared to the bare PIMs although there are cracks on the PIM surface as higher w.t% of Ag NPs are loaded into the PIM surface. The nanocomposite PIM with (40 w.t% D2EHPA, 10 w.t% Ag NPs and 50 w.t% PVC) was the optimum composition. Parameters that are important for the extraction of trace metal ions were optimised as sample pH 5, 1 M HNO_3 of the receiving solution and 120 hrs for the extraction time. The selectivity was investigated and it has been observed that the optimised PIM extracts metal ions from synthetic waters in order of Cd^{2+} > Cu^{2+} > Ni^{2+} > Co^{2+}, which is based on the corresponding recovery factor values and is in line with the *Hard* and *Soft Acids* and *Bases Theory* and the corresponding hydration energies. However, the stability of the PIM is still compromised during repeated cycle operations despite an improvement of hydrophilicity as demonstrated by the mass loss of 21% when the membrane was reused ten times. The individual contributions to the mass loss were 82.4% for D2EHPA and 17.6% Ag NPs. These mass losses are in the ratio of approximately 4:1, which is in agreement with the mass ratios of the corresponding components in the original membrane (i.e. 40 w.t% D2EHPA and 10 w.t% Ag NPs).

The optimised silver nanocomposite PIM was then tested in environmental samples collected from Donaldson dam and tap water from Braamfontein. The obtained LOD values for all analytes were higher as compared to EPA, WHO and DWWSA standards for drinking water. Thus, showing that the proposed method is not good for monitoring metal ions in drinking water. However, it can be used in dams and rivers since there was no significant difference in the transport efficiencies of target analytes even though the water samples tested had different compositions. Considering the simplicity and the improved hydrophilicity, the silver nanocomposite PIM can be viewed as an attractive alternative to existing membranes for the design of passive samplers to monitor metal ions in natural waters.

7.2 Recommendations and future work

- To avoid loss of membrane performance due to reusability, investigations should be conducted on the use of cleaning agents that would prevent accumulations of foreign substances on or inside the membrane surface that promote fouling.
- The proposed nanocomposite membrane should be tested in other environmental samples such as acid mine drainage, wastewater and sea water to investigate its performance in different water samples.
- Study the effect of membrane thickness and how the shape and size of the incorporated nanoparticles affect membrane morphology and transport efficiency.
- Deploy the optimised membrane directly into the field as passive sampler to investigate differences in lab-and field results.

REFERENCES

Aguilar, J.C., Miguel, E.R. de S., Gyves, J. de, Bartsch, R.A., Kim, M., 2001. Design, synthesis and evaluation of diazadibenzocrown ethers as Pb2+ extractants and carriers in plasticized cellulose triacetate membranes. *Talanta* **54**, 1195–1204. https://doi.org/10.1016/S00399140(01)00387-3

Ahkola, H., Herve, S., Knuutinen, J., 2013. Overview of passive Chemcatcher sampling with SPE pretreatment suitable for the analysis of NPEOs and NPs. *Environ. Sci. Pollut. Res.* **20**, 1207–1218. https://doi.org/10.1007/s11356-012-1153-0

Ahmaruzzaman, M., 2009. Role of Fly Ash in the Removal of Organic Pollutants from Wastewater. *Energy Fuels* **23**, 1494–1511. https://doi.org/10.1021/ef8002697

Ahmed, M.J.K., Ahmaruzzaman, M., 2016. A review on potential usage of industrial waste materials for binding heavy metal ions from aqueous solutions. *J. Water Process Eng.* **10**, 39–47. https://doi.org/10.1016/j.jwpe.2016.01.014

Akar, N., Asar, B., Dizge, N., Koyuncu, I., 2013. Investigation of characterization and biofouling properties of PES membrane containing selenium and copper nanoparticles. *J. Membr. Sci.* **437**, 216–226. https://doi.org/10.1016/j.memsci.2013.02.012

Al Aani, S., Wright, C.J., Atieh, M.A., Hilal, N., 2017. Engineering nanocomposite membranes: Addressing current challenges and future opportunities. *Desalination*, 50th anniversary of Desalination **401**, 1–15. https://doi.org/10.1016/j.desal.2016.08.001

Almeida, M.I.G.S., Cattrall, R.W., Kolev, S.D., 2017. Polymer inclusion membranes (PIMs) in chemical analysis - A review. *Anal. Chim. Acta* **987**, 1–14. https://doi.org/10.1016/j.aca.2017.07.032

Almeida, M.I.G.S., Cattrall, R.W., Kolev, S.D., 2012. Recent trends in extraction and transport of metal ions using polymer inclusion membranes (PIMs). *J. Membr. Sci.* **415–416**, 9–23. https://doi.org/10.1016/j.memsci.2012.06.006

Almeida, M.I.G.S., Chan, C., Pettigrove, V.J., Cattrall, R.W., Kolev, S.D., 2014. Development of a passive sampler for Zinc(II) in urban pond waters using a polymer inclusion membrane. *Environ. Pollut.* **193**, 233–239. https://doi.org/10.1016/j.envpol.2014.06.040

Almeida, M.I.G.S., Silva, A.M.L., Coleman, R.A., Pettigrove, V.J., Cattrall, R.W., Kolev, S.D., 2016. Development of a passive sampler based on a polymer inclusion membrane for total ammonia monitoring in freshwaters. *Anal. Bioanal. Chem.* **408**, 3213–3222. https://doi.org/10.1007/s00216-016-9394-2

Alula, M.T., Karamchand, L., Hendricks, N.R., Blackburn, J.M., 2018. Citrate-capped silver nanoparticles as a probe for sensitive and selective colorimetric and spectrophotometric sensing of creatinine in human urine. *Anal. Chim. Acta* **1007**, 40–49. https://doi.org/10.1016/j.aca.2017.12.016

Andrade, P.F., de Faria, A.F., Oliveira, S.R., Arruda, M.A.Z., Gonçalves, M. do C., 2015. Improved antibacterial activity of nanofiltration polysulfone membranes modified with silver nanoparticles. *Water Res.* **81**, 333–342. https://doi.org/10.1016/j.watres.2015.05.006

Annane, K., Sahmoune, A., Montels, P., Tingry, S., 2015. Polymer inclusion membrane extraction of cadmium(II) with Aliquat 336 in micro-channel cell. *Chem. Eng. Res. Des.* **94**, 605–610. https://doi.org/10.1016/j.cherd.2014.10.004

A Saf, S Alpaydin, A Coskun, M Ersoz, 2011. Selective transport and removal of Cr(VI) through polymer inclusion membrane containing 5 - (4-phenoxyphe- nyl)- 6H - 1,3,4-thiadiazin- 2- amine as a carrier. *J.Membr.Sci.* **377**, 241–248.

Argiropoulos, G., Cattrall, R.W., Hamilton, I.C., Kolev, S.D., Paimin, R., 1998. The study of a membrane for extracting gold(III) from hydrochloric acid solutions. *J. Membr. Sci.* **138**, 279–285. https://doi.org/10.1016/S0376-7388(97)00235-4

Arous, O., Amara, M., Kerdjoudj, H., 2010a. SELECTIVE TRANSPORT OF METAL IONS USING POLYMER INCLUSION MEMBRANES CONTAINING CROWN ETHERS AND CRYPTANDS 16.

Arous, O., Amara, M., Trari, M., Bouguelia, A., Kerdjoudj, H., 2010b. Cadmium (II) and lead (II) transport in a polymer inclusion membrane using tributyl phosphate as mobile carrier and CuFeO2 as a polarized photo electrode. *J. Hazard. Mater.* **180**, 493–498. https://doi.org/10.1016/j.jhazmat.2010.04.057

Arous, O., Kerdjoudj, H., Seta, P., 2004. Comparison of carrier-facilitated silver (i) and copper

(ii) ions transport mechanisms in a supported liquid membrane and in a plasticized cellulose triacetate membrane. *J. Membr. Sci.* **241**, 177–185. https://doi.org/10.1016/j.memsci.2004.04.024

Ashok Kumar, S.K., Shipra, Manjusha, 2010. Dual behavior of thiuram sulphide: Highly selective transport and ion-selective electrode for Ag(I) ions under two different conditions. *J. Membr. Sci.* **350**, 161–171. https://doi.org/10.1016/j.memsci.2009.12.024

Atkins, P., Overton, T., 2010. Shriver and Atkins' Inorganic Chemistry. OUP Oxford.

Bassyouni, M., Abdel-Aziz, M.H., Zoromba, M.S., Abdel-hamid, S.M.S., Drioli, E., 2019. A review of polymeric nanocomposite membranes for water purification. *J. Ind. Eng. Chem.* https://doi.org/10.1016/j.jiec.2019.01.045

Behl, M., Stout, M.D., Herbert, R.A., Dill, J.A., Baker, G.L., Hayden, B.K., Roycroft, J.H., Bucher, J.R., Hooth, M.J., 2015. Comparative toxicity and carcinogenicity of soluble and insoluble cobalt compounds. *Toxicology* **333**, 195–205. https://doi.org/10.1016/j.tox.2015.04.008

Bempah, C.K., Ewusi, A., Obiri-Yeboah, S., Asabere, B., Mensah, F., Boateng, J., Voigt, H.-J., 2013. Distribution of Arsenic and Heavy Metals from Mine Tailings dams at Obuasi Municipality of Ghana. *Am. J. Eng. Res.* 10.

Bonggotgetsakul, Y.Y.N., Cattrall, R.W., Kolev, S.D., 2016. Recovery of gold from aqua regia digested electronic scrap using a poly(vinylidene fluoride-co-hexafluoropropene) (PVDF-HFP) based polymer inclusion membrane (PIM) containing Cyphos® IL 104. *J. Membr. Sci.* **514**, 274–281. https://doi.org/10.1016/j.memsci.2016.05.002

Bonggotgetsakul, Y.Y.N., Cattrall, R.W., Kolev, S.D., 2015. A method for coating a polymer inclusion membrane with palladium nanoparticles. *React. Funct. Polym.* **97**, 30–36. https://doi.org/10.1016/j.reactfunctpolym.2015.10.003

C Harman, J Allan, ELM Vermeirssen, 2012. Calibration and use of the polar organic chemical integrative sampler—a critical review [WWW Document]. URL https://setac.onlinelibrary.wiley.com/doi/full/10.1002/etc.2011 (accessed 2.7.19).

Cai, C., Yang, F., Zhao, Z., Liao, Q., Bai, R., Guo, W., Chen, P., Zhang, Y., Zhang, H., 2019. Promising transport and high-selective separation of Li(I) from Na(I) and K(I) by a functional

polymer inclusion membrane (PIM) system. *J. Membr. Sci.* **579**, 1–10. https://doi.org/10.1016/j.memsci.2019.02.046

Calzadilla, A., Rehdanz, K., Tol, R.S.J., 2011. Water scarcity and the impact of improved irrigation management: a computable general equilibrium analysis. *Agric. Econ.* **42**, 305–323. https://doi.org/10.1111/j.1574-0862.2010.00516.x

Cempel, M., Nikel, G., 2006. Nickel: A review of its sources and environmental toxicology. *Pol. J. Environ. Stud.* **15**, 375–382.

Chen, L., Wu, Y., Dong, H., Meng, M., Li, C., Yan, Y., Chen, J., 2018. An overview on membrane strategies for rare earths extraction and separation. *Sep. Purif. Technol.* **197**, 70–85. https://doi.org/10.1016/j.seppur.2017.12.053

Chen, Y., Feng, S., Huang, Y., Yuan, D., 2015. Redox speciation analysis of dissolved iron in estuarine and coastal waters with on-line solid phase extraction and graphite furnace atomic absorption spectrometry detection. *Talanta* **137**, 25–30. https://doi.org/10.1016/j.talanta.2015.01.017

Cho, Y., Xu, C., Cattrall, R.W., Kolev, S.D., 2011. A polymer inclusion membrane for extracting thiocyanate from weakly alkaline solutions. *J. Membr. Sci.* **367**, 85–90. https://doi.org/10.1016/j.memsci.2010.10.040

Criquet, J., Dumoulin, D., Howsam, M., Mondamert, L., Goossens, J.-F., Prygiel, J., Billon, G., 2017. Comparison of POCIS passive samplers vs. composite water sampling: A case study. *Sci. Total Environ.* **609**, 982–991. https://doi.org/10.1016/j.scitotenv.2017.07.227

Croft, C.F., Almeida, M.I.G.S., Cattrall, R.W., Kolev, S.D., 2018. Separation of lanthanum(III), gadolinium(III) and ytterbium(III) from sulfuric acid solutions by using a polymer inclusion membrane. *J. Membr. Sci.* **545**, 259–265. https://doi.org/10.1016/j.memsci.2017.09.085

Danesi, P.R., Reichley-Yinger, L., Rickert, P.G., 1987. Lifetime of supported liquid membranes: the influence of interfacial properties, chemical composition and water transport on the long-term stability of the membranes. *J. Membr. Sci.* **31**, 117–145. https://doi.org/10.1016/S0376-7388(00)82223-1

Dasari, A., Quirós, J., Herrero, B., Boltes, K., García-Calvo, E., Rosal, R., 2012. Antifouling membranes prepared by electrospinning polylactic acid containing biocidal nanoparticles. *J. Membr. Sci.* **405–406**, 134–140. https://doi.org/10.1016/j.memsci.2012.02.060

Davison, W., Zhang, H., 2012. Progress in understanding the use of diffusive gradients in thin films (DGT) – back to basics. *Environ. Chem.* **9**, 1–13. https://doi.org/10.1071/EN11084

Dharmadasa, P., Kim, N., Thunders, M., 2017. Maternal cadmium exposure and impact on foetal gene expression through methylation changes. *Food Chem. Toxicol.* **109**, 714–720. https://doi.org/10.1016/j.fct.2017.09.002

Distefano, T., Kelly, S., 2017. Are we in deep water? Water scarcity and its limits to economic growth. *Ecol. Econ.* **142**, 130–147. https://doi.org/10.1016/j.ecolecon.2017.06.019

Durand, J.F., 2012. The impact of gold mining on the Witwatersrand on the rivers and karst system of Gauteng and North West Province, South Africa. *J. Afr. Earth Sci.* **68**, 24–43. https://doi.org/10.1016/j.jafrearsci.2012.03.013

Elias, G., Díez, S., Fontàs, C., 2019. System for mercury preconcentration in natural waters based on a polymer inclusion membrane incorporating an ionic liquid. *J. Hazard. Mater.* **371**, 316–322. https://doi.org/10.1016/j.jhazmat.2019.03.017

El-Kady, A.A., Abdel-Wahhab, M.A., 2018. Occurrence of trace metals in foodstuffs and their health impact. *Trends Food Sci. Technol.* **75**, 36–45. https://doi.org/10.1016/j.tifs.2018.03.001

Ershad, M., Almeida, M.I.G.S., Spassov, T.G., Cattrall, R.W., Kolev, S.D., 2018. Polymer inclusion membranes (PIMs) containing purified dinonylnaphthalene sulfonic acid (DNNS): Performance and selectivity. *Sep. Purif. Technol.* **195**, 446–452. https://doi.org/10.1016/j.seppur.2017.12.037

Esteve-Turrillas, F.A., Yusà, V., Pastor, A., de la Guardia, M., 2008. New perspectives in the use of semipermeable membrane devices as passive samplers. *Talanta* **74**, 443–457. https://doi.org/10.1016/j.talanta.2007.06.019

Facchinelli, A., Sacchi, E., Mallen, L., 2001. Multivariate statistical and GIS-based approach to identify heavy metal sources in soils. *Environ. Pollut. Barking Essex 1987* **114**, 313–324.

Fadel, M., Hassanein, N.M., Elshafei, M.M., Mostafa, A.H., Ahmed, M.A., Khater, H.M., 2017. Biosorption of manganese from groundwater by biomass of Saccharomyces cerevisiae. *HBRC J.* **13**, 106–113. https://doi.org/10.1016/j.hbrcj.2014.12.006

Farooq, U., Kozinski, J.A., Khan, M.A., Athar, M., 2010. Biosorption of heavy metal ions using wheat based biosorbents – A review of the recent literature. *Bioresour. Technol.* **101**, 5043–5053. https://doi.org/10.1016/j.biortech.2010.02.030

Fashola, M., Ngole-Jeme, V., Babalola, O., 2016. Heavy Metal Pollution from Gold Mines: Environmental Effects and Bacterial Strategies for Resistance. *Int. J. Environ. Res. Public. Health* **13**, 1047. https://doi.org/10.3390/ijerph13111047

Figueiredo, A.S., Sánchez-Loredo, M.G., Maurício, A., Pereira, M.F.C., Minhalma, M., Pinho, M.N. de, 2015. Tailoring of structures and permeation properties of asymmetric nanocomposite cellulose acetate/silver membranes. *J. Appl. Polym. Sci.* **132**. https://doi.org/10.1002/app.41796

Fontàs, C., Tayeb, R., Tingry, S., Hidalgo, M., Seta, P., 2005. Transport of platinum(IV) through supported liquid membrane (SLM) and polymeric plasticized membrane (PPM). *J. Membr. Sci.* **263**, 96–102. https://doi.org/10.1016/j.memsci.2005.04.008

Fontàs, C., Vera, R., Batalla, A., Kolev, S.D., Anticó, E., 2014. A novel low-cost detection method for screening of arsenic in groundwater. *Environ. Sci. Pollut. Res.* **21**, 11682–11688. https://doi.org/10.1007/s11356-014-2917-5

Frost, M.S., Dempsey, M.J., Whitehead, D.E., 2017. The response of citrate functionalised gold and silver nanoparticles to the addition of heavy metal ions. *Colloids Surf. Physicochem. Eng. Asp.* **518**, 15–24. https://doi.org/10.1016/j.colsurfa.2016.12.036

Fu, F., Wang, Q., 2011. Removal of heavy metal ions from wastewaters: A review. *J. Environ. Manage.* **92**, 407–418. https://doi.org/10.1016/j.jenvman.2010.11.011

G. Wulfsberg, 1987. Principles of Descriptive Cheistry [WWW Document]. URL https://www.wou.edu/las/physci/ch412/Table1.htm (accessed 5.1.19).

Garcia-Rodríguez, A., Fontàs, C., Matamoros, V., Almeida, M.I.G.S., Cattrall, R.W., Kolev, S.D., 2016. Development of a polymer inclusion membrane-based passive sampler for monitoring of sulfamethoxazole in natural waters. Minimizing the effect of the flow pattern of the aquatic system. *Microchem. J.* **124**, 175–180. https://doi.org/10.1016/j.microc.2015.08.017

Garcia-Rodríguez, A., Matamoros, V., Kolev, S.D., Fontàs, C., 2015. Development of a polymer inclusion membrane (PIM) for the preconcentration of antibiotics in environmental water samples. *J. Membr. Sci.* **492**, 32–39. https://doi.org/10.1016/j.memsci.2015.05.037

Gega, J., Otrembska, P., 2014. Separation of Ni(II) and Cd(II) Ions with Supported Liquid Membranes (SLM) using D2EHPA as a Carrier. *Sep. Sci. Technol.* **49**, 1756–1760. https://doi.org/10.1080/01496395.2014.906463

Geng, H.-X., Wang, L., 2019. Cadmium: Toxic effects on placental and embryonic development. *Environ. Toxicol. Pharmacol.* **67**, 102–107. https://doi.org/10.1016/j.etap.2019.02.006

Gherasim, C.-V.I., Bourceanu, G., Olariu, R.-I., Arsene, C., 2011. Removal of lead(II) from aqueous solutions by a polyvinyl-chloride inclusion membrane without added plasticizer. *J. Membr. Sci.* **377**, 167–174. https://doi.org/10.1016/j.memsci.2011.04.042

Gherrou, A., Kerdjoudj, H., Molinari, R., Seta, P., 2005. Preparation and characterization of polymeric plasticized membranes (PPM) embedding a crown ether carrier application to copper ions transport. *Mater. Sci. Eng. C* **25**, 436–443. https://doi.org/10.1016/j.msec.2004.11.002

Gherrou, A., Kerdjoudj, H., Molinari, R., Seta, P., Drioli, E., 2004. Fixed sites plasticized cellulose triacetate membranes containing crown ethers for silver(I), copper(II) and gold(III) ions transport. *J. Membr. Sci.* **228**, 149–157. https://doi.org/10.1016/j.memsci.2003.10.003

Gille, D., Schmid, A., 2015. Vitamin B12 in meat and dairy products. *Nutr. Rev.* **73**, 106–115. https://doi.org/10.1093/nutrit/nuu011

Gordon, C.S., Lowe, J.T., 1927. Carbon-monoxide detector. US1644014A.

Górecki, T., Namieśnik, J., 2002. Passive sampling. *TrAC Trends Anal. Chem.* **21**, 276–291. https://doi.org/10.1016/S0165-9936(02)00407-7

Granado-Castro, M.D., Casanueva-Marenco, M.J., Galindo-Riaño, M.D., El Mai, H., Díaz-deAlba, M., 2018. A separation and preconcentration process for metal speciation using a liquid membrane: A case study for iron speciation in seawater. *Mar. Chem.* **198**, 56–63. https://doi.org/10.1016/j.marchem.2017.11.009

Gujja, P., Rosing, D.R., Tripodi, D.J., Shizukuda, Y., 2010. Iron Overload Cardiomyopathy: Better Understanding of an Increasing Disorder. *J. Am. Coll. Cardiol.* **56**, 1001–1012. https://doi.org/10.1016/j.jacc.2010.03.083

Guo, L., Zhang, J., Zhang, D., Liu, Y., Deng, Y., Chen, J., 2012. Preparation of Poly(vinylidene fluoride -tetrafluoroethylene)-Based Polymer Inclusion Membrane Using Bifunctional Ionic Liquid Extractant for Cr(VI) Transport. *Ind. Eng. Chem. Res.* **51**, 2714–2722. https://doi.org/10.1021/ie201824s

de Gyves, J., Rodríguez de San Miguel, E., 1999. Metal Ion Separations by Supported Liquid Membranes. *Ind. Eng. Chem. Res.* **38**, 2182–2202. https://doi.org/10.1021/ie980374p

Hashim, M.A., Mukhopadhyay, S., Sahu, J.N., Sengupta, B., 2011. Remediation technologies for heavy metal contaminated groundwater. *J. Environ. Manage.* **92**, 2355–2388. https://doi.org/10.1016/j.jenvman.2011.06.009

Hodson, M.E., 2004. Heavy metals—geochemical bogey men? *Environ. Pollut.* **129**, 341–343. https://doi.org/10.1016/j.envpol.2003.11.003

Hussain, M.B., Ali, S., Azam, A., Hina, S., Ahsan, M., Farooq, B.A., Bharwana, S.A., Gill, M.B., 2013. Morphological, physiological and biochemical responses of plants to nickel stress: a review. *Afr J Agric Res* **8**, 1596–1602.

Ihsanullah, Abbas, A., Al-Amer, A.M., Laoui, T., Al-Marri, M.J., Nasser, M.S., Khraisheh, M., Atieh, M.A., 2016. Heavy metal removal from aqueous solution by advanced carbon nanotubes: Critical review of adsorption applications. *Sep. Purif. Technol.* **157**, 141–161. https://doi.org/10.1016/j.seppur.2015.11.039

Ivanov, I., 2004. Increased current efficiency of zinc electrowinning in the presence of metal impurities by addition of organic inhibitors. *Hydrometallurgy* **72**, 73–78. https://doi.org/10.1016/S0304-386X(03)00129-4

Jacob, J.M., Karthik, C., Saratale, R.G., Kumar, S.S., Prabakar, D., Kadirvelu, K., Pugazhendhi, A., 2018. Biological approaches to tackle heavy metal pollution: A survey of literature. *J. Environ. Manage.* **217**, 56–70. https://doi.org/10.1016/j.jenvman.2018.03.077

Jean, E., Villemin, D., Hlaibi, M., Lebrun, L., 2018. Heavy metal ions extraction using new supported liquid membranes containing ionic liquid as carrier. *Sep. Purif. Technol.* **201**, 1–9. https://doi.org/10.1016/j.seppur.2018.02.033

Jhaveri, J.H., Murthy, Z.V.P., 2016. Nanocomposite membranes. *Desalination Water Treat.* **57**, 26803–26819. https://doi.org/10.1080/19443994.2015.1120687

Johary, F., Jamaluddin, N.A., Rohani, R., Hassan, A.R., Sharifuddin, S.S., Isa, M.H.M., 2018a. Development of polyethersulfone (PES)/silver nanoparticles (AgNPs)/polyethylene glycol (PEG) nanofiltration membrane. p. 030022. https://doi.org/10.1063/1.5041243

Kang, G., Cao, Y., 2014. Application and modification of poly(vinylidene fluoride) (PVDF) membranes – A review. *J. Membr. Sci.* **463**, 145–165. https://doi.org/10.1016/j.memsci.2014.03.055

Karthik, C., Oves, M., Thangabalu, R., Sharma, R., Santhosh, S.B., Indra Arulselvi, P., 2016. Cellulosimicrobium funkei-like enhances the growth of Phaseolus vulgaris by modulating oxidative damage under Chromium(VI) toxicity. *J. Adv. Res.* **7**, 839–850. https://doi.org/10.1016/j.jare.2016.08.007

Kaufmann, R.B., Staes, C.J., Matte, T.D., 2003. Deaths related to lead poisoning in the United States, 1979-1998. *Environ. Res.* **91**, 78–84.

Kaya, A., Onac, C., Alpoguz, H.K., Yilmaz, A., Atar, N., 2016. Removal of Cr(VI) through calixarene based polymer inclusion membrane from chrome plating bath water. *Chem. Eng. J.* **283**, 141–149. https://doi.org/10.1016/j.cej.2015.07.052

Kebiche-Senhadji, O., Bey, S., Clarizia, G., Mansouri, L., Benamor, M., 2011. Gas permeation behavior of CTA polymer inclusion membrane (PIM) containing an acidic carrier for metal recovery (DEHPA). *Sep. Purif. Technol.* **80**, 38–44. https://doi.org/10.1016/j.seppur.2011.03.032

Khalid, A., Ibrahim, A., Al-Hamouz, O.C.S., Laoui, T., Benamor, A., Atieh, M.A., 2017a. Fabrication of polysulfone nanocomposite membranes with silver-doped carbon nanotubes and their antifouling performance. *J. Appl. Polym. Sci.* **134**. https://doi.org/10.1002/app.44688

Khalid, S., Shahid, M., Niazi, N.K., Murtaza, B., Bibi, I., Dumat, C., 2017b. A comparison of technologies for remediation of heavy metal contaminated soils. *J. Geochem. Explor.*, Remediation of Polluted Soils - Part 2 **182**, 247–268. https://doi.org/10.1016/j.gexplo.2016.11.021

Khan, M.S., Zaidi, A., Wani, P.A., Oves, M., 2009. Role of plant growth promoting rhizobacteria in the remediation of metal contaminated soils. *Environ. Chem. Lett.* **7**, 1–19. https://doi.org/10.1007/s10311-008-0155-0

Kim, J.S., Kim, S.K., Cho, M.H., Lee, S.H., Kim, J.Y., Kwon, S.G., Lee, E.H., 2001. Permeation of silver ion through polymeric CTA membrane containing acyclic polyether bearing amide and amine end-group. *Bull. Korean Chem. Soc.* **22**, 1076–1080.

Kim, J.S., Kim, S.K., Ko, J.W., Kim, E.T., Yu, S.H., Cho, M.H., Kwon, S.G., Lee, E.H., 2000. Selective transport of cesium ion in polymeric CTA membrane containing calixcrown ethers. *Talanta* **52**, 1143–1148. https://doi.org/10.1016/S0039-9140(00)00489-6

Kim, J.S., Kuk, E., Yu, K.N., Kim, J.-H., Park, S.J., Lee, H.J., Kim, S.H., Park, Y.K., Park, Y.H., Hwang, C.-Y., Kim, Y.-K., Lee, Y.-S., Jeong, D.H., Cho, M.-H., 2007. Antimicrobial effects of silver nanoparticles. *Nanomedicine Nanotechnol. Biol. Med.* **3**, 95–101. https://doi.org/10.1016/j.nano.2006.12.001

Kolev, S.D., St John, A.M., Cattrall, R.W., 2013. Mathematical modeling of the extraction of uranium(VI) into a polymer inclusion membrane composed of PVC and di-(2-ethylhexyl) phosphoric acid. *J. Membr. Sci.* **425–426**, 169–175. https://doi.org/10.1016/j.memsci.2012.08.050

Koseoglu-Imer, D.Y., Kose, B., Altinbas, M., Koyuncu, I., 2013. The production of polysulfone (PS) membrane with silver nanoparticles (AgNP): Physical properties, filtration performances, and biofouling resistances of membranes. *J. Membr. Sci.* **428**, 620–628. https://doi.org/10.1016/j.memsci.2012.10.046

Kozlowski, C.A., Walkowiak, W., 2005. Applicability of liquid membranes in chromium(VI) transport with amines as ion carriers. *J. Membr. Sci.* **266**, 143–150. https://doi.org/10.1016/j.memsci.2005.04.053

Kubota, F., Kono, R., Yoshida, W., Sharaf, M., Kolev, S.D., Goto, M., 2019. Recovery of gold ions from discarded mobile phone leachate by solvent extraction and polymer inclusion membrane (PIM) based separation using an amic acid extractant. *Sep. Purif. Technol.* **214**, 156–161. https://doi.org/10.1016/j.seppur.2018.04.031

Kumar, M., Lawler, J., 2014. Preparation and characterization of negatively charged organicinorganic hybrid ultrafiltration membranes for protein separation. *Sep. Purif. Technol.* **130**, 112–123. https://doi.org/10.1016/j.seppur.2014.04.027

Kumar, P., Kim, K.-H., Bansal, V., Lazarides, T., Kumar, N., 2017. Progress in the sensing techniques for heavy metal ions using nanomaterials. *J. Ind. Eng. Chem.* **54**, 30–43. https://doi.org/10.1016/j.jiec.2017.06.010

Lacan, P., Guizard, C., Le Gall, P., Wettling, D., Cot, L., 1995. Facilitated transport of ions through fixed-site carrier membranes derived from hybrid organic-inorganic materials. *J. Membr. Sci.* **100**, 99–109. https://doi.org/10.1016/0376-7388(94)00259-2

Lakhal-Littleton, S., 2019. Mechanisms of cardiac iron homeostasis and their importance to heart function. *Free Radic. Biol. Med.*, Iron as Soul of Life on Earth Revisited: From Chemical

Reaction, Ferroptosis to Therapeutics **133**, 234–237. https://doi.org/10.1016/j.freeradbiomed.2018.08.010

Lamb, J.D., Nazarenko, A.Y., 1997. Lead(II) ion sorption and transport using polymer inclusion membranes containing tri-octylphosphine oxide. *J. Membr. Sci.* **134**, 255–259. https://doi.org/10.1016/S0376-7388(97)00115-4

Larsson, S.C., Wolk, A., 2016. Urinary cadmium and mortality from all causes, cancer and cardiovascular disease in the general population: systematic review and meta-analysis of cohort studies. *Int. J. Epidemiol.* **45**, 782–791. https://doi.org/10.1093/ije/dyv086

Lee, P.C., Meisel, D., 2002. Adsorption and surface-enhanced Raman of dyes on silver and gold sols [WWW Document]. https://doi.org/10.1021/j100214a025

Levitskaia, T.G., Lamb, J.D., Fox, K.L., Moyer, B.A., 2002. Selective carrier-mediated cesium transport through polymer inclusion membranes by calix[4]arene-crown-6 carriers from complex aqueous mixtures. *Radiochim. Acta* **90**, 43–52.

Levitskaia, T.G., Macdonald, D.M., Lamb, J.D., Moyer, B.A., 2000. Prediction of the carriermediated cation flux through polymer inclusion membranes via fundamental thermodynamic quantities: complexation study of bis(dodecyloxy)calix[4]arene-crown-6 with alkali metal cations. *Phys. Chem. Chem. Phys.* **2**, 1481–1491. https://doi.org/10.1039/A908840G

Leyssens, L., Vinck, B., Van Der Straeten, C., Wuyts, F., Maes, L., 2017. Cobalt toxicity in humans—A review of the potential sources and systemic health effects. *Toxicology* **387**, 43–56. https://doi.org/10.1016/j.tox.2017.05.015

Linder, M.C., 2013. Biochemistry of Copper. Springer Science & Business Media.

Lytle, D.A., Wahman, D.G., Schock, M.R., Nadagouda, M.N., Harmon, S., Webster, K., Botkins, J., 2019. Georgeite: A rare copper mineral with important drinking water implications. *Chem. Eng. J.* **355**, 1–10. https://doi.org/10.1016/j.cej.2018.08.106

Ma, Q., Song, J., Zhang, S., Wang, M., Guo, Y., Dong, C., 2016. Colorimetric detection of riboflavin by silver nanoparticles capped with β-cyclodextrin-grafted citrate. *Colloids Surf. B Biointerfaces* **148**, 66–72. https://doi.org/10.1016/j.colsurfb.2016.08.040

Maret, W., 2016. The Metals in the Biological Periodic System of the Elements: Concepts and

Conjectures. *Int. J. Mol. Sci.* **17**, 66. https://doi.org/10.3390/ijms17010066 Marulasiddeshwara, M.B., Dakshayani, S.S., Sharath Kumar, M.N., Chethana, R., Raghavendra Kumar, P., Devaraja, S., 2017. Facile-one pot-green synthesis, antibacterial, antifungal, antioxidant and antiplatelet activities of lignin capped silver nanoparticles: A promising therapeutic agent. *Mater. Sci. Eng. C* **81**, 182–190. https://doi.org/10.1016/j.msec.2017.07.054

Mekonnen, M.M., Hoekstra, A.Y., 2016. Four billion people facing severe water scarcity. *Sci. Adv.* **2**, e1500323. https://doi.org/10.1126/sciadv.1500323

Miège, C., Mazzella, N., Allan, I., Dulio, V., Smedes, F., Tixier, C., Vermeirssen, E., Brant, J., O'Toole, S., Budzinski, H., Ghestem, J.-P., Staub, P.-F., Lardy-Fontan, S., Gonzalez, J.-L., Coquery, M., Vrana, B., 2015. Position paper on passive sampling techniques for the monitoring of contaminants in the aquatic environment – Achievements to date and perspectives. *Trends Environ. Anal. Chem.* **8**, 20–26. https://doi.org/10.1016/j.teac.2015.07.001

Moghimi Benhangi, H., Ahmadi, S., Hakimi, M., Molafilabi, A., Faraji, H., Mashkani, B., 2019. Protective effects of isatin and its synthetic derivatives against iron, copper and lead toxicity. *Toxicol. In Vitro* **54**, 232–236. https://doi.org/10.1016/j.tiv.2018.10.004

Mokkapati, V.R.S.S., Koseoglu-Imer, D.Y., Yilmaz-Deveci, N., Mijakovic, I., Koyuncu, I., 2017. Membrane properties and anti-bacterial/anti-biofouling activity of polysulfone–graphene oxide composite membranes phase inversed in graphene oxide non-solvent †Electronic supplementary information (ESI) available. See DOI: 10.1039/c6ra25015g Click here for additional data file. *Rsc Adv.* **7**, 4378–4386. https://doi.org/10.1039/c6ra25015g

M.S, J., Soontarapa, K., Padaki, M., Geetha, B., Isloor, A., 2017. Favorable influence of mPIAM on PSf blend membranes for ion rejection. *J. Membr. Sci.* **533**, 229–240. https://doi.org/10.1016/j.memsci.2017.03.039

Nasir, A.M., Goh, P.S., Ismail, A.F., 2019. Highly adsorptive polysulfone/hydrous iron-nickelmanganese (PSF/HINM) nanocomposite hollow fiber membrane for synergistic arsenic removal. *Sep. Purif. Technol.* **213**, 162–175. https://doi.org/10.1016/j.seppur.2018.12.040

Nghiem, L., Mornane, P., Potter, I., Perera, J., Cattrall, R., Kolev, S., 2006. Extraction and transport of metal ions and small organic compounds using polymer inclusion membranes (PIMs). *J. Membr. Sci.* **281**, 7–41. https://doi.org/10.1016/j.memsci.2006.03.035

Nguyen, T.A.H., Ngo, H.H., Guo, W.S., Zhang, J., Liang, S., Yue, Q.Y., Li, Q., Nguyen, T.V., 2013. Applicability of agricultural waste and by-products for adsorptive removal of heavy metals from wastewater. *Bioresour. Technol.* **148**, 574–585. https://doi.org/10.1016/j.biortech.2013.08.124

Nthunya, L.N., Masheane, M.L., Malinga, S.P., Nxumalo, E.N., Mamba, B.B., Mhlanga, S.D., 2017. Determination of toxic metals in drinking water sources in the Chief Albert Luthuli Local Municipality in Mpumalanga, South Africa. *Phys. Chem. Earth Parts ABC*, Infrastructural Planning for Water Security in Eastern and Southern Africa **100**, 94–100. https://doi.org/10.1016/j.pce.2017.04.006

Nuapia, Y., Chimuka, L., Cukrowska, E., 2018. Assessment of heavy metals in raw food samples from open markets in two African cities. *Chemosphere* **196**, 339–346. https://doi.org/10.1016/j.chemosphere.2017.12.134

Ocampo, A.L., Aguilar, J.C., Rodríguez de San Miguel, E., Monroy, M., Roquero, P., de Gyves, J., 2009. Novel proton-conducting polymer inclusion membranes. *J. Membr. Sci.* **326**, 382–387. https://doi.org/10.1016/j.memsci.2008.10.010

Okem, A., Southway, C., Stirk, W.A., Street, R.A., Finnie, J.F., Van Staden, J., 2014. Heavy metal contamination in South African medicinal plants: A cause for concern. *South Afr. J. Bot.* **93**, 125–130. https://doi.org/10.1016/j.sajb.2014.04.001

Onac, C., Kaya, A., Ataman, D., Gunduz, N.A., Alpoguz, H.K., 2019. The removal of Cr(VI) through polymeric supported liquid membrane by using calix[4]arene as a carrier. *Chin. J. Chem. Eng.* **27**, 85–91. https://doi.org/10.1016/j.cjche.2018.01.029

Palmes, E.D., Gunnison, A.F., 1973. Personal monitoring device for gaseous contaminants. *Am. Ind. Hyg. Assoc. J.* **34**, 78–81. https://doi.org/10.1080/0002889738506810

Panzarini, E., Mariano, S., Vergallo, C., Carata, E., Fimia, G.M., Mura, F., Rossi, M., Vergaro, V., Ciccarella, G., Corazzari, M., Dini, L., 2017. Glucose capped silver nanoparticles induce cell cycle arrest in HeLa cells. *Toxicol. In Vitro* **41**, 64–74. https://doi.org/10.1016/j.tiv.2017.02.014

Papanikolaou, G., Pantopoulos, K., 2005. Iron metabolism and toxicity. *Toxicol. Appl. Pharmacol.* **202**, 199–211. https://doi.org/10.1016/j.taap.2004.06.021

Patil, D.S., Chavan, S.M., Oubagaranadin, J.U.K., 2016. A review of technologies for manganese removal from wastewaters. *J. Environ. Chem. Eng.* **4**, 468–487. https://doi.org/10.1016/j.jece.2015.11.028

Patil, M.P., Singh, R.D., Koli, P.B., Patil, K.T., Jagdale, B.S., Tipare, A.R., Kim, G.-D., 2018. Antibacterial potential of silver nanoparticles synthesized using Madhuca longifolia flower extract as a green resource. *Microb. Pathog.* **121**, 184–189. https://doi.org/10.1016/j.micpath.2018.05.040

Paustenbach, D.J., Tvermoes, B.E., Unice, K.M., Finley, B.L., Kerger, B.D., 2013. A review of the health hazards posed by cobalt. *Crit. Rev. Toxicol.* **43**, 316–362. https://doi.org/10.3109/10408444.2013.779633

Pellera, F.-M., Giannis, A., Kalderis, D., Anastasiadou, K., Stegmann, R., Wang, J.-Y., Gidarakos, E., 2012. Adsorption of Cu(II) ions from aqueous solutions on biochars prepared from agricultural by-products. *J. Environ. Manage.* **96**, 35–42. https://doi.org/10.1016/j.jenvman.2011.10.010

Pereira, N., St John, A., Cattrall, R.W., Perera, J.M., Kolev, S.D., 2009. Influence of the composition of polymer inclusion membranes on their homogeneity and flexibility. *Desalination*, International Membrane Science and Technology Conference 2007 **236**, 327–333. https://doi.org/10.1016/j.desal.2007.10.083

Pont, N., Salvadó, V., Fontàs, C., 2008. Selective transport and removal of Cd from chloride solutions by polymer inclusion membranes. *J. Membr. Sci.* **318**, 340–345. https://doi.org/10.1016/j.memsci.2008.02.057

Pourret, O., Bollinger, J.-C., 2018. "Heavy metal" - What to do now: To use or not to use? *Sci. Total Environ.* **610–611**, 419–420. https://doi.org/10.1016/j.scitotenv.2017.08.043

Ramanathan, S., Gopinath, S.C.B., Anbu, P., Lakshmipriya, T., Kasim, F.H., Lee, C.-G., 2018. Eco-friendly synthesis of Solanum trilobatum extract-capped silver nanoparticles is compatible with good antimicrobial activities. *J. Mol. Struct.* **1160**, 80–91. https://doi.org/10.1016/j.molstruc.2018.01.056

Rangabhashiyam, S., Balasubramanian, P., 2018. Characteristics, performances, equilibrium and kinetic modeling aspects of heavy metal removal using algae. *Bioresour. Technol. Rep.* https://doi.org/10.1016/j.biteb.2018.07.009

Rasheed, T., Bilal, M., Li, C., Nabeel, F., Khalid, M., Iqbal, H.M.N., 2018. Catalytic potential of bio-synthesized silver nanoparticles using Convolvulus arvensis extract for the degradation of environmental pollutants. *J. Photochem. Photobiol. B* **181**, 44–52. https://doi.org/10.1016/j.jphotobiol.2018.02.024

Rivaro, P., Luisa Abelmoschi, M., Grotti, M., Ianni, C., Magi, E., Margiotta, F., Massolo, S., Saggiomo, V., 2012. Combined effects of hydrographic structure and iron and copper availability on the phytoplankton growth in Terra Nova Bay Polynya (Ross Sea, Antarctica). *Deep Sea Res. Part Oceanogr. Res. Pap.* **62**, 97–110. https://doi.org/10.1016/j.dsr.2011.12.008

Ruihua, L., Lin, Z., Tao, T., Bo, L., 2011. Phosphorus removal performance of acid mine drainage from wastewater. *J. Hazard. Mater.* **190**, 669–676. https://doi.org/10.1016/j.jhazmat.2011.03.097

SANS, 2006. Drinking water quality requirements. **241,** 1-3.

Safarpour, M., Vatanpour, V., Khataee, A., Esmaeili, M., 2015. Development of a novel high flux and fouling-resistant thin film composite nanofiltration membrane by embedding reduced graphene oxide/TiO2. *Sep. Purif. Technol.* **154**, 96–107. https://doi.org/10.1016/j.seppur.2015.09.039

Sastre, A.M., Kumar, A., Shukla, J.P., Singh, R.K., 1998. Improved Techniques in Liquid Membrane Separations: An Overview. *Sep. Purif. Methods* **27**, 213–298. https://doi.org/10.1080/03602549809351641

Scindia, Y.M., Pandey, A.K., Reddy, A.V.R., 2005. Coupled-diffusion transport of Cr(VI) across anion-exchange membranes prepared by physical and chemical immobilization methods. *J. Membr. Sci.* **249**, 143–152. https://doi.org/10.1016/j.memsci.2004.10.015

Seethapathy, S., Górecki, T., Li, X., 2008. Passive sampling in environmental analysis. *J. Chromatogr. A*, 50 Years Journal of Chromatography **1184**, 234–253. https://doi.org/10.1016/j.chroma.2007.07.070

Sellami, F., Kebiche-Senhadji, O., Marais, S., Couvrat, N., Fatyeyeva, K., 2019. Polymer inclusion membranes based on CTA/PBAT blend containing Aliquat 336 as extractant for removal of Cr(VI): Efficiency, stability and selectivity. *React. Funct. Polym.* **139**, 120–132. https://doi.org/10.1016/j.reactfunctpolym.2019.03.014

Shahzad, B., Tanveer, M., Rehman, A., Cheema, S.A., Fahad, S., Rehman, S., Sharma, A.,

2018. Nickel; whether toxic or essential for plants and environment - A review. *Plant Physiol. Biochem.* **132**, 641–651. https://doi.org/10.1016/j.plaphy.2018.10.014

Sikder, M.T., Rahman, M.M., Jakariya, M., Hosokawa, T., Kurasaki, M., Saito, T., 2019. Remediation of water pollution with native cyclodextrins and modified cyclodextrins: A comparative overview and perspectives. *Chem. Eng. J.* **355**, 920–941. https://doi.org/10.1016/j.cej.2018.08.218

Simões, L.C., Simões, M., 2013. Biofilms in drinking water: problems and solutions. *RSC Adv.* **3**, 2520–2533. https://doi.org/10.1039/C2RA22243D

Sobol, Z., Schiestl, R.H., 2012. Intracellular and extracellular factors influencing Cr(VI and Cr(III) genotoxicity. *Environ. Mol. Mutagen.* **53**, 94–100. https://doi.org/10.1002/em.20679

Sole, K.C., Feather, A.M., Cole, P.M., 2005. Solvent extraction in southern Africa: An update of some recent hydrometallurgical developments. *Hydrometallurgy*, Special Issue To Honour Mike Slater **78**, 52–78. https://doi.org/10.1016/j.hydromet.2004.11.012

Song, J., Huang, T., Qiu, H., Niu, X., Li, X.-M., Xie, Y., He, T., 2018. A critical review on membrane extraction with improved stability: Potential application for recycling metals from city mine. *Desalination*, Membrane Engineering for Desalination in the Mining and Extraction Industry **440**, 18–38. https://doi.org/10.1016/j.desal.2018.01.007

Sribudda, D., Sunsandee, N., Ramakul, P., Pancharoen, U., Phatanasri, S., 2015. Separation of Cd(II) from industrial wastewater via HFSLM: Equilibrium, kinetic and thermodynamic investigation. *J. Ind. Eng. Chem.* **25**, 22–28. https://doi.org/10.1016/j.jiec.2014.10.008

St John, A.M., Cattrall, R.W., Kolev, S.D., 2013. Determination of the initial flux of polymer inclusion membranes. *Sep. Purif. Technol.* **116**, 41–45. https://doi.org/10.1016/j.seppur.2013.05.021

St John, A.M., Cattrall, R.W., Kolev, S.D., 2012. Transport and separation of uranium(VI) by a polymer inclusion membrane based on di-(2-ethylhexyl) phosphoric acid. *J. Membr. Sci.* **409–410**, 242–250. https://doi.org/10.1016/j.memsci.2012.03.061

Strachan, S., 2010. Trace elements. *Curr. Anaesth. Crit. Care* **21**, 44–48. https://doi.org/10.1016/j.cacc.2009.08.004

Tayeb, R., Fontas, C., Dhahbi, M., Tingry, S., Seta, P., 2005. Cd(II) transport across supported liquid membranes (SLM) and polymeric plasticized membranes (PPM) mediated by Lasalocid A. *Sep. Purif. Technol.* **42**, 189–193. https://doi.org/10.1016/j.seppur.2004.07.006

Teow, Y.H., Latif, A.A., Lim, J.K., Ngang, H.P., Susan, L.Y., Ooi, B.S., 2015. Hydroxyl functionalized PVDF-TiO2 ultrafiltration membrane and its antifouling properties. *J. Appl. Polym. Sci.* **132**, 41844. https://doi.org/10.1002/app.41844

Thunhorst, K.L., Noble, R.D., Bowman, C.N., 1999. Properties of the transport of alkali metal salts through polymeric membranes containing benzo-18-crown-6 crown ether functional groups. *J. Membr. Sci.* **156**, 293–302. https://doi.org/10.1016/S0376-7388(98)00358-5

Tor, A., Arslan, G., Muslu, H., Celiktas, A., Cengeloglu, Y., Ersoz, M., 2009. Facilitated transport of Cr(III) through polymer inclusion membrane with di(2-ethylhexyl)phosphoric acid (DEHPA). *J. Membr. Sci.* **1–2**, 169–174. https://doi.org/10.1016/j.memsci.2008.12.032

Turner, A., 2019. Cadmium pigments in consumer products and their health risks. *Sci. Total Environ.* **657**, 1409–1418. https://doi.org/10.1016/j.scitotenv.2018.12.096

Tutu, H., McCarthy, T.S., Cukrowska, E., 2008. The chemical characteristics of acid mine drainage with particular reference to sources, distribution and remediation: The Witwatersrand Basin, South Africa as a case study. *Appl. Geochem.* **23**, 3666–3684. https://doi.org/10.1016/j.apgeochem.2008.09.002

USEPA, 2000. Risk Based Concentration Table.

Vatanpour, V., Madaeni, S.S., Moradian, R., Zinadini, S., Astinchap, B., 2011. Fabrication and characterization of novel antifouling nanofiltration membrane prepared from oxidized multiwalled carbon nanotube/polyethersulfone nanocomposite. *J. Membr. Sci.* **375**, 284–294. https://doi.org/10.1016/j.memsci.2011.03.055

Vrana, B., Allan, I.J., Greenwood, R., Mills, G.A., Dominiak, E., Svensson, K., Knutsson, J., Morrison, G., 2005. Passive sampling techniques for monitoring pollutants in water. *TrAC Trends Anal. Chem.* **24**, 845–868. https://doi.org/10.1016/j.trac.2005.06.006

Wang, D., Cattrall, R.W., Li, J., Almeida, M.I.G.S., Stevens, G.W., Kolev, S.D., 2017. A poly(vinylidene fluoride-co-hexafluoropropylene) (PVDF-HFP)-based polymer inclusion membrane (PIM) containing LIX84I for the extraction and transport of Cu(II) from its

ammonium sulfate/ammonia solutions. *J. Membr. Sci.* **542**, 272–279. https://doi.org/10.1016/j.memsci.2017.08.027

Wang, D., Hu, J., Li, Y., Fu, M., Liu, D., Chen, Q., 2016. Evidence on the 2-nitrophenyl octyl ether (NPOE) facilitating Copper(II) transport through polymer inclusion membranes. *J. Membr. Sci.* **501**, 228–235. https://doi.org/10.1016/j.memsci.2015.12.013

Wang, L., Paimin, R., Cattrall, R.W., Shen, W., Kolev, S.D., 2000. The extraction of cadmium(II) and copper(II) from hydrochloric acid solutions using an Aliquat 336/PVC membrane. *J. Membr. Sci.* **176**, 105–111. https://doi.org/10.1016/S0376-7388(00)00436-1

Wongkaew, K., Pancharoen, U., Phatanasri, S., Leepipatpiboon, N., Lothongkum, A.W., 2015. Effect of diluent polarity on membrane stability in the separation of trace Pd(II) from wastewater by HFSLM using LIX84-I. *J. Ind. Eng. Chem.* **21**, 212–220. https://doi.org/10.1016/j.jiec.2014.02.027

World Health Organisation [WWW Document], 2018. . *WHO*. URL http://www.who.int/mediacentre/factsheets/fs391/en/ (accessed 4.20.18).

World Health Organization, 2015. Progress on Sanitation and Drinking Water–2015 Update and MDG Assessment; World Health Organization. Geneva, Switzerland.

X. J. Yang, *, A. G. Fane, † and, Soldenhoff‡, K., 2002. Comparison of Liquid Membrane Processes for Metal Separations: Permeability, Stability, and Selectivity [WWW Document]. https://doi.org/10.1021/ie011044z

Yaftian, M.R., Almeida, M.I.G.S., Cattrall, R.W., Kolev, S.D., 2018. Selective extraction of vanadium(V) from sulfate solutions into a polymer inclusion membrane composed of poly(vinylidenefluoride-co-hexafluoropropylene) and Cyphos® IL 101. *J. Membr. Sci.* **545**, 57–65. https://doi.org/10.1016/j.memsci.2017.09.058

Yin, J., Deng, B., 2015. Polymer-matrix nanocomposite membranes for water treatment. *J. Membr. Sci.* **479**, 256–275. https://doi.org/10.1016/j.memsci.2014.11.019

Yoshida, W., Baba, Y., Kubota, F., Kolev, S.D., Goto, M., 2019. Selective transport of scandium(III) across polymer inclusion membranes with improved stability which contain an amic acid carrier. *J. Membr. Sci.* **572**, 291–299. https://doi.org/10.1016/j.memsci.2018.11.021

Zeng, Z., Liu, J., Savenije, H.H.G., 2013. A simple approach to assess water scarcity integrating

water quantity and quality. *Ecol. Indic.* **34**, 441–449. https://doi.org/10.1016/j.ecolind.2013.06.012

Zhang, L.L., Cattrall, R.W., Ashokkumar, M., Kolev, S.D., 2012a. On-line extractive separation in flow injection analysis based on polymer inclusion membranes: A study on membrane stability and approaches for improving membrane permeability. *Talanta* **97**, 382– 387. https://doi.org/10.1016/j.talanta.2012.04.049

Zhang, X., Yang, L., Li, Y., Li, H., Wang, W., Ye, B., 2012b. Impacts of lead/zinc mining and smelting on the environment and human health in China. *Environ. Monit. Assess.* **184**, 2261–2273. https://doi.org/10.1007/s10661-011-2115-6

Zoroddu, M.A., Aaseth, J., Crisponi, G., Medici, S., Peana, M., Nurchi, V.M., 2019. The essential metals for humans: A brief overview. *J. Inorg. Biochem.* https://doi.org/10.1016/j.jinorgbio.2019.03.013

Zukowska, J., Biziuk, M., 2008. Methodological evaluation of method for dietary heavy metal intake. *J. Food Sci.* **73**, 21–29. https://doi.org/10.1111/j.1750-3841.2007.00648.x

APPENDIX

Table A1 ANOVA analysis of PIMs water contact angle at different Ag NPs loadings

Anova: Single Factor						
SUMMARY						
Groups	*Count*	*Sum*	*Average*	*Variance*		
0 % AgNPS	10	886.40	88.64	35.23889		
5 % AgNPs	10	708.60	70.860	5.96328889		
10 % AgNPs	10	703.80	70.380	11.0557822		
15 % AgNPs	10	666.73	66.673	12.9525122		
ANOVA						
Source of Variation	*SS*	*df*	*MS*	*F*	*P-value*	*F crit*
Between Groups	2086.1875	3	695.3958333	42.6554691	0.001	2.86626555
Within Groups	586.89426	36	16.30261833			
Total	2673.08176	39				

Table A2 *t*-Test analysis of PIMs water contact angle at different Ag NPs loadings

Bonferroni's correction p= 0.0083

t-Test: Two-Sample Assuming Unequal Variances

	0% AgNPS	*5 % AgNPs*
Mean	88.64	70.860
Variance	35.23889	5.96328888 9
Observations	10	10
Hypothesized Mean Difference	0	
Df	12	
t Stat	7.63954855	
P(T<=t) one-tail	3.0042E-06	
t Critical one-tail	1.78228755 6	
P(T<=t) two-tail	0.001	
t Critical two-tail	2.17881283	

t-Test: Two-Sample Assuming Unequal Variances

	0% AgNPS	*10% AgNPs*
Mean	86.807	70.380
Variance	35.2388	11.0557
Observations	9	8222
Hypothesized Mean Difference	10	10
df	0	
t Stat	14	
P(T<=t) one-tail	7.39489 427 E-06	
t Critical one-tail	1.68951 0136	
P(T<=t) two-tail	0.001	
t Critical two-tail	2.14478 6688	

t-Test: Two-Sample Assuming Unequal Variances

	0% AgNPS	*15% AgNPs*
Mean	88.64	66.673
Variance	35.2388	12.9525
Observations	9	1222
Hypothesized Mean Difference	10	10
df	0	
t Stat	15	
P(T<=t) one-tail	8.26054 7443 E-07	
t Critical one-tail	2.89495 1.75305 0356	
P(T<=t) two-tail	0.001	
t Critical two-tail	2.13144 9546	

t-Test: Two-Sample Assuming Unequal Variances

	5 % AgNPs	*10% AgNPs*
Mean	70.860	70.380
	5.96328888	11.0557822
Variance	9	2
Observations	10	10
Hypothesized Mean Difference	0	
df	17	
t Stat	0.3096802	
	0.38028396	
P(T<=t) one-tail	7	
	1.73960672	
t Critical one-tail	6	
P(T<=t) two-tail	0.76	
	2.10981557	
t Critical two-tail	8	

t-Test: Two-Sample Assuming Unequal Variances

	5 % AgNPs	*15% AgNPs*
Mean	70.860	66.673
	5.96328	12.9525
Variance	8889	1222
Observations	10	10
Hypothesized Mean Difference	0	
df	16	
	1.91006	
t Stat	305	
	0.03710	
P(T<=t) one-tail	9192	
	1.74588	
t Critical one-tail	3676	
P(T<=t) two-tail	0.07	
	2.11990	
t Critical two-tail	5299	

t-Test: Two-Sample Assuming Equal Variances

	10% AgNPs	*15% AgNPs*
Mean	70.380	66.673
	11.0557	12.9525
Variance	8222	1222
Observations	10	10
	12.0041	
Pooled Variance	4722	
Hypothesized Mean Difference	0	
df	18	
	1.43469	
t Stat	2435	
	0.08426	
P(T<=t) one-tail	0906	
	1.73406	
t Critical one-tail	3607	
P(T<=t) two-tail	0.16	
	2.10092	
t Critical two-tail	204	

Table A3 ANOVA analysis of PIMs water uptake at different Ag NPs loadings

Anova: Single Factor

SUMMARY

Groups	*Count*	*Sum*	*Average*	*Variance*
0 % AgNPs	3	42.574238	14.191413	20.925546
5 % AgNPs	3	53.247531	17.749177	80.833000 2
10 % AgNPs	3	71.812029	23.937343	66.422893 9
15 % AgNPs	3	59.834747	19.944916	110.39769 3

ANOVA

Source of Variation	*SS*	*df*	*MS*	*F*	*P-value*	*F crit*
Between Groups	149.8483	3	49.949445	0.7172029 7	0.56	4.066181
Within Groups	557.1583	8	69.644783			
Total	707.0066	11				

Figure A1 Calibration curves obtained with a nanocomposite PIM (n=3) (40 w.t% D2EHPA, 10 w.t% Ag NPs and 50 w.t% PVC). Feed phase: 3500 mL with 0.5 – 2.0 mg L^{-1} analytes and extraction period: 24 hrs. The stripping solution contained 8 mL 1 M HNO_3.

